

T-Cell Stimulation by Melanoma RNA-Pulsed Dendritic Cells

Dissertation zur Erlangung
des Doktorgrades der Naturwissenschaften
an der Fakultät für Biologie
der Ludwig-Maximilians-Universität München

Angefertigt am

Institut für Molekulare Immunologie
GSF – Forschungszentrum für Umwelt und Gesundheit
unter der Betreuung von Prof. Dolores J. Schendel

und im

Labor für Tumorimmunologie
Urologische Abteilung des Klinikums Großhadern
Ludwig-Maximilians-Universität München
unter der Betreuung von Dr. Heike Pohla

vorgelegt von

Miran Javorović

am 15. Januar 2004

1. Berichterstatter: Prof. Dr. Dirk Eick
2. Berichterstatter: Prof. Dr. Hans Weiher

Tag der mündlichen Prüfung: 28. Mai 2004

For my mom

Table of contents

1. Introduction	1
1.1 Tumour immunoediting and immunosurveillance	1
1.2 Tumour immune escape	4
1.3 Dendritic cells	9
1.4 Danger model	12
1.5 Tolerance to self-antigens	13
1.6 RNA-pulsed DCs in tumour immunotherapy	16
1.8 Melanoma model	19
1.9 Aims of the study	23
2. Materials	25
2.1 Instruments and other equipment	25
2.2 Commonly used material	26
2.3 Chemicals and biological reagents	26
2.4 Kits	28
2.5 Cell culture media, buffers and solutions	29
2.6 Cells	31
2.7 Antibodies	31
2.8 Molecular biology media, buffers and gels	32
2.9 Plasmids	33
2.10 Peptides	33
2.11 Primers	34
2.12 List of manufacturers and persons	34
3. Methods	37
3.1 Cell culture	37
3.1.1 Cell counting	37
3.1.2 Cryopreservation of cells	37
3.1.3 Thawing of cryopreserved cells	38

3.1.4	Culture of adherent tumour cell lines	38
3.1.5	Culture of suspension tumour cell lines	38
3.1.6	CTL restimulation and culture	39
3.1.7	Isolation of PBMCs from a leukapheresis product	39
3.1.8	DC generation and culture	40
3.2	Flow cytometry	40
3.2.1	Direct staining of cell-surface molecules	41
3.2.2	Indirect staining of intracellular molecules	41
3.3	Production of amplified total cellular mRNA	42
3.3.1	Total cellular RNA isolation from tumour cells	43
3.3.2	Reverse transcription of isolated RNA into cDNA	43
3.3.3	Amplification of cDNA	44
3.3.4	Purification of cDNA	45
3.3.5	<i>In vitro</i> transcription of total cellular cDNA into cRNA	45
3.4	Production of single-species cRNA	46
3.4.1	Transformation of competent bacteria with plasmid DNA	47
3.4.2	Selection and expansion of transformed bacteria	48
3.4.3	Freezing of transformed bacteria	48
3.4.4	Plasmid DNA extraction from transformed bacteria	49
3.4.5	<i>In vitro</i> transcription of single-species cDNA into cRNA	49
3.4.6	Purification of cRNA	50
3.5	Electrophoresis	51
3.5.1	DNA agarose gel electrophoresis	51
3.5.2	RNA denaturing-agarose gel electrophoresis	51
3.6	RNA transfection into DCs	52
3.6.1	Lipofection	52
3.6.2	Electroporation	53
3.7	Functional assay	54
3.7.1	DC or tumour cell co-incubation with CTLs	54
3.7.2	IFN- γ ELISA	55
3.8	RNA quantitation	56
3.8.1	Total cellular RNA isolation from transfected DCs	56
3.8.2	Reverse transcription of <i>in vitro</i> transcribed cRNA and dendritic cell-derived RNA into cDNA	57
3.8.3	Real-time PCR	58
4.	Results	63
4.1	Transfection of DCs with RNA encoding EGFP	63
4.1.1	Generation of DCs	64

4.1.2	Lipofection vs. electroporation and immature DCs vs. mature DCs	66
4.1.3	Phenotype of electroporated DCs	70
4.1.4	Electroporation with increasing amounts of EGFP cRNA	72
4.1.5	Kinetics of EGFP cRNA degradation and EGFP expression	75
4.1.6	Summary of the data obtained in the EGFP system	79
4.2	Transfection of DCs with RNA encoding tyrosinase	81
4.2.1	Time in culture needed for CTLs to most efficiently react to antigen presentation	82
4.2.2	Time needed for transfected DCs to most effectively present the antigen	84
4.2.3	Controls in the DC-RNA-CTL system	85
4.2.4	Electroporation with increasing amounts of tyrosinase cRNA	87
4.2.5	RNA and DC concentrations in electroporation	88
4.2.6	Reproducibility of results in a standardised system	89
4.2.7	Kinetics of tyrosinase cRNA degradation	90
4.2.8	Summary of the data obtained in the tyrosinase system	95
4.3	Transfection of DCs with RNA encoding a combination of antigens	96
4.3.1	Amount of antigen message in different RNA samples	97
4.3.2	Different CTL reactivities upon exposure to synthetic peptides	101
4.3.3	Correlation between amount of antigen message and epitope recognition by CTLs	103
4.3.4	Efficiency of electroporation with single-species tumour-antigen cRNA	106
4.3.5	Stimulatory capacity of DCs pulsed with single-species tumour-antigen RNA and total cellular tumour RNA	107
4.3.6	Summary of the data obtained in the three-antigen system	112
5.	Discussion	114
5.1	Efficiency of RNA transfection into DCs	114
5.2	Antigen processing in immature and mature DCs	116
5.3	Quantitation of antigen presentation on RNA-pulsed DCs	119
5.4	Correct and incorrect peptide sequences	123
5.5	Priming T-helper cells in addition to CTLs	127
5.6	Overcoming tumour immune escape	129
5.7	Antigen competition and immunodominance	131
5.8	Dangers of autoimmunity associated with immunotherapy	134

5.9	Conclusions and prospects	141
6.	Summary	143
7.	References	146
8.	Abbreviations	163
9.	Acknowledgments	166
10.	Curriculum vitae	168

1. Introduction

Interest in vaccinating against tumours dates back to the 1890s when the New York surgeon William B Coley successfully treated some patients with sarcoma using bacterial toxins. In 1909, Paul Ehrlich successfully carried out immunisation in animals with tumour cells and suggested that tumours occur in humans at a high frequency but are kept under control by the immune system. Whereas this hypothesis may be simplistic, it has become clear that some tumour cells can indeed be distinguished from corresponding normal cells due to the existence of so-called tumour-associated antigens (TAAs) that are sometimes recognised by the immune system (reviewed in Dermime S *et al.* 2002). Once the immune system perceives an antigen as dangerous, it is likely that this antigen and antigen-bearing particles or cells will be completely eliminated by the immune system with high specificity and efficiency. Therefore, in situations where well-established approaches such as surgery, radiation therapy and chemotherapy fail to help cancer patients, therapeutic approaches based on activated effectors of the immune system have the potential to be effective alternatives.

1.1 Tumour immunoediting and immunosurveillance

The concept that the immune system can recognise and destroy tumour cells was postulated in the cancer immunosurveillance hypothesis proposed by Burnet and Thomas (Burnet FM 1970). The logical prediction from this hypothesis is that immunodeficient or immunosuppressed humans should show a greater incidence of cancer. Based on long-term studies of transplant patients and individuals with primary immunodeficiencies, it is clear that some of the observed higher risk was due to the development of tumours of viral origin (Penn I 1999). However, greater risk ratios have also been documented for a broad range of tumours with no apparent viral etiology. For example, one study showed increased occurrence of colon, lung, bladder, kidney, ureter and endocrine tumours, as well as malignant melanomas, in patients who received renal transplants, as compared with the general population (Birkeland SA *et al.* 1995). These and other data strongly indicate that individuals with severe deficits of immunity indeed have a higher probability of developing a variety of cancers. In addition to supporting epidemiological studies, there is accumulating evidence showing a positive correlation between the presence of

lymphocytes in a tumour and increased patient survival. Based on statistical observations in one study, it was calculated that patients with tumour infiltrating lymphocytes (TILs) in their melanomas survived one and a half to three-fold longer than patients with no TILs (Clemente CG *et al.* 1996).

During tumour formation, the immune system may select for tumour variants that are better suited to survive in an immunologically intact environment, very much like it does with viruses, bacteria and parasites. This was demonstrated in many murine studies when the repassaging of transplantable tumours through immunocompetent hosts resulted in the generation of tumour variants with reduced immunogenicity (Uyttenhove C *et al.* 1980, Urban JL *et al.* 1982). In other words, tumours are imprinted by the immunologic environment in which they form. This imprinting process can often result in the generation of tumours that are better able to fight the tumour-suppressing actions of the immune system by eliminating tumour cells of high immunogenicity but leaving behind tumour variants of reduced immunogenicity or that have acquired other mechanisms to evade or suppress immune attack. These cells have a better chance of surviving in the immunocompetent host. The alterations that must occur during the immunologic sculpting of a developing tumour are probably facilitated by the genetic instability of tumours (Lengauer C *et al.* 1998).

The term "immunosurveillance" only implies protection of the host by the immune system at the earliest stages of cellular transformation. Therefore, it does not accurately describe the whole process. As argued above, immunosurveillance also shapes tumours by exerting selective pressure. To more appropriately describe the dual host-protecting and tumour-sculpting actions of the immune system, Dunn and colleagues proposed the use of a broader term "cancer immunoediting" (Dunn GP *et al.* 2002). They envisage immunoediting as a result of processes in three phases: elimination, equilibrium and escape (Figure 1.1).

The elimination phase encompasses the original concept of immunosurveillance. If the developing tumour is successfully deleted, this phase represents the complete editing process without progression to the subsequent phases. It is possible that, at first, tumour cells appear immunologically as healthy growing cells that do not send out danger signals to activate the immune system because they express neither microbial immune-recognition

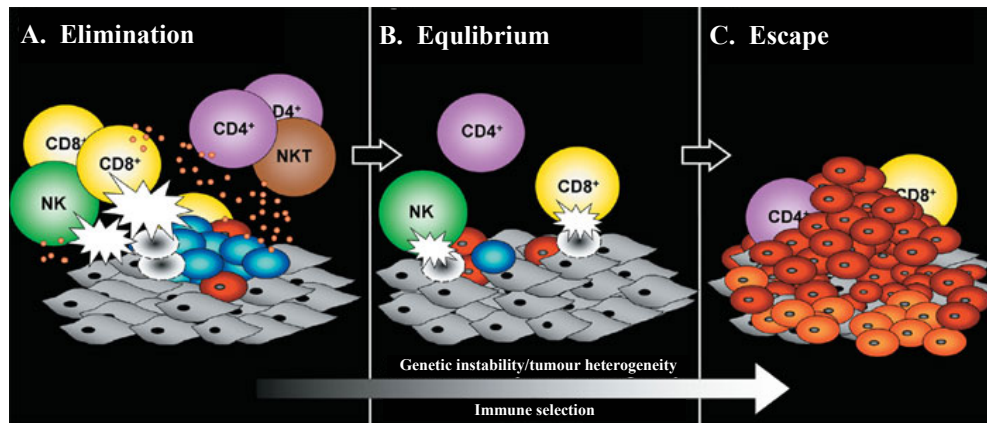


Figure 1.1 The three Es of cancer immunoediting. Cancer immunoediting encompasses three phases. Elimination corresponds to immunosurveillance (A). Equilibrium represents the process by which the immune system iteratively selects and/or promotes the generation of tumour cell variants with increasing capacities to survive the immune attack (B). Escape is the process wherein the immunologically sculpted tumour expands in an uncontrolled manner in the immunocompetent host (C). In A and B, developing tumour cells (blue), tumour cell variants (red) and underlying stroma and nontransformed cells (gray) are shown. In C, additional tumour variants (orange) that have formed as a result of the equilibrium process are shown. Different lymphocyte populations are as marked. The small orange circles represent cytokines and the white flashes represent cytotoxic activity of lymphocytes against tumour cells. Abbreviations: NK (natural killer) cells, NKT (natural killer T-) cells. From Dunn GP *et al.* 2002.

patterns nor release distress signals to alarm the innate immune cells (Restifo NP *et al.* 2002). However, once tumours reach a certain size, they begin to disrupt surrounding tissue and stress signals are triggered when oxygen and nutrient supplies become scarce. Metabolic disturbance, generation of reactive oxygen species such as OH and H₂O₂, up-regulation of protective stress factors and death by apoptosis or necrosis may all act as alarm signals to recruit and activate local innate immune cells such as dendritic cells (DCs), macrophages, neutrophils and natural killer (NK) cells. They in turn activate T-cells to mount an adaptive immune response against tumours. In the equilibrium phase, all tumour cell variants that have survived the elimination phase enter a dynamic equilibrium with the host immune system. Actions of the immune system are the driving force behind the Darwinian selective pressure which is enough to contain but not fully extinguish a tumour mass containing many genetically unstable and rapidly mutating malignant cells. Many of the original escape variants of tumour cells are destroyed, but new variants appear, carrying different mutations that provide them with increased resistance to the immune attack. It is likely that equilibrium is the longest of the three phases and may occur over a period of many years. In the escape phase, surviving tumour variants that have acquired insensitivity to immunologic detection and/or elimination through genetic or

epigenetic changes begin to expand in an uncontrolled manner. Only then does the malignant disease become clinically observable.

1.2 Tumour immune escape

One study estimated that an average malignancy contains more than 1×10^4 mutations (Stoler DL *et al.* 1999). Genomic instability creates a vast repertoire of tumour cells. Some of these cells are selected for survival simply because they possess certain genetic and epigenetic traits that are beneficial in their environment. In other words, already existing genes and environmental factors define the passive process of natural selection. Terms such as "tumour evasion" or "tumour escape" are not really appropriate because evasion and escape imply active acquisition of certain characteristics or phenotypes, rather than the differential propagation of tumour subclones. The same concept also applies to tumour growth in the face of an effective immunotherapy.

In a review by Khong and Restifo, the following tumour immune mechanisms are described (Khong HT and Restifo NP 2002):

- loss or down-regulation of HLA (human leukocyte antigen) class I molecules
- loss of tumour antigens and immunodominance
- defective death receptor signalling
- apoptosis of activated T-cells
- lack of co-stimulation
- secretion of immunosuppressive cytokines
- presentation of altered peptide ligands

Decreased or absent HLA class I expression is associated with invasive and metastatic lesions. Seven major altered HLA class I phenotypes have been defined in tumour tissues (Garrido F *et al.* 1997) and are explained in Figure 1.2:

1. **HLA class I total loss.** This phenotype is characterised by the absence of any HLA class I molecule expression in tumour cells. One of the mechanisms that underlie this loss involves mutations in one copy of the β_2 -microglobulin gene in combination with the loss of heterozygosity involving the second allele (Hicklin DJ *et al.* 1998). Other detected causes include defects in HLA genes and in the antigen processing and

transport pathway, such as down-regulation of proteasome subunits, LMP-2 and LMP-7 (low molecular protein 2 and 7), and peptide transporters, TAP-1 and TAP-2 (transporter associated with antigen processing 1 and 2). However, in these situations, HLA class I can often be up-regulated by treatment with IFN- γ (interferon γ).

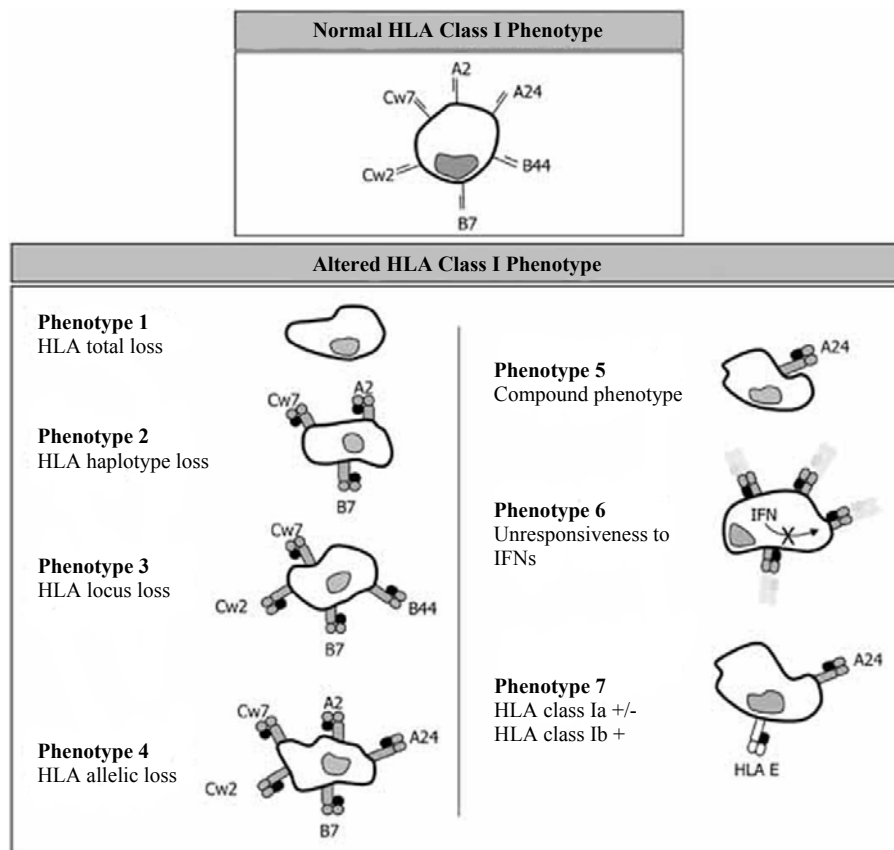


Figure 1.2 Normal and altered HLA class I phenotypes found in human tumours. Normal cells express 6 HLA class I alleles (2 HLA-A, 2 HLA-B and 2 HLA-C). HLA molecules can be totally or partially absent from tumour cells (Phenotype I-Phenotype V). In addition, tumour cells may not respond to IFNs (Phenotype VI), or may also express aberrant HLA-E molecules in cells with low expression of HLA-A, B, or C classical class I antigens (Phenotype VII). Abbreviations: HLA (human leukocyte antigen), IFN (interferon). From Garcia-Lora A *et al.* 2003.

2. **HLA haplotype loss.** Tumours can partially or entirely lose one of the two HLA haplotypes due to the loss of heterozygosity on chromosome 6 (Ramal LM *et al.* 2000).
3. **HLA A, B or C locus product down-regulation.** This altered phenotype is found when both products of HLA-A, B or C loci are coordinately down-regulated. It is more frequent with HLA-A and HLA-B molecules and is associated with changes in

the transcription of corresponding genes (Soong TW and Hui KM 1992, Peltenburg LT and Schrier PI 1994).

4. **HLA allelic loss.** This alteration is defined as the loss of a single HLA class I allele that might be the result of point mutations, partial deletions of HLA class I genes, chromosomal breakage or somatic recombination (Brady CS *et al.* 2000).
5. **Compound phenotypes.** To produce this phenotype a combination of two different alterations is required, for example, an HLA haplotype loss and HLA-B and C locus down-regulation (combination of phenotypes II and III). The final result is a tumour cell expressing only one HLA class I allele.
6. **Unresponsiveness to interferons (IFNs).** Some tumour cells express basal levels of HLA class I molecules but have lost their capacity to up-regulate them in response to different cytokines, including IFN- α and IFN- γ .
7. **Downregulation of classical HLA-A, B and C molecules and appearance of HLA-E molecules.** HLA-E has a strong NK inhibition capacity (Marin R *et al.* 2003).

A direct consequence of partial or complete loss of HLA class I is increased susceptibility to NK cell lysis. Therefore, in addition to mechanisms helping them escape recognition by T-cells, tumours need other modifications that render them resistant to attacks by NK cells. A tumour escape strategy that has yet to be demonstrated in humans is down-regulation of MICA and MICB (MHC class I chain-related genes A and B) ligands that engage NK activating receptors (Garrido F and Algarra I 2001). It is also possible that strong NK stimulatory factors, such as IL-12 (interleukin 12), IL-2, IL-15 and type 1 IFNs, usually associated with microbial infection, are not readily available in tumour environments. Furthermore, cross-talk between DCs and NK cells might be lacking (Gerosa F *et al.* 2002). In some situations, tumours may produce immunomodulatory cytokines, such as TGF- β (transforming growth factor β) or MIF (macrophage migration inhibitory factor), which can directly inhibit NK cell activation and function.

Most examples of antigen down-regulation by tumour cells come from the melanoma model. In one study, cells were observed to be melanoma antigen A (Melan-A)-positive in 100% of stage I lesions but in only 75% of stage IV lesions (Hofbauer GF *et al.* 1998). Decreased antigen expression was also found in non-regressing tumours after peptide vaccination. Expression of gp100 (glycoprotein 100) was reduced from 47% to 32% after vaccination with the corresponding peptide (Lee KH *et al.* 1998). In most cases, the exact

mechanisms that control down-regulation of tumour antigens are not known. Nevertheless, propagation of such antigen loss variants may be facilitated by epitope immunodominance. The theory of immunodominance, as it relates to tumour escape, predicts that antigen-loss variants within a tumour are shielded from immune pressure. Parental tumour cells carrying an immunodominant epitope serve as a distraction, thereby diverting attention from the tumour variants. Once the parental cells are eliminated, a new hierarchy is established among the variant subpopulations, and formerly immunorecessive epitopes become dominant (Schreiber H *et al.* 2002).

Fas and TRAIL (TNF-related apoptosis inducing ligand) receptors are called "death receptors" because they contain cytoplasmic sequences described as "death domains" that are essential for the transmission of apoptotic signals into the cells. Defective death receptor signalling is another mechanism that may contribute to the survival and proliferation of tumour cells. Various tumours express cFLIP (cellular FLICE-inhibitory protein), a protein that inhibits the Fas signalling pathway, thereby, rendering tumour cells resistant to death receptor-mediated apoptosis (Irmeler M *et al.* 1997). Down-regulation or loss of Fas expression and loss of expression of all TRAIL receptors may also contribute to tumour escape (Hersey P and Zhang XD 2001 *Nature Rev Cancer*, Shin MS *et al.* 1999).

One of the more controversial mechanisms of tumour escape is the expression of death receptor ligands by tumour cells. A variety of cancer cells express the functional Fas ligand, which induces apoptosis of Fas-susceptible target cells, possibly including T-cells (Niehans GA *et al.* 1997). TRAIL is also expressed by tumours but there is no convincing evidence that it plays a major role in the induction of tumour-specific T-cell apoptosis in human cancers (Cappello P *et al.* 2002).

Unlike professional antigen-presenting cells (APCs), most cells, including tumour cells, do not express the co-stimulatory molecules, CD80, CD86, CD40 and CD70. Presentation of tumour antigens to T-cells without appropriate co-stimulation may lead to T-cell anergy. Lack of expression of co-stimulatory molecules by tumours may also hinder optimal NK cell activation via CD28 and CD27 pathways (Takeda K *et al.* 2000). In an experimental setting, insertion of genes encoding CD80, CD86 or both into tumours generally increased the immunogenicity of those tumours but did not necessarily lead to regression (Chen L *et al.* 1994).

Tumour cells produce a variety of cytokines and chemokines that can negatively effect maturation and function of immune cells. Most tumours secrete VEGF (vascular endothelial growth factor), a cytokine known to inhibit DC differentiation and maturation (Toi M *et al.* 1996, Oyama T *et al.* 1998). Increased concentrations of IL-10 are frequently detected in the sera of cancer patients. This cytokine negatively influences DCs at many different levels. It interferes with DC differentiation from stem cell precursors (Girolomoni G 1997), compromises DC maturation and function, inhibits antigen presentation, IL-12 production and induction of T-helper type 1 responses by DCs (Sharma S *et al.* 1999), helps induce spontaneous DC apoptosis (Ludewig B *et al.* 1995) and enhances DC susceptibility to NK cell lysis (Carbone E *et al.* 1999). IL-10 has also been shown to down-regulate TAP-1 and TAP-2 peptide transporters and HLA class I/II antigen-presenting molecules in tumour cells thereby protecting them from recognition by cytotoxic T-lymphocytes (CTLs). The proinflammatory factor PGE₂ (prostaglandin E2) is another cytokine expressed by tumours. It increases the production of IL-10 by lymphocytes and macrophages and inhibits IL-12 production by macrophages (Huang M *et al.* 1998). High concentrations of TGF- β are also frequently found in cancer patients and are associated with disease progression and poor responses to immunotherapy. It inhibits the activation, proliferation and activity of lymphocytes (Fontana A *et al.* 1989).

It has been proven that each individual T-cell receptor (TCR) is a very adaptable and finely-tunable structure that differentially responds not only to one but to a broad spectrum of presented peptides. Analogues of immunogenic peptides which maintain the capacity to induce some TCR-mediated responses, despite changed amino acids at TCR contact sites, are defined as altered peptide ligands (APLs). *In vitro* studies have shown that APLs can mediate a number of different outcomes in interacting T-cells, ranging from anergy and partial activation to increased and optimal activation (Kersh GJ and Allen PM 1996 Nature). Peptides mimicking the Melan-A immunogenic epitope can be found in peptide fractions eluted from melanoma cells and are thought to induce antigen-specific T-cell anergy (Rivoltini L *et al.* 2002).

1.3 Dendritic cells

DCs (Figure 1.3) represent a heterogenous cell population, residing in most peripheral tissues, particularly at sites of interface with the environment, i.e. skin and mucosae. Here, they represent 1-2% of the total cell number (Banchereau J *et al.* 2000). In the absence of ongoing inflammatory and immune responses, DCs constitutively patrol through the blood, peripheral tissues, lymph and lymphoid organs. In peripheral tissues, DCs capture self and non-self antigens via specific receptors (FcR, MMR, DEC-205 and DC-SIGN), and various mechanisms, such as macropinocytosis, receptor-mediated endocytosis and phagocytosis. Internalised antigens are then processed into proteolytic peptides, and these peptides are loaded onto major histocompatibility complex (MHC) class I and class II molecules. The steps of antigen uptake, degradation, loading and transfer to the cell surface as part of a peptide-MHC (pMHC) complex are altogether called "antigen processing and presentation". Constitutively, however, peripheral DCs present antigens quite inefficiently. Signals from pathogens or pathogen-induced tissue damage, often referred to as "danger signals", induce DCs to enter a developmental program, called "maturation", which transforms DCs into efficient antigen-presenting cells and T-cell activators. Danger signals are generated when receptors on DCs recognise an encounter with bacteria, bacterial products (DNA and LPS), fungal products (hyphae), viruses, viral products (dsRNA), cytokines, molecules on T-cells (CD40L) and molecules derived from self cells (tumour cell lysates and heat-shock proteins).

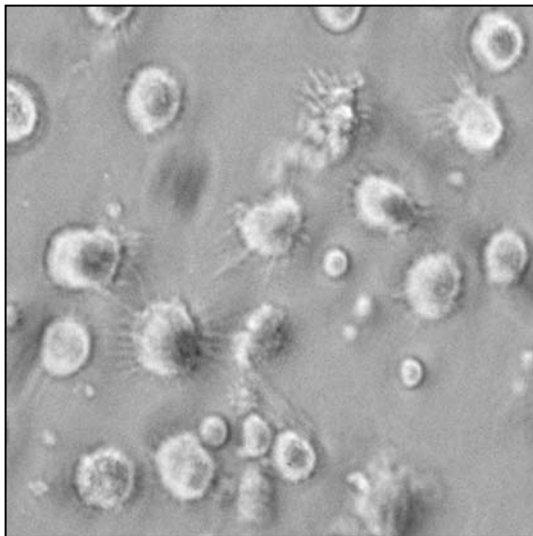


Figure 1.3 Mature monocyte-derived DCs. DCs were given their name because of the dendrite-like cytoplasmic processes protruding from the cell bodies into their environment. Once DCs arrive in the secondary lymphoid organs, interaction with many T-cells takes place. The processes increase the surface of DCs thereby enabling antigen presentation to an increased number of T-cells.

During maturation, antigen uptake is down-regulated. Peptide loading as well as the half-life and delivery of pMHC complexes to the cell surface are increased. The expression of co-stimulatory molecules (CD80, CD86, CD40 and OX-40L) is also up-regulated. One study demonstrated that mature DCs are up to 1000-fold more efficient in activating resting T-cells, compared to other professional APCs, such as monocytes, macrophages and B-cells (Bhardwaj N *et al.* 1993). Therefore, DCs can be described as the most potent APCs. They are also the only cells capable of activating naïve T-cells and, thereby, of initiating adaptive immune responses. In addition to up-regulation of antigen-presenting and co-stimulatory molecules, maturation includes enhancing the ability of DCs to migrate out of the tissues and into secondary lymphoid organs, where interactions with T-cells take place. This includes modifications in the expression of chemokine receptors, such as CCR7 (chemokine CC motif receptor 27) and adhesion molecules, as well as profound changes in the cytoskeleton organisation. DCs simultaneously become primed to synthesise cytokines essential for the development of CTLs and T-helper cells (IL-12, IL-15 and IL-18) and chemokines which attract naïve and memory cells (Sallusto F and Lanzavecchia A 1999). The maturation state is accompanied by the development of resistance to immunosuppressive factors, such as IL-10, and to infection by several organisms.

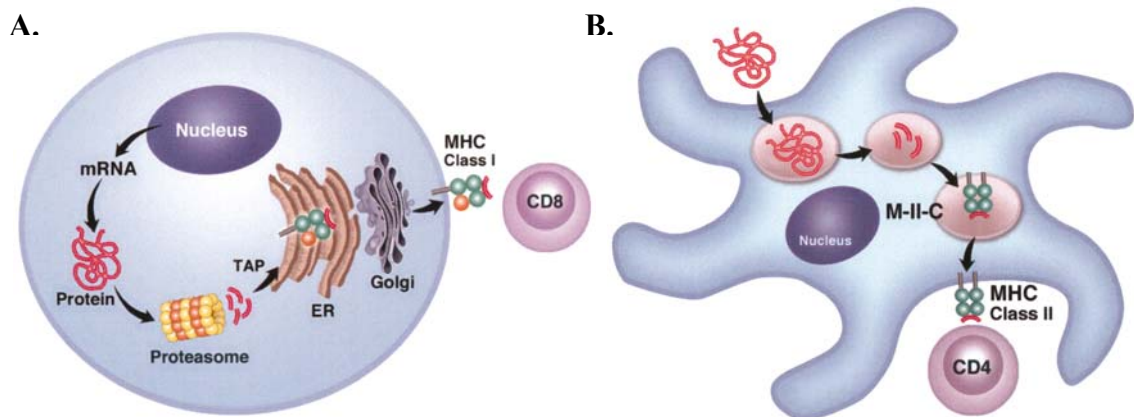


Figure 1.4 MHC class I and class II antigen processing and presentation pathways in DCs. Intracellular proteins (A) undergo degradation by the proteasome complex, are brought into the ER where they bind to MHC class I molecules and traffic through the Golgi apparatus on their way to the cell surface. On the cell surface, they are recognised by CTLs ($CD8^+$ T-cells). Exogenous proteins (B) enter the endosome/lysosome vesicles in antigen presenting cells after internalisation by phagocytosis or endocytosis. Here they are degraded into peptides by proteases. These peptides bind to MHC class II molecules in compartments called MIIC, from where they are transferred to the cell surface by transport vesicles. On the cell surface, they are recognised by T-helper cells ($CD4^+$ T-cells). Abbreviations: TAP (transporter associated with antigen processing), ER (endoplasmic reticulum), MHC (major histocompatibility complex), MIIC (MHC class II rich compartments). From Ribas A *et al.* 2003.

Antigenic peptides from exogenously acquired proteins are produced by proteases in incoming endosomes (Figure 1.4A). These endosomes fuse with vesicles carrying MHC class II antigen-presenting molecules from the endoplasmic reticulum (ER) to form the so-called MHC class II rich compartments (MIICs). Inside MIICs, peptides bind to antigen-presenting molecules. Subsequently, pMHC class II complexes are exported to the cell surface for activation of T-helper cells. These complexes are generated only in a narrow time-frame after induction of DC maturation but persist with extremely long half-lives of several days (Cella M *et al.* 1997). Endogenously synthesised antigens, such as self proteins and viral proteins, are cleaved by proteasomes into peptides in the cytoplasm and transported into the endoplasmic reticulum via TAP transporters (Figure 1.4B). There they are loaded onto MHC class I molecules. When displayed at the cell surface, pMHC class I complexes are recognised by CTLs. The average pMHC class I complex has a half-life of only 5-10 hr at the cell surface and therefore decays reasonably quickly. Nevertheless, these complexes are continuously assembled in the biosynthetic pathway (Cella M *et al.* 1999).

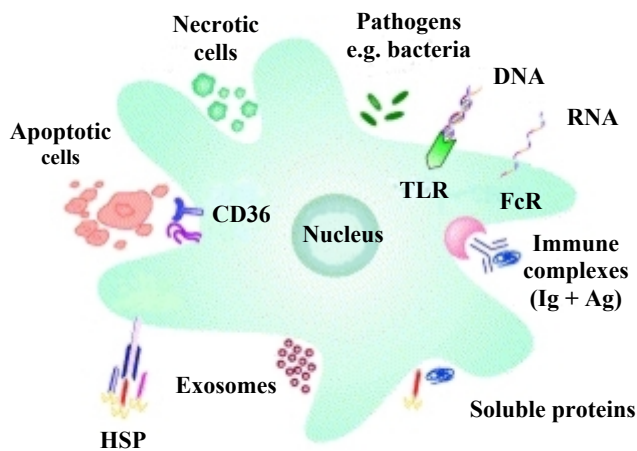


Figure 1.5 Exogenously derived antigens access the MHC class I processing pathway of DCs and are presented on MHC class I molecules. Multiple forms of exogenous antigens that access the MHC class I processing pathway of DCs are shown. Abbreviations: TLR (Toll-like receptor), Ig (immunoglobulin), FcR (Fc receptor), Ag (antigen), HSP (heat shock protein). From Bhardwaj N 2001.

"Cross-priming" is the term used to describe the ability of DCs to present antigens from other cells and mount CTL responses against these antigens. Since its discovery (Bevan MJ 1976), this phenomenon has been implicated in tolerance to self-antigens and in immune responses to viruses, transplantation antigens and tumours. As shown in Figure 1.5, antigens from multiple extracellular sources can be taken up and presented by DCs within MHC class I molecules (Yewdell JW *et al.* 1999). How exactly peptides derived from exogenous antigens gain access to MHC class I molecules is still being deciphered. TAP-dependent cross-priming suggests that exogenous antigens somehow enter the

cytoplasm from endosomes following internalisation (Sigal LJ and Rock KL 2000). Soluble antigens or antigens within immune complexes appear to access the cytoplasm (Rodriguez A *et al.* 1999). Only small molecules can traverse the endosomal membrane, suggesting the existence of active transporters, pores or leaky junctions that allow exogenous antigens to enter the cytoplasm. It is also possible that antigens processed inside endosomes have access to recycling MHC class I molecules that re-appear on the cell surface (Yewdell JW *et al.* 1999). However, it is not clear whether endosomal proteases generate peptides for MHC class I. In terms of immunotherapy, the exogenous pathway is attractive because it can be exploited to introduce antigens in different forms into DCs and, thereby, activate a broad repertoire of antigen-specific CTLs and T-helper cells.

1.4 Danger model

According to the danger model proposed by Matzinger (Matzinger P 1994), the immune system does not necessarily respond only to what is foreign but to anything that is dangerous. DCs acquire antigens from the cell debris generated during an inflammatory response but do not discriminate between self and pathogen-specific antigens. They process and present both. Whereas immature and semi-mature DCs induce T-cell anergy and activate regulatory T-cells (Lutz MB and Schuler G 2002), only mature DCs are capable of efficiently activating T-cells. The consequence is that antigens are presented in a T-cell stimulatory fashion exclusively in the context of danger, which induces the process of DC maturation in the first place. The prerequisite of DC maturation increases the probability that a high percentage of antigens presented by the DC is indeed foreign.

The danger model is based on the existence of the so-called second signal, in addition to the first signal directed at T-cells. Whereas the first signal comes from specific recognition of antigenic peptides presented within MHC molecules, the second signal is either mediated through co-stimulatory molecules on professional APCs or delivered by T-helper cells. The main principle of the model is that the presence or absence of the second signal determines immune responsiveness or tolerance. The main rules to generate an immune response or tolerant state are as follows.

Naïve T-cells

- undergo apoptosis if they receive signal one in the absence of signal two
- second signal may be offered only by DCs

Memory T-cells

- undergo apoptosis if they receive signal one in the absence of signal two
- second signal may be offered from all professional APCs, i.e. monocytes, macrophages, B-cells or DCs

B-cells

- undergo apoptosis if they receive signal one in the absence of signal two
- second signal may be offered only by memory/effector T-cells

Effector T and B-cells

- perform functions after antigen recognition regardless of the presence or absence of signal two
- undergo apoptosis or revert to a resting state after a reasonably short period of time

In the danger model, it is assumed that the main determinant leading to the initiation of an immune response is the presence of an antigen in the context of tissue destruction. If there is no damage and cells are unharmed or they die by apoptosis, no immune response ensues. However, if cells are injured, stressed or die by necrosis, an immune response is induced. Since an absolute majority of body cells present only signal one, the default reaction of a responding T-cell for an antigen should be tolerance. This kind of behaviour is very beneficial to sustain the tolerant state and to avoid auto-aggression against self-tissues (Kowalczyk DW 2002).

1.5 Tolerance to self-antigens

The establishment of T-cell tolerance to self-antigens has two components: central (intrathymic) and peripheral (extrathymic). In the thymus, T-cells are subjected to the rigorous process of negative selection before they are released into peripheral circulation. High-avidity T-cells that recognise presented self-antigens are eliminated. Low-avidity T-

cells specific for the same antigens and low to high-avidity T-cells specific not only for foreign, but also self-antigens that were not presented in the thymus, escape negative selection and become part of the mature naïve T-cell population. Even if their TCRs recognise self-antigens, all T-cells that have not been stopped in the thymus are functionally competent. For example, CTLs specific for ubiquitous proteins such as β_2 -microglobulin, hemoglobin (Schild H 1990) and kallikrein (Heiser A 2000) are part of the peripheral T-cell repertoire and can be activated under appropriate conditions. In the periphery, the immune system either ignores autoreactive T-cells or deals with them before activation through mechanisms that include tolerance and regulation (defensive strategies). If these approaches are inefficient, the system tries to minimise an autoimmune response before it causes too much damage (reactive strategies).

The defensive strategies include passive and active approaches. Passive maintenance of peripheral tolerance is based on simply ignoring existing autoreactive T-cells (Zinkernagel RM 1996). This is possible because their distribution is restricted to hematopoietic and lymphoid tissues. Therefore, T-cells do not circulate throughout the body in search of antigens (Mackay CR 1993). As explained above, somatic cells present their own antigens, but lack co-stimulatory molecules and therefore can neither prime naïve T-cells nor activate memory T-cells. Instead, the contact of T-cells with antigens and their subsequent activation depend on professional APCs. The function of APCs is to shuttle antigens to the T-cells, most of which are waiting in the lymphoid tissues. If T-cells specific for self-antigens had access to other tissues in the body and if they could be activated there without the help of APCs, immunological ignorance would not be possible. Indeed, it appears that the majority of self-antigens are not actively tolerised, but ignored because they are either expressed at immunologically privileged sites (Barker CF and Billingham RE 1977, Oldstone MB *et al.* 1991) or they are not expressed above a certain threshold required to overcome central or peripheral tolerance (Kurts C 1998). However, not all autoreactive T-cells are ignored in the periphery. Their potential activation is prevented by APC-based and T-cell-based active tolerance mechanisms.

During homeostasis, DCs constantly acquire self-antigens, primarily from somatic tissues that are frequently targeted by pathogenic infections. These immature-like DCs migrate to the lymph nodes and present antigens to autoreactive T-cells in a tolerogenic manner (Steinman RM 2000). As a consequence, self-specific T-cells are removed from the

circulation. During infection, DCs originating from the same tissues present self-antigens together with pathogenic antigens in a stimulating manner, but not many self-epitopes are recognised in the lymphoid organs because most autoreactive T-cells have already been eliminated. Autoreactive T-cells can be, and probably constantly are, activated by APCs during infection and would induce autoimmune pathology if it were not for the presence of regulatory T-cells. These $CD4^+CD25^+$ cells prevent the activation, expansion and function of autoreactive T-cells. It has been shown in mice that depletion of this T-cell subpopulation induces a broad range of autoimmune pathologies (Shevach EM 2001). Since they purge the body of autoreactive T-cells that may have escaped elimination by tolerising APC, regulatory T-cells seem to be the last line of defence before the onset of autoimmunity. It is still unclear what proportion and which subsets of autoreactive T-cells are ignored, tolerised by APCs or regulated by T-cells (Gilboa E 2001).

Reactive strategies are used by the immune system to minimise the effects of already existing autoimmune responses. Activated autoreactive T-helper cells die by neglect because most somatic cells do not express MHC class II molecules. This phenomenon is also known as programmed cell death. CTLs that repeatedly encounter self-antigen on somatic cells in the absence of co-stimulation die in a process known as activation-induced cell death. Regulatory T-cells also contribute to the reactive strategies.

Mechanisms in charge of maintaining tolerance are not perfect. Low-avidity self-specific T-cells are able to avoid negative selection in the thymus. In order to be activated in the periphery, such cells need strong stimulatory signals to compensate for their low avidity. Evolutionary calibration within the immune system ensures that, in most situations, somatic cells and APCs in the periphery do not express stimulatory molecules above the threshold of APCs in the thymus. Whereas low-avidity self-specific T-cells are more difficult to stimulate, there are high-avidity autoreactive T-cells that need weaker stimuli for activation. These high-avidity cells can reach the periphery if corresponding epitopes are not presented in the thymus. Most of them are then ignored because the antigens for which they are specific are not accessible. Outside the thymus, multiple mechanisms are in charge of eliminating or controlling both low and high-avidity self-specific T-cells, but even they can fail. The consequence is that the repertoire of T-cells in the periphery includes cells specific for self-antigens with avidities ranging from low to high. As explained above, DCs needed for T-cell stimulation efficiently present everything they

capture, not discriminating between harmless and dangerous. Therefore, whether an antigen is seen as foreign or self, is not really predetermined, but strongly depends on the context in which the antigen is presented to the immune system.

Most TAAs are self-antigens. For example, indirect assays in different studies revealed that Melan-A-specific CTLs are present in 20-75% of healthy individuals. Pittet and colleagues (Pittet MJ *et al.* 1999) used the direct method of tetramer-staining and confirmed these findings by detecting CTLs specific for Melan-A in 60% of healthy donors. These cells were of naïve phenotype and had a high frequency of 1 in every 1500 CTLs. It was also demonstrated that autoreactive T-cells may even be of high avidity (Yee C *et al.* 1999). It is thought that active central and/or peripheral tolerance mechanisms usually do not exist against these TAAs (Ludewig B *et al.* 2000). They seem instead to be immunologically ignored. The idea of attacking tumours with effectors of the immune system is to a large extent based on breaking the tolerance to self, and the outcome of successful immunotherapy is actually a form of autoimmunity.

1.6 RNA-pulsed DCs in tumour immunotherapy

The fact that functionally-competent autoreactive T-cells specific for TAAs have not been completely eliminated from the body does not guarantee tumour regression but it is the foundation of tumour immunotherapy. TAAs must be presented to the T-cells in a stimulatory manner and, therefore, strategies have to be developed that use the flexibility of the immune system in interpreting an antigen as foreign or self. Vaccination with tumour antigen-pulsed DCs was shown to elicit protective immunity in a variety of animal models. This can be explained by the high antigen-presenting and T-cell stimulatory capacities of DCs that are the most potent professional APCs and the only APCs able to prime naïve T-cells. It was observed that the cellular arm of the immune system is most efficient at specifically recognising tumour cells and eliminating them. Therefore, the emphasis in vaccination has shifted from humoral immunity towards the induction of cellular responses, especially CTLs. The attention CTLs received is not only due to their effective killing of malignant cells but also to limitations imposed by available technology. Depending on antigen loading methods and the antigen itself, in most cases, engineered DCs stimulated CTLs and not T-helper cells. However, it is becoming increasingly clear

that inducing antigen-specific T-helper cells, in addition to CTLs, is necessary to improve initiation and maintenance of anti-tumour immunity (Wang RF 2001).

In DC-based tumour immunotherapy, an important decision involves the choice of TAAs with which to load the DCs. Equally important are the composition and the form of the antigen in which it should be introduced into the DCs. Different approaches are summarised in Table 1.1. They are thoroughly evaluated and compared in a review by Mitchell and Nair (Mitchell DA and Nair S 2000).

Table 1.1 Delivery of antigens into DCs

<p>Individual tumour-associated antigens: synthetic or eluted peptides soluble protein cDNA or cRNA encoding the antigen</p> <p>Whole tumour antigenic repertoires: differentiation of DCs from malignant cells (leukemia) tumour lysates apoptotic bodies or necrotic cells total cellular tumour RNA DC-tumour cell hybrids peptide-HSP complexes DC-derived exosomes</p>

Abbreviations: cDNA (complementary DNA), cRNA (complementary RNA), HSP (heat shock protein).

Exogenous loading of a synthetic peptide, representing an antigenic epitope known to be immunogenic, onto empty MHC molecules expressed on the DCs is an efficient and very often used strategy (Thurner B *et al.* 1999). Alternatively, DCs can be pulsed with a recombinant protein to induce immune responses against all potentially immunogenic epitopes from one antigen (Santin AD *et al.* 1999). However, vaccine strategies based on synthetic proteins and peptides require the identification of relevant antigens and their epitopes. Unfortunately, the number of described immunogenic TAAs is small, even for melanoma which is the best-defined type of tumour in this respect. Once chosen, it is assumed but not guaranteed that these proteins or peptides will be the ones best recognised by the immune system of a certain patient. Peptides also have the disadvantage of MHC-

restriction, meaning that each peptide binds to molecules of only one specific HLA allotype, thereby restricting immunotherapy to patients whose haplotypes include the allotype in question.

By using total tumour preparations, DCs can be engineered to present a full spectrum of epitopes from different TAAs, even when the identities of the antigens are not known. Such approaches include loading of DCs with peptides eluted from tumour cells (Herr W *et al.* 2000), pulsing DCs with tumour lysates (Schott M *et al.* 2000) and fusing DCs and tumour cells into tumour-DC hybrids (Kugler A 2000). However, these methods are highly dependent on the amount of tumour tissue available. The problem of limited tumour material can be overcome by using TAAs in the form of nucleic acids, DNA or RNA, because they can be easily amplified in PCR. Most importantly, if nucleic acids are transfected into DCs, all the critical decisions are not made by the scientists but are left to the DCs themselves. DCs choose the antigen(s) and the epitope(s) for presentation by all available MHC class I and class II molecules.

Many viral and non-viral gene transfer technologies have been tested on DCs (Kirk CJ and Mulé JJ 2000). While viral vectors have high transduction efficiency (Jenne L *et al.* 2001), their clinical applicability may be hampered by safety issues involving viral proteins that might be co-expressed with tumour proteins. Furthermore, immunodominance may occur, whereby viral antigens mask or suppress the response to less potent tumour antigens. The consequence of this phenomenon may be that DCs expressing both viral and tumour antigens are eliminated by virus-specific CTLs before they can activate a tumour-specific response. Plasmid DNA transfer into DCs has not been very efficient (van Tendeloo VF *et al.* 1998).

Immunisation of mice with RNA was first described in 1995 (Conry RM *et al.* 1995). Shortly after, the first successful attempts to load DCs with tumour antigens in the form of RNA and prime T-cells with RNA-transfected DCs were described by the Gilboa group (Boczkowski D *et al.* 1996). Even though RNA molecules are very unstable and, therefore, difficult to work with, RNA transfection into DCs may be advantageous over DNA in several respects. A single cell is sufficient for the establishment of a cDNA library. Subsequent amplification of the total cellular antigenic repertoire in the form of DNA is feasible but complicated cloning steps have to be performed. RNA can also be

isolated from a few tumour cells. The total cellular mRNA amplification technology developed by Boczkowski and colleagues is simple and yields unlimited amounts of biologically functional RNA (Boczkowski D *et al.* 2000). As opposed to transfected DNA, which has to be transcribed following entry into the nucleus of DCs, RNA only has to reach the cytoplasm where it is directly translated into protein. Whereas the half-life of stable mRNA species in mammalian cells is less than 24 hr, unintegrated DNA can persist and function in non-dividing cells for months. Vaccination with total tumour-derived antigens in the form of DNA is, therefore, of greater concern when tumour antigens involved in tumourigenesis, such as the products the human papilloma virus *E6* or *E7* genes, are introduced into the DCs. Finally, if cDNA encoding individual TAAs is available, corresponding cRNA can be synthesised by *in vitro* transcription. Multiple cRNA species can easily be transfected into the target cell, leading to the translation of several different gene products within the same cell. In contrast, only one or a few copies of a DNA vector are usually incorporated into each cell, thereby limiting expression to only a few proteins within each DC. Whereas additional cloning steps are required with DNA, the RNA technology makes it possible to simply add additional RNA species into the mixture in order to include a desired antigen in the repertoire of antigens to be presented by transfected DCs.

The immune system has learned to deal with self-specific T-cells that were activated during infection. Nevertheless, immunotherapy using effective and repeated vaccinations is capable of activating more autoreactive T-cells than the immune system has evolved to tolerate. Depending on the immunotherapeutic approach, other self-antigens are likely to be presented alongside TAAs, most of which are self-antigens themselves. Therefore, by trying to manipulate the immune system into specifically recognising and killing tumour cells, the thin line between breaking tolerance and inducing autoimmune disease can be easily crossed.

1.8 Melanoma model

In recent decades, melanoma incidence and mortality rates have been steadily and markedly increasing, particularly among Caucasian populations. Most melanomas are thought to be caused by intermittent, not chronic, exposure to UV radiation, especially

during childhood. Nevertheless, exposure in adulthood certainly also plays a role. In older people, melanomas appear to be more related to chronic exposure. This is suggested by the body site distribution of melanomas in the elderly, with more melanomas on chronically exposed body sites (de Vries E *et al.* 2003). In Europe, the highest melanoma incidence rates have been reported in Scandinavia (about 15 cases per 1×10^5 inhabitants and year) and the lowest in the Mediterranean countries (about 5-7 cases per 1×10^5 inhabitants and year). In comparison, both the United States (10-20 cases per 1×10^5 inhabitants and year) and Australia (40-60 cases per 1×10^5 inhabitants and year) have higher incidence rates (Garbe C and Blum A 2001). In 90% of patients with early-stage disease, melanoma is curable with surgery alone. However, the prognosis for patients with more advanced disease involving regional lymph nodes or distant metastases is poor, with median survival rates of 24 and 6 months, respectively (Kim CJ *et al.* 2002). In its metastatic stage, melanoma is highly resistant to traditional forms of therapy (e.g. surgery, radiation and chemotherapy) and causes substantial mortality (Helmbach H *et al.* 2001). Therefore, clinicians have been more inclined to explore novel approaches, including immunotherapy.

Adoptive transfer of TILs in combination with IL-2 resulted in tumour regressions in approximately 30% of melanoma patients (Rosenberg SA 1992), suggesting that the immune system can play a critical role in the elimination of malignant cells. To further understand the molecular nature of the observed immune responses, much effort has been devoted to the characterisation of melanoma-associated antigens (MAAs) with the help of T-cells displaying *in vitro* reactivity against melanoma cells. Since melanoma is easily adapted for laboratory tissue culture, in contrast to most other human cancers, many melanoma cell lines were established and used in mixed lymphocyte tumour cell cultures. As a result, a wide array of different MAAs have been molecularly identified, which are specifically recognised on tumour cells by CTLs in association with MHC class I molecules (Boon T and van der Bruggen P 1996). Even though there is no direct evidence that melanoma is more immunogenic than other tumours, identification of these antigens has made melanoma the most informative model for understanding cancer immunity.

Given the fact that cancer arises from the host's own tissues, it is no surprise that the large majority of TAAs characterised to date are unaltered self-antigens well known to the immune system. In rare cases, mutations can create alterations in individual amino acids

or *de novo* open reading frames yielding new antigens. The functional genome of melanoma cells almost completely reflects the genes expressed by normal melanocytes at the same stage of differentiation and similar physiologic context, i.e. proliferation. As shown in Table 1.2, antigens associated with melanoma are divided into three main groups: cancer-testis antigens, melanocyte differentiation antigens and melanoma-specific antigens (reviewed in Kirkin AF *et al.* 1998, Turk MJ *et al.* 2002, Ramirez-Montagut T *et al.* 2003).

Table 1.2 Melanoma-associated antigens.

Cancer-testis antigens	Melanocyte differentiation antigens	Melanoma-specific antigens (mutated)
MAGE	tyrosinase	CDK4
GAGE	Melan-A (MART-1)	β -catenin
BAGE	gp100 (pmel17)	CDC27
RAGE	TRP-1 (gp75)	GnT-V
PRAME	TRP-2 (DCT)	LDLR
P15		gp100 (pmel17)
NY-ESO-1 (CAG3)		
LAGE (CAMEL)		

Abbreviations: CAMEL (CTL-recognised antigen on melanoma), CDC27 (cell division control 27), CDK4 (cyclin-dependent kinase 4), GnT-V (beta 1,6-N-acetylglucosaminyltransferase V), gp (glycoprotein), LDLR (low density lipoprotein receptor), MAGE (melanoma antigen gene), Melan-A (melanoma antigen A), MART-1 (melanoma antigen recognised by T-cells 1), PRAME (preferentially expressed antigen of melanoma).

The cancer-testis group of antigens represents proteins expressed in several different tumours, including melanoma, but not in normal tissues except for testes. This appears to be due to demethylation of the genes in testes and cancer cells. Since germ cells in testes do not express MHC class I molecules and have no direct contact with the cells of the immune system, vaccination against these antigens should cause no side-effects, i.e. autoimmunity. MAGE-1 (melanoma antigen gene) was the first ever tumour-derived (melanoma) human gene product to be identified as a CTL target (van der Bruggen P *et al.* 1991). Since then, many cancer-testis antigens and their epitopes have been identified, including members of the MAGE, GAGE and BAGE families. NY-ESO-1 has both class I and class II-restricted epitopes and is one of the most immunogenic TAAs, described to date.

A differentiation antigen is an antigen expressed by both cancer cells and their normal cell counterparts. Such antigens are structurally or functionally associated with a particular point in cell differentiation and they are usually found at relatively low concentrations on a small subset of normal cells. In the case of cancer, differentiation antigens are good potential targets for the immune system based on clonal expansion of the tumour and its abnormal differentiation. Differentiation antigens relevant to anti-melanoma immunity are proteins required for melanin synthesis in cellular compartments called melanosomes. This is why they are called melanocyte differentiation antigens. These antigens are normally expressed in melanocytes in the skin and retinal epithelium in the eye. They include tyrosinase, tyrosinase-related protein 1 (TRP-1), tyrosinase-related protein 2 (TRP-2) and gp100. Tyrosinase is the rate-limiting enzyme, which catalyses two initial steps of the melanin biosynthetic pathway. TRP-1 stabilises tyrosinase, TRP-2 is a tautomerase and gp100 is involved in melanin polymerisation (Prota G *et al.* 2000). Melan-A is also a differentiation antigen with melanosomal localisation, but its function is currently unknown (de Mazière AM 2002).

The process of carcinogenesis is thought to involve accumulation of mutations that act collectively to transform normal cells into malignant cells. These mutations, in addition to being oncogenic, may be immunogenic by creating completely new antigenic epitopes or by enhancing the binding of poorly reactive or non-reactive epitopes to MHC molecules, TCRs or antibodies. Changes in the genes for CDK4 (cyclin-dependent kinase 4), β -catenin, CDC27 (cell division control 27) and triosephosphate isomerase are among the few examples of mutations that also encode potentially immunogenic epitopes in melanoma. Since they are altered, these antigens are no longer self-antigens but can be classified as unique tumour antigens. In the case of melanoma, they are called melanoma-specific antigens. If an immune response is mounted against any of these molecules, only malignant cells are targeted and, therefore, damage to normal tissue is unlikely. The problem with these mutated proteins as targets for vaccination strategies is that, in most cases, the site of the mutation or rearrangement tends to vary among patients, which results in the generation of antigenic epitopes restricted to a few individuals. In the case of the CDK4 antigen, the particular mutation, an arginine (R) to cysteine (C) exchange at residue 24, was found in only 5% of tested melanomas (Wölfel T *et al.* 1995). The CDK4 protein is a cell-cycle activator that propagates progression through the G1 phase of the cell cycle.

Its mutated form, CDK4-R24C is resistant to inhibition by the cell-cycle inhibitor p16/INK4 α (Vax VV *et al.* 2003).

1.9 Aims of the study

The goal of this work was to find optimal conditions for producing a DC-based vaccine for cancer patients using tumour antigens in the form of RNA. As explained above, there are three main advantages to pulsing DCs with RNA. Even if only a small amount of tumour tissue is available, isolated RNA can easily be amplified in reverse transcription PCR (RT-PCR). By using tumour RNA, the identities of TAAs and their T-cell epitopes do not have to be known, but one can count on the fact that messages encoding these antigens are part of the total cellular RNA pool. The DC, not the scientist, chooses the antigen(s) and, depending on its MHC repertoire, decides which epitope(s) will be presented.

T-cell priming based on *in vitro* RNA-pulsed DCs was first described in 1996 (Boczkowski D *et al.* 1996). Since then, most publications have concentrated on clinical applications, without further exploring cellular events following RNA entry into the DC that precede antigen presentation on its surface. Published protocols for RNA transfection into DCs have used different forms of RNA: total cellular tumour RNA, amplified total cellular tumour mRNA and single-species tumour-antigen cRNA. A wide range of RNA concentrations have been applied either by lipofection, electroporation or through simple DC co-incubation with naked RNA. No agreement has been reached on how much and what kind of RNA should be used and how this RNA should be brought into the DCs. Therefore, my studies were designed to quantitate RNA transfer into DCs, to determine intracellular stability of transfected RNA in DCs and to analyse the kinetics of protein expression and the generation of functional pMHC ligands that can activate effector memory CTLs. Simultaneous activation of CTLs with specificities for different antigens minimises the potential for tumour escape through immune selection of tumour variants showing loss of individual antigens. Thus, generation of multiplex pMHC ligands for CTLs may improve clinical efficiency. On the other hand, peptide competition for MHC molecules within the DC may limit pMHC ligand generation. This central immunological question was addressed by comparing DCs loaded with total cellular tumour RNA, amplified total cellular tumour mRNA and pools of defined single-species tumour-antigen

cRNAs versus individual single-species tumour-antigen cRNAs for their capacity to display various pMHC ligands and activate CTLs of corresponding specificities.

RNA encoding the enhanced green fluorescence protein (EGFP), an antigen not associated with tumours, was used to determine the optimal conditions for RNA transfection into DCs using a simple read-out system of flow cytometry. Subsequent work was based on melanoma using a more complicated analysis of effector CTL function. This tumour model was chosen as the most suitable because it is well characterised at both the cellular and the molecular levels. The CTL stimulatory capacity of DCs pulsed with RNA was first investigated using one MAA, tyrosinase. An RNA mixture of three antigens, tyrosinase, Melan-A and CDK4-R24C, was compared with total cellular melanoma RNA for processing and presentation to antigen-specific CTLs to evaluate the role of antigen competition at the level of pMHC generation.

2. Materials

2.1 Instruments and other equipment

Bacteria shaker <i>Certomat H</i>	B. Braun Biotech Int.
Balance <i>BP 2100</i>	Sartorius
Balance (analytical) <i>MCI</i>	Sartorius
Cooling block (for LightCycler®)	Roche
Cell counting chamber <i>Neubauer</i>	Brand
Centrifuge <i>Megafuge 2.0</i>	Heraeus
Centrifuge <i>5417R</i>	Eppendorf
Controlled-freezing box	Nalgene
Electrophoresis chamber	Invitrogen
Electroporator <i>Gene Pulser Xcell™</i>	Bio-Rad
ELISA reader <i>E max</i>	Molecular Devices
Flow cytometer <i>FACSCalibur™</i>	Becton Dickinson
Freezer (-20°C) <i>Premium</i>	Liebherr
Freezer (-80°C) <i>HFU86</i>	Heraeus
Fridge (4°C)	Bosch
Gel scanner <i>Fluor-S™ MultiImager</i>	Bio-Rad
Heating block <i>Thermomixer Comfort</i>	Eppendorf
Incubator (human cells)	Heraeus
Incubator (bacteria)	Memmert
Irradiation chamber <i>Gammacell 40</i>	Atomic Energy
Liquid nitrogen tank <i>Chronos Biosafe</i>	Messer Griesheim
Multichannel pipettes (5-50 µL, 25-200 µL)	Dunn Labor Technik
Micropipettes (0.5-10 µL, 10-100 µL, 20-200 µL, 100-1000 µL)	Eppendorf
Microscope <i>Leica DMIL</i>	Leica
Microscope (fluorescence) <i>Axiovert 10</i> with camera	Zeiss
Microwave oven <i>Micromat</i>	AEG
Pipetting assistant <i>Easypet</i>	Eppendorf
Spectrophotometer <i>GeneQuant II</i>	Amersham Biosciences
Sterile bench	Heraeus
Thermocycler <i>LightCycler®</i>	Roche
Thermocycler <i>PTC-200</i>	MJ Research

Vortexer	Bender & Hobein
Water bath <i>SUB</i>	Julabo
Water purification system <i>Easypure RF</i>	Barnstead
Vacuum manifold for plasmid preps <i>QIAvac® 6S</i>	Qiagen

2.2 Commonly used material

Cryovials	Nunc
Capillaries (for LightCycler®)	Roche
ELISA plates <i>Immuno F96 Maxi-Sorp</i>	Nunc
Filters for cells <i>Cellstrainer</i>	Falcon
Filters for solutions (0.2 µm and 0.8 µm)	Schleicher und Schüll
Flasks for cell culture (75 cm ² and 175 cm ²)	Falcon
Gloves (nitrile)	Semperit
Pasteur pipettes	Peske OHG
Petri dishes	Falcon
Pipettes (2, 5, 10 and 25 mL)	Falcon
Pipette tips (10, 200 and 1000 µL)	Greiner
Pipette tips (10, 200 and 1000 µL with a filter)	Biozym
Plates for cell culture (6-well, 24-well and 96-well)	TPP
Scalpels (Nr. 20)	Feather
Tubes for cell culture (polystyrene, 15 mL)	Falcon
Tubes for cell culture (polypropylene, 15 mL and 50 mL)	Falcon
Tubes for molecular biology (0.5 mL)	Starlab
Tubes for molecular biology <i>Safelock</i> (1.5 mL and 2 mL)	Eppendorf
Tubes for FACS™ (1.2 mL)	Peske OHG
Tubes for FACS™ (5 mL)	Falcon

2.3 Chemicals and biological reagents

0.24-95 Kb RNA Ladder	Invitrogen
Agar	Sigma

Agarose	Invitrogen
AIM V medium	Invitrogen
Ampicillin	Merck
β -mercaptoethanol	Sigma
Blue Juice Gel Loading Buffer	Invitrogen
Chloroform	Merck
Carbonate-bicarbonate buffer capsules	Sigma
DEPC (diethyl pyrocarbonate)	Sigma
DMSO (dimethyl sulfoxide)	Merck
Ethidium bromide	Bio-Rad
Ethanol	Merck
FACS™ Flow	Becton Dickinson
FACS™ Rinse	Becton Dickinson
FACS™ Safe	Becton Dickinson
Ficoll	Biochrom
FBS (fetal bovine serum)	Invitrogen
Formamide	Invitrogen
HEPES	Invitrogen
Glycerol	Merck
GM-CSF (granulocyte macrophage colony stimulating factor)	Essex Pharma
HS (human serum)	LTI
IL-1 β (interleukin 1 β)	R&D Systems
IL-2 (interleukin 2)	R&D Systems
IL-4 (interleukin 4)	R&D Systems
IL-6 (interleukin 6)	R&D Systems
Isopropanol	Sigma
LB Broth Base	Invitrogen
L-glutamine	Invitrogen
MEM	Invitrogen
One Shot TOP10F' competent cells	Invitrogen
OptiMEM I medium	Invitrogen
Ortho-phosphoric acid	Merck
PBS (phosphate buffered saline)	Cell Concepts
Peptone	Invitrogen

Penicillin/streptomycin	Invitrogen
PGE ₂ (prostaglandin E2)	Sigma
PstI restriction enzyme	Roche
Ready-Load 1 Kb DNA Ladder	Invitrogen
RNase A (ribonuclease A)	Roche
RPMI 1640 medium	Invitrogen
Sodium chloride	Merck
Sodium pyruvate	Invitrogen
SpeI restriction enzyme	New England BioLabs
Substrate Reagents A and B	Becton Dickinson
TAE (tris acetate EDTA) buffer	Invitrogen
TBE (tris borate EDTA) buffer	Ambion
TransFast™	Promega
Tri Reagent	Sigma
Trypan blue	Sigma
Trypsin/EDTA	Invitrogen
Tween 20	Merck
TNF- α (tumour necrosis factor α)	R&D Systems
XbaI restriction enzyme	Fermentas
X-vivo 15 medium	Biowhittaker
Yeast extract	Invitrogen
Yeast tRNA	Roche
Zeocin	Invitrogen

2.4 Kits

1st Strand cDNA Synthesis Kit for RT-PCR (AMV)	Roche
Advantage® 2 PCR Enzyme System	Becton Dickinson
Fix&Perm Cell Permeabilisation Kit	An der Grub
LightCycler® – FastStart DNA Master SYBR Green I	Roche
LightCycler® – Primer Set for Human Tyrosinase	Search LC
mMESSAGE mMACHINE™ T7	Ambion
OptEIA™ Human IFN- γ Set	Becton Dickinson

Poly(A) Tailing Kit	Ambion
QIAquick® PCR Purification Kit	Qiagen
QIAwell® 8 Ultra Plasmid Kit	Qiagen
RNeasy® Mini Kit	Qiagen
SMART™ PCR cDNA Synthesis Kit	Becton Dickinson

2.5 Cell culture media and solutions

Standard tumour medium:

500 mL	RPMI 1640	
50 mL	FBS	= 10%
5 mL	MEM (100×)	= 1×
5 mL	L-glutamine (200 mM)	= 2 mM
5 mL	Sodium-pyruvate (100 mM)	= 1 mM

RPMI III:

500 mL	RPMI 1640	
5 mL	L-glutamine (200 mM)	= 2 mM
5 mL	Na-pyruvate (100 mM)	= 1 mM
5 mL	Pen/Strep (10 ⁴ U/mL)	= 100 U/mL

AIMV III:

500 mL	AIM V	
5 mL	L-glutamine (200 mM)	= 2 mM
5 mL	Na-pyruvate (100 mM)	= 1 mM
5 mL	Pen/Strep (10 ⁴ U/mL)	= 100 U/mL

CTL co-incubation medium:

16 mL	RPMI III	
4 mL	HS or autologous plasma	= 20%
8 µL	IL-2 (100 U/mL)	= 40 U/mL

B-cell medium:

45 mL	RPMI III	
5 mL	FBS	= 10%

Trypsin/EDTA 2×:

20 mL	PBS	
5 mL	Trypsine-EDTA (10×)	= 2×

DMSO 20%:

40 mL	RPMI III	
10 mL	DMSO	= 20%

Freezing Medium:

½	FBS	
½	DMSO 20%	= 10%

Dendritic cell medium:

250 mL	X-Vivo 15	
2.5 mL	L-glutamine (200 mM)	= 2 mM
2.5 mL	Pen/Strep (10 ⁴ U/mL)	= 100 U/mL

FACS™ Buffer:

49 mL	PBS	
1 mL	FBS	= 2%

DEPC water:

400 mL	double distilled water	
400 µL	DEPC	= 0.1%

2.6 Cells

Name	Description	Source	Reference
11/33 CTL	monoclonal CTL line; HLA-A*0201-restricted; specific for the Melan-A ₂₆₋₃₅ epitope	Wölfel T	Wölfel T <i>et al.</i> 1993
14/35 CTL	monoclonal CTL line; HLA-A*0201-restricted; specific for the CDK4-R24C ₂₃₋₃₂ epitope	Wölfel T	Wölfel T <i>et al.</i> 1995
624.38 MEL	melanoma cell line; HLA-A2-positive; CDK4-R24C-negative	Panelli MC	Rivoltini <i>et al.</i> 1995
A375 MEL	melanoma cell line; HLA-A2-positive; tyrosinase, Melan-A and CDK4-R24C-negative	ATCC (CRL-1619)	
A42 CTL	monoclonal CTL line; HLA-A*0201-restricted; specific for the Melan-A ₂₆₋₃₅ epitope	Panelli MC	Kawakami Y <i>et al.</i> 1994
AK-EBV-B	Epstein-Barr virus transformed lymphoblastoid cell line established from a healthy donor	Wölfel T	Wölfel T <i>et al.</i> 1994
DC	differentiated from monocytes of the healthy HLA-A*0201-positive blood donor PH	generated in the lab	
IL-2 MEL	93.04A12 melanoma cell line; HLA-A2-positive; CDK4-R24C-negative; stable IL-2 transfectant	Schrier P	
IVS B CTL	polyclonal CTL line; HLA-A*0201-restricted; specific for the tyrosinase ₃₆₉₋₃₇₇ epitope	Wölfel T	Wölfel T <i>et al.</i> 1993
LAZ388	Epstein-Barr virus transformed lymphoblastoid cell line	Schrier P	
RCC26	human renal cell carcinoma cell line; HLA-A2-positive	Schendel DJ	Schendel DJ <i>et al.</i> 1993
SK23 MEL	human melanoma cell line; HLA-A2-positive	Panelli MC	
SK29 MEL	human melanoma cell line; HLA-A2-positive; heterozygous for CDK4-R24C	Wölfel T	Wölfel T <i>et al.</i> 1994a
T2	hybrid of a T and a B lymphoblastoid cell line; TAP-deficient	Panelli MC	Salter RD <i>et al.</i> 1985
TyrF8 CTL	monoclonal CTL line; HLA-A*0201-restricted; specific for the tyrosinase ₃₆₉₋₃₇₇ epitope	Schrier P	MJ Visseren <i>et al.</i> 1995

2.7 Antibodies

Specificity	Clone	Isotype	Conjugation	Application	Manufacturer
CD1a	HI 149	IgG ₁	PE	primary	Becton Dickinson
CD11c	B-ly6	IgG ₁	PE	primary	Becton Dickinson
CD14	RM052	IgG _{2a}	FITC	primary	Beckman Coulter
CD40	5C3	IgG ₁	PE	primary	Becton Dickinson
CD80	L307.4	IgG ₁	FITC	primary	Becton Dickinson
	MAB104	IgG ₁	PE	primary	Beckman Coulter

CD83	HB15e	IgG ₁	PE	primary	Becton Dickinson
CD86	FUN-1	IgG ₁	PE	primary	Becton Dickinson
CD206	19	IgG ₁	PE	primary	Becton Dickinson
mouse IgG + IgM		F(ab') ₂	FITC	secondary	Dianova
HLA-A,B,C	G46-2.6	IgG ₁	FITC	primary	Becton Dickinson
HLA-DR	Immu-357	IgG ₁	PE	primary	Beckman Coulter
HLA-DP,DQ,DR	TÜ39	IgG _{2a}	FITC	primary	Becton Dickinson
isotype control IgG₁	X40	IgG ₁	FITC and PE	primary	Becton Dickinson
isotype control IgG_{2a}	G155-178	IgG _{2a}	FITC	primary	Becton Dickinson
Melan-A	A103	IgG ₁	none	primary	Dako Cytomation

All anti-human antibodies originate from a mouse. Anti-mouse IgG and IgM F(ab')₂ fragments originate from a goat.

2.8 Molecular biology media, buffers and gels

LB medium:

10 g Peptone
 5 g Yeast extract
 10 g (5 g) Sodium chloride (low salt)
 ad 1 L Distilled water

LB agar medium:

10 g LB Broth Base
 7.5 g Agar
 ad 500 mL Distilled water

DNA electrophoresis gel:

27 mL Distilled water
 3 mL TAE buffer (10×) = 1×
 0.36 g agarose = 1.2%

DNA electrophoresis running buffer:

180 mL	Distilled water	
20 mL	TAE buffer (10×)	= 1×
8 µL	Ethidium bromide (10 µg/µL)	= 0.4 µg/mL

RNA electrophoresis gel:

27 mL	DEPC water	
3 mL	TBE buffer (10×)	= 1×
0.36 g	agarose	= 1.2%

RNA electrophoresis running buffer:

180 mL	DEPC water	
20 mL	TAE buffer (10×)	= 1×
8 µL	Ethidium bromide (10 µg/µL)	= 0.4 µg/mL

2.9 Plasmids

Plasmid	cDNA insert	resistance	source
pcDNAI/Amp/Aa1.2	Melan-A	ampicillin	Wölfel T
pcDNAI/Amp/C11.1	CDK4-R24C	ampicillin	Wölfel T
pGEM4Z/GFP/A64	EGFP	ampicillin	Su Z
pZeoSV2+/huTyr	tyrosinase	zeocin	Sutter G

2.10 Peptides

Epitope	Peptide sequence
CDK4-R24C ₂₃₋₃₂	ACDPHSGHFV
influenza matrix protein ₅₈₋₆₆	GILGFVTL
Melan-A ₂₆₋₃₅	ELAGIGILTV
tyrosinase ₃₆₉₋₃₇₇	YMNGTMSQV and YMDGTMSQV

All peptides were synthesised at the Genzentrum.

2.11 Primers

Sequence specificity	Primers	Sequence	PCR product size	Application
α-enolase	forward	5' GTTAGCAAGAACTGAACGTCACA 3'	619 bp	real-time PCR
	reverse	5' TGAAGGACTTGTACAGGTCAG 3'		
total cellular mRNA	forward	5' TAATACGACTCACTATAGGGAGG AAGCAGTGGTAACAACGCAGAGT 3'	depends on mRNA size	total cellular mRNA amplification
	reverse	5' AAGCAGTGGTAACAACGCAGAGT 3'		
CDK4	forward	5' CGATATGAGCCAGTGGCTG 3'	134 bp	real-time PCR
	reverse	3' AGGCCTCCTCCACCTCCT 3'		
EGFP	forward	5' GCTACCCCGACCACATGAAG 3'	485 bp	real-time PCR
	reverse	5' GTCCATGCCGAGAGTGATCC 3'		
Melan-A	forward	5' ACTGCTCATCGGCTGTTG 3'	267 bp	real-time PCR
	reverse	5' CACCTGAGACATGCTGA 3'		
tyrosinase	forward	not defined	not defined	real-time PCR
	reverse	not defined		

All primers were synthesised at the Genzentrum except for tyrosinase primers which were part of the LightCycler® – Primer Set for Human Tyrosinase.

2.12 List of manufacturers and persons

AEG	Nürnberg, Germany
Ambion	Austin, Texas, USA
Amersham Biosciences	Piscataway, New Jersey, USA
An der Grub	Kaumberg, Austria
ATCC	Rockyville, Maryland, USA
Atomic Energy	Ottawa, Ontario, Canada
Barnstead	Dubuque, Iowa, USA
B. Braun Biotech Int.	Melsungen, Germany
Beckman Coulter	Palo Alto, California, USA
Becton Dickinson	Jersey City, New Jersey, USA
Bender & Hobein	Ismaning, Germany
Biochrom	Berlin, Germany
Bio-Rad	Richmond, California, USA
Biowhittaker	East Rutherford, New Jersey, USA

Biozym	Hess. Olendorf, Germany
Cell Concepts	Umkirch, Germany
Dako Cytomation	Glostrup, Denmark
Dianova	Hamburg, Germany
Dunn Labortechnik	Asbach, Germany
Eppendorf	Hamburg, Germany
Essex Pharma	München, Germany
Falcon	Oxnard, California, USA
Fermentas	Leon-Rot, Germany
Genzentrum	Martinsried, Germany
Greiner	Nürtingen, Germany
Heraeus	Hanau, Germany
Invitrogen	Karlsruhe, Germany
Julabo	Seelbach, Germany
Leica	Wetzlar, Germany
Liebherr	Bierbach an der Riss, Germany
Memmert	Schwabach, Germany
Merck	Darmstadt, Germany
Messer Griesheim	Krefeld, Germany
MJ Research	Watertown, Massachusetts, USA
Molecular Devices	Sunnyvale, California, USA
Nalgene	Rochester, New York, USA
New England BioLabs	Frankfurt am Main, Germany
Nunc	Naperville, USA
Panelli MC*	National Institutes of Health, Bethesda, Maryland, USA
Peske OHG	München, Germany
Promega	Madison, Wisconsin, USA
Qiagen	Chatsworth, California, USA
R&D Systems	Minneapolis, Minnesota, USA
Roche	Mannheim, Germany
Sartorius	Göttingen, Germany
Schendel DJ*	Institute of Molecular Immunology, GSF, München, Germany

Schleicher und Schüll	Dassel, Germany
Schrier P*	Leiden University Medical Center, Leiden, The Netherlands
Search LC	Heidelberg, Germany
Semperit	Wien, Austria
Sigma	St. Louis, Missouri, USA
Starlab	Ahrensburg, Germany
Sutter G*	Technical University, München, Germany
Su Z*	Duke University Medical Center, Durham, North Carolina, USA
TPP	Trasadingen, Switzerland
Wölfel T*	Johannes Gutenberg-University, Mainz, Germany
Zeiss	Jena, Germany

* These individuals are thanked for kindly providing cells and plasmids listed above.

3. Methods

3.1 Cell culture

3.1.1 Cell counting

The cell count and viability was assessed by trypan blue exclusion. Live cells did not take up the trypan blue. The cell suspension was diluted 1:10 with trypan blue by adding 10 μL of the cell suspension to 90 μL of trypan blue in a well of a 96-well plate. A Neubauer counting chamber was filled with the trypan blue-diluted cell suspension using a pipette and capillary action. Care was taken not to over or underfill the chamber. Using an inverted microscope, the number of viable (unstained) cells in the four corner squares was counted. Either the cells touching the top and left of the ruled squares or those touching the bottom and right were counted, but not both. Formulas used to calculate cell concentrations and total cell numbers are shown in Figure 3.1.

$$\text{cell concentration} = \frac{\text{average number of cells per square} \times 10^5}{10^6} \times 10^6 / \text{mL}$$
$$\text{total cell number} = \text{cell concentration} \times \text{volume of cell suspension}$$

Figure 3.1 Formulas used to calculate cell concentrations and total cell numbers.

3.1.2 Cryopreservation of cells

Tumour cell lines and CTL clones were frozen at concentrations between 2×10^6 and $5 \times 10^6 / \text{mL}$ in 1 mL volumes. Peripheral blood mononuclear cells (PBMCs) were frozen at $40 \times 10^6 / \text{mL}$ in 1.5 mL volumes. Pelleted cells were first resuspended in an appropriate volume of FBS. The same volume of pre-cooled 20% DMSO was then gradually added to the cell suspension. After thorough mixing, 1 mL or 1.5 mL aliquots of the cell suspension were transferred into pre-cooled cryovials. The cryovials were placed into controlled-freezing boxes and stored at -80°C overnight. The following day, the cryovials were transferred into the liquid nitrogen freezer for long-term storage at -196°C .

3.1.3 Thawing of cryopreserved cells

The thawing medium used was FBS. The cryovials were retrieved from the liquid nitrogen freezer and thawed rapidly in a water bath at 37°C. As soon as only a small ice crystal was seen floating inside the cryovial, the contents of a vial were transferred into a 15 mL Falcon tube containing 1 mL of FBS. Additional 2 mL of FBS were slowly added in a drop-wise manner with continual mixing. The tube was immediately centrifuged at 540×g for 5 min. Pelleted cells were then resuspended in the corresponding culture medium pre-warmed to 37°C.

3.1.4 Culture of adherent tumour cell lines

SK23 MEL, SK29 MEL, IL-2 MEL, 624.38 MEL, IL-2 MEL, A375 MEL and RCC26 tumour cell lines were cultured in the standard tumour medium. Volume of the medium in a middle-sized culture flask (75 cm² adherence surface) was 10 mL. Volume of the medium in a large-sized flask (175 cm² adherence surface) was 25 mL. Approximately every 3-4 days cells grew to confluence. At that time point, their medium was exchanged and they were split 1:2 to 1:10, depending on the growth rate of individual cell lines. The medium was removed, cells were washed once with warm PBS and then incubated with 1 mL (middle-sized flask) or 2 mL (large-sized flask) trypsin/EDTA 2× for 3 min at room temperature. Detached cells were resuspended in fresh standard tumour medium and distributed in new culture flasks.

3.1.5 Culture of suspension tumour cell lines

LAZ388, AK-EBV-B and T2 tumour cell lines were cultured in the B-cell medium. Volume of the medium was 20 mL in a middle-sized culture flask. Approximately every 4 days, $\frac{3}{4}$ of the cell suspension were removed and the same volume of fresh medium was added.

3.1.6 CTL restimulation and culture

All CTL clones were first expanded in restimulation cultures. Large stocks were aliquoted and frozen. Each time they were needed for an experiment, CTLs were taken from the same stock, thawed, placed into wells of a 24-well plate and restimulated according to one of the following standardised protocols.

For restimulation, thawed TyrF8 CTLs (5×10^5 per well) were mixed with IL-2 MEL cells as stimulators (irradiated with 1×10^4 rad, 8×10^4 cells per well), LAZ388 cells as feeders (irradiated with 1.5×10^4 rad, 1×10^5 cells per well) and PBMCs pooled from several donors as feeders (irradiated with 5×10^3 rad, 1.5×10^6 cells per well) in RPMI III medium (1.5 mL per well) supplemented with 7.5% human serum, 7.5% FBS and 100 U/mL IL-2. Half of the medium was substituted with fresh medium approximately every 2 days. During expansion, TyrF8 CTLs were restimulated every 2 weeks. They were harvested, counted and used for co-incubation experiments with DCs or tumour cells on days 7 or 14 after thawing and restimulation.

For restimulation, thawed IVS B, A42, 11/33 and 14/35 CTLs (5×10^5 per well) were mixed with SK 29 MEL cells as stimulators (irradiated with 1×10^4 rad, 1×10^5 cells per well) and AK-EBV-B cells as feeders (irradiated with 1×10^4 rad, 2×10^5 cells per well) in AIM V III medium (1.5 mL per well) supplemented with 10% human serum and 500 U/mL IL-2. Half of the medium was substituted with fresh medium, with the IL-2 concentration reduced to 250 U/mL, approximately every 2 days. During expansion IVS B, A42, 11/33 and 14/35 CTLs were restimulated once a week. They were harvested, counted and used for co-incubation experiments with DCs or tumour cells on day 7 after thawing and restimulation.

3.1.7 Isolation of PBMCs from a leukapheresis product

The leukapheresis product was diluted 1:2 with dilution medium pre-warmed to 37°C. Using a pipette, 30 mL of the diluted sample were carefully layered onto 20 mL of Ficoll in a 50 mL Falcon tubes. The tubes were centrifuged at $840 \times g$ for 30 min without brake. Using a Pasteur pipette, the white ring (composed of PBMCs) at the interface between the

Ficoll and plasma was removed and transferred into a cell culture flask. Isolated PBMCs were diluted 1:2 with warm dilution medium and aliquoted into 50 mL Falcon tubes. The tubes were centrifuged at 760×g for 10 min. Pelleted cells were resuspended in 50 mL of washing medium pre-warmed to 37°C. The following centrifugation programme was performed to separate cells from platelets: 75×g for 20 min, gradual increase of 15×g/min to 540×g, stop without a brake. Pelleted cells were again resuspended in 50 mL of warm washing medium and centrifuged at 540×g. Pelleted cells were then resuspended in FBS, counted and frozen according to the procedure described below.

3.1.8 DC generation and culture

A large stock of PBMCs from donor PH was obtained from a leukapheresis product by Ficoll density gradient centrifugation. These PBMCs were aliquoted and frozen. For each DC culture, PBMCs from the same stock were used. Thawed PBMCs were resuspended in RPMI 1640 medium supplemented with 1% autologous plasma at 5-10×10⁶ cells per 2 mL per well of a 6-well plate. The plates were incubated at 37°C and 5% CO₂ for 2 hr. Non-adherent cells were carefully washed away. Adhering monocytes were cultured in 2 mL per well of dendritic cell medium supplemented with 1% autologous plasma, 800 U/mL GM-CSF and 800 U/mL IL-4. After 3 days of culture, 800 U/mL GM-CSF and 800 U/mL IL-4 were added again. On day 6 of culture, immature DCs were harvested, counted and resuspended in fresh dendritic cell medium supplemented with 1% autologous plasma, 800 U/mL GM-CSF, 500 U/mL IL-4, 5 ng/mL IL-1 β , 9 ng/mL IL-6, 9 ng/mL TNF- α and 2 μ M PGE₂ at 0.5×10⁶ cells per 1 mL per well of a 24-well plate for maturation. Mature DCs were harvested on day 8 of culture.

3.2 Flow cytometry

Flow cytometry was used to measure the cellular expression of chosen molecules. These molecules either fluoresce themselves (e.g. EGFP) or they are specifically stained with monoclonal antibodies attached to fluorescent dyes. Flow cytometric analysis was performed in the fluorescence-activated cell sorter (FACS™). In the FACSCalibur™, the suspension of stained cells was forced through a nozzle, creating a fine stream of liquid

containing cells spaced singly at intervals. As each cell passed through a laser beam, it scattered the laser light and fluorescent molecules associated with the cell were excited. Sensitive photomultiplier tubes detected both the scattered light, which gave information about the size and granularity of the cell, and the fluorescence emissions, which gave information about the binding of the labelled monoclonal antibodies and, hence, the expression of targeted molecules by each cell.

3.2.1 Direct staining of cell-surface molecules

In order to measure the expression of cell-surface molecules CD14, CD1a, CD206, CD11c, CD83, CD40, CD80, CD86, HLA-A,B,C and HLA-DP,DQ,DR, specific monoclonal antibodies conjugated with FITC (fluorescein isothiocyanate) or PE (phycoerythrin) were used for the direct staining on the cell surface. Approximately 5×10^4 untransfected or EGFP cRNA-transfected DCs per well of a 96-well plate were washed twice. Each washing step included resuspension of cells in 150 μ L of FACS™ buffer, centrifugation at $300 \times g$ for 3 min and discarding of the supernatant. After washing, 3 μ L of each antibody were added separately to the pellets. After a 30 min incubation on ice and in the dark, cells were washed twice. Finally, cells were resuspended in 200 μ L of FACS™ buffer and flow cytometric analysis was performed.

3.2.2 Indirect staining of intracellular molecules

In order to measure the expression of Melan-A inside RNA-transfected DCs, cells were first fixed and permeabilised using Reagents A and B from the Fix&Perm Cell Permeabilisation Kit. Briefly, approximately 3×10^5 cells were placed into each well of a 96-well plate and washed twice. Each washing step included resuspension of cells in 200 μ L of PBS, centrifugation at $300 \times g$ for 3 min and discarding of supernatant. After washing, 50 μ L of Reagent A (fixation medium) were added to the pellet and mixed gently. After a 15 min incubation at room temperature, cells were washed twice. Subsequently, 50 μ L of Reagent B (permeabilisation medium) and 17 μ L of the Melan-A-specific primary antibody were added to the pellet and mixed gently. After a 15 min incubation at room temperature, cells were washed three times and then 20 μ L of the

FITC-conjugated secondary antibody specific for the primary antibody were added to the pellet and mixed gently. After a 20 min incubation at room temperature in the dark, the cells were washed three times. Finally, pelleted cells were resuspended in 200 μ L of PBS and flow cytometric analysis was performed.

In order to measure the expression of EGFP inside RNA-transfected DCs, no staining was necessary, since EGFP itself is a fluorescent molecule. DCs were washed twice with PBS, as described above. Pellets were resuspended in 200 μ L of PBS and flow cytometric analysis was performed.

3.3 Production of amplified total cellular mRNA

In transfection experiments described below, either total cellular tumour RNA was used or amplified total cellular mRNA. The unspecific amplification procedure included five steps: reverse transcription of mRNA into cDNA, amplification of cDNA in PCR, purification of amplified cDNA, *in vitro* transcription of amplified cDNA into cRNA and cRNA purification (Figure 3.2).

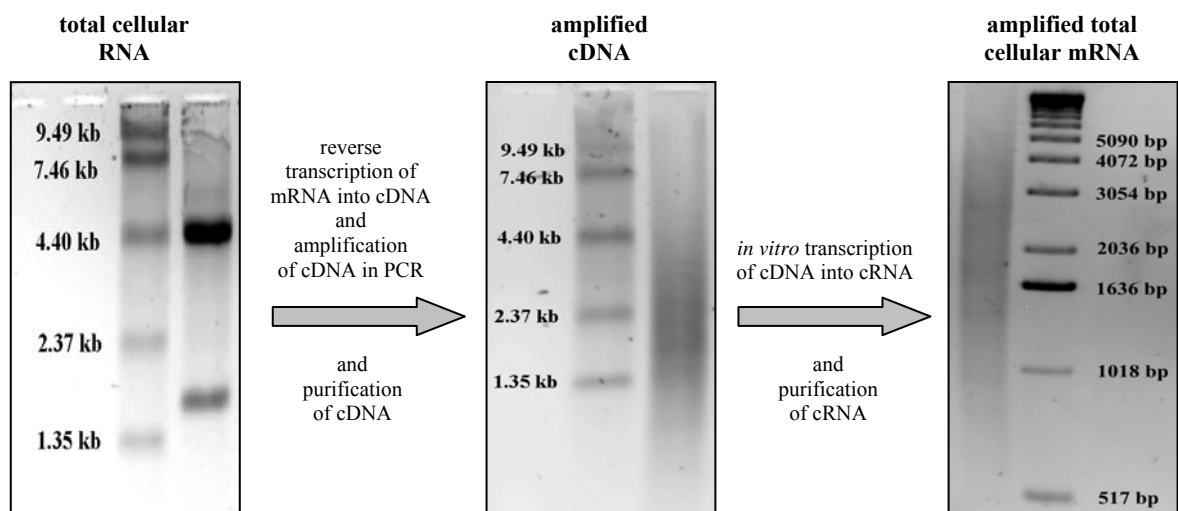


Figure 3.2 The principle of total cellular mRNA amplification. On the left agarose gel electrophoresis picture, total cellular RNA isolated from 624.38 MEL melanoma cells is shown. The thicker upper band (5 kb) corresponds to 28S rRNA and the lower thinner band (1.9 kb) to 18S rRNA. The existence of these two bands and the 2-fold higher amount of 28S rRNA, compared to 18S rRNA, indicate that the integrity of RNA was not compromised by the isolation procedure. Only mRNA contained in the total cellular sample was reverse transcribed into cDNA. On the middle picture, a smear of different cellular cDNA species after amplification and purification is shown. This cDNA was *in vitro* transcribed into cRNA. On the right picture, a smear of different cellular cRNA species after purification i.e. amplified total cellular mRNA is shown.

3.3.1 Total cellular RNA isolation from tumour cells

Total cellular RNA was isolated from tumour cells using the RNeasy® Mini Kit. The isolation procedure was performed with up to 10×10^6 cells per column according to manufacturer's instructions. Cellular plasma membranes and organelles were first disrupted by vortexing cells with a buffer containing guanidine isothiocyanate. Centrifugation through a QIAshredder® column sheared the high molecular weight genomic DNA and other high-molecular-weight cellular components to create a homogenous lysate. The lysate was mixed with an ethanol containing buffer and transferred onto an RNeasy® column. Ethanol provided conditions which promoted selective binding of RNA to a silica-gel membrane during centrifugation of the solution through the column. Washing buffers were then used to eliminate contaminants while RNA remained attached to the membrane inside the column. Finally, DEPC water was used to elute the RNA from the column. Isolated and purified RNA was stored at -80°C . The average yield was 100 μg total cellular RNA from 10×10^6 cells, depending on the cell line. The integrity and size distribution of isolated RNA were examined by denaturing-agarose gel electrophoresis and ethidium bromide staining. Only RNA samples were used in further experiment whose relevant ribosomal species, 28S rRNA (5 kb) and 18S rRNA (1.9 kb), appeared as bands on the stained gel, as opposed to smears which would have indicated RNA degradation (Figure 3.2).

3.3.2 Reverse transcription of isolated RNA into cDNA

Reverse transcription of total cellular mRNA into cDNA was performed using the SMART™ PCR cDNA Synthesis Kit according to manufacturer's instructions. The method relied on the ability of reverse transcriptase (RT) to transcribe mRNA into single-stranded DNA in the so called first-strand reaction. This reaction was primed by a modified oligo(dT) primer that bound to the 3' poly(A) tail of mRNA species. When RT reached the 5' end of the mRNA, the terminal transferase activity of the enzyme added a few additional nucleotides, primarily deoxycytidine, to the 3' end of the cDNA. The SMART™ oligonucleotide, with an oligo(G) sequence at its 3' end, base-paired with the deoxycytidine stretch on the 3' end of cDNA, creating an extended template. RT then switched templates and continued replicating to the end of the nucleotide. The resulting

full-length, single-stranded cDNA contained the complete 5' end of the mRNA, as well as the sequence that was complementary to the SMART™ oligonucleotide. In cases where RT paused before the end of the template, the addition of deoxycytidine nucleotides was much less efficient than with full length cDNA-RNA hybrids, thus preventing base-pairing with the SMART™ oligonucleotide. The SMART™ anchor sequence and the poly(A) sequence served as universal priming sites for end-to-end cDNA amplification in PCR. Therefore, cDNA lacking these sequences, due to prematurely terminated cDNAs caused by incomplete RT activity, contaminating genomic DNA or cDNA transcribed from poly(A)-negative RNA was not exponentially amplified. The reverse transcription reaction was performed under conditions suggested by the manufacturer. These are described in Figure 3.3.

Annealing		
3 µL	RNA (1 µg) + deionised water	
1 µL	CDS primer (10 µM)	= final 2 µM
1 µL	SMART™ oligonucleotide (10 µM)	= final 2 µM
<hr/>		
5 µL	total	
Incubation at 72°C for 5 min followed by incubation on ice for 2 min.		
Reverse transcription		
5 µL	Annealing reaction mixture	
2 µL	First-Strand Buffer (5×)	= 1×
1 µL	DTT (20 mM)	= 2 mM
1 µL	dNTP Mix (10 mM)	= 1 mM
1 µL	PowerScript Reverse Transcriptase	
<hr/>		
10 µL	total	
Incubation at 42°C for 1 hr followed by incubation on ice for 5 min.		

Figure 3.3 Contents of the reverse transcription reaction mixture and reaction conditions.

3.3.3 Amplification of cDNA

Single-stranded cDNA, synthesised in the reverse transcription reaction with total cellular mRNA as a template, was amplified in PCR using the Advantage® 2 PCR Enzyme System. Primers were designed to specifically bind to 5' (5' SMART™ + T7 primer) and 3' (3' CDS PCR primer) sequences that were integrated into cDNA during the reverse

transcription step. In addition to the sequence that is complementary to the SMART™ oligonucleotide sequence, the 5' SMART™ + T7 primer contained the T7 promoter sequence. Therefore, in PCR performed with this primer, the T7 promoter was integrated into every cDNA molecule synthesised during PCR. This was the prerequisite for subsequent *in vitro* transcription of cDNA into cRNA. The PCR reaction was performed under conditions suggested by the manufacturer. These are described in Figure 3.4.

2 µL	cDNA	
80 µL	PCR-grade water	
10 µL	Advantage 2 PCR Buffer (10×)	= 1×
2 µL	dNTP Mix (10 mM)	= 0.2 mM
2 µL	5' SMART™ + T7 primer (10 µM)	= 0.2 µM
2 µL	3' CDS PCR primer (10 µM)	= 0.2 µM
2 µL	Advantage® 2 Polymerase Mix (50×)	= 1×
<hr/>		
100 µL	total	
Initial denaturation at 95°C for 1 min. Amplification (20 cycles): 95°C for 15 sec, 65°C for 30 sec and 68°C for 6 min. Cooling at 4°C.		

Figure 3.4 Contents of the PCR reaction mixture and reaction conditions.

3.3.4 Purification of cDNA

Amplified cDNA was purified using the QIAquick® PCR Purification Kit according to manufacturer's instruction. The method is based on DNA adsorption to a silica-gel membrane in the presence of high salt concentrations. Briefly, whereas DNA remains attached to the membrane, contaminants pass through the column during centrifugation. In a washing step, impurities, such as salts, enzymes, primers and unincorporated nucleotides, are removed with a washing buffer. Finally, DNA is eluted in Tris buffer.

3.3.5 *In vitro* transcription of total cellular cDNA into cRNA

The *in vitro* transcription of amplified cDNA into cRNA was performed using the mMMESSAGE mMACHINE™ T7 kit. Any sufficiently pure DNA with a promoter site can serve as a template for an RNA polymerase. As shown in Figure 3.5, the minimal promoter sequence required by the T7 RNA polymerase was part of the 5' SMART™ + T7

primer which was used in the cDNA PCR amplification step. The mMACHINE™ T7 kit was designed for *in vitro* synthesis of capped RNA. Capped RNA mimics eukaryotic mRNA found *in vivo*, because it has a 7-methyl guanosine cap structure at the 5' end. The cap analogue available in this kit, m⁷G(5')ppp(5')G, was incorporated only as the first 5' terminal G of the transcript because its structure inhibited its incorporation at any other position in the RNA molecule.

primer:	5' TAATACGACTCACTATAGGGAGGAAGCAGTGGTAACAACGCAGAGT 3'
promoter:	5' TAATACGACTCACTATAGGGAGA 3'

Figure 3.5 The 5' SMART™ + T7 primer and the minimal sequence of the T7 promoter required for recognition by the T7 RNA polymerase. The primer was used in amplification of total cellular cDNA amplification. Thereby, the T7 promoter was integrated into each cDNA molecule synthesised in PCR.

The reaction was performed under conditions suggested in the manufacturer's instructions and described in Figure 3.6. After *in vitro* transcription and cRNA purification (described below) the measured yield of amplified total cellular mRNA was 20-30 µg per 20 µL of the *in vitro* transcription reaction mixture.

6 µL	cDNA (1 µg) + Nuclease-free water	
10 µL	NTP/Cap (2×)	= 1×
2 µL	Reaction Buffer (10×)	= 1×
2 µL	Enzyme Mix	
<hr/>		
20 µL	total	
Incubation at 37°C for 4 hr, followed by DNA digestion by DNase (1 µL) at 37°C for 30 min.		

Figure 3.6 Contents of the *in vitro* transcription reaction mixture and reaction conditions.

3.4 Production of single-species cRNA

Production of single-species cRNA included four steps: linearisation of the plasmid containing a cDNA insert, *in vitro* transcription based on the promoter sequence and the cDNA template in the linearised plasmid, polyadenylation of synthesised cRNA and cRNA purification (Figure 3.7). Since substantial amounts of the cDNA template, i.e. plasmid

DNA (pDNA), were needed for *in vitro* transcription reactions, the plasmid had to be amplified in competent bacteria.

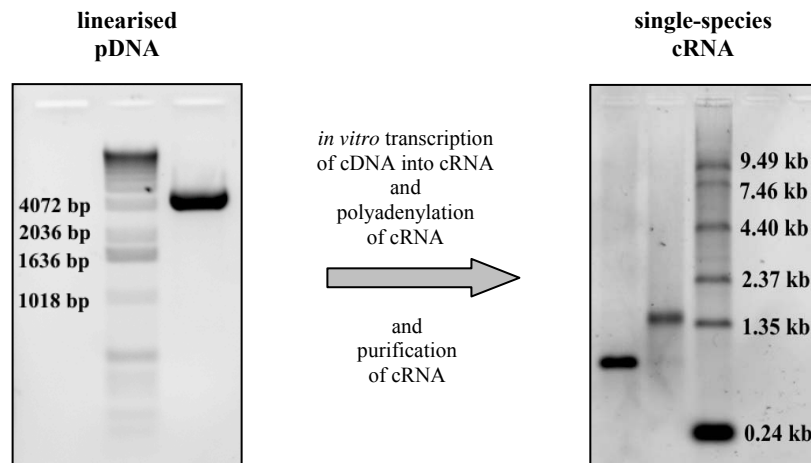


Figure 3.7 The principle of single-species cRNA production. The left agarose gel electrophoresis picture shows the pcDNA1/Amp plasmid with the Melan-A cDNA insert after linearisation with the XbaI restriction endonuclease. Linearised pDNA served as a template for *in vitro* transcription of Melan-A cDNA into Melan-A cRNA. On the right picture, the left band corresponds to shorter Melan-A cRNA before polyadenylation and the right band to longer Melan-A cRNA after polyadenylation and purification. The same strategy was used to produce tyrosinase and CDK4-R24C cRNAs. EGFP cRNA was not polyadenylated after *in vitro* transcription because its poly(A) tail was encoded in the plasmid.

3.4.1 Transformation of competent bacteria with plasmid DNA

In order to obtain larger amounts of pDNA that was received from other groups as a kind gift, competent bacteria had to be transformed with the pDNA in question and expanded. A 50 μ L vial of One Shot TOP10F' competent cells was slowly defrosted on melting ice, a small volume of pDNA (Table 3.1) was added and mixed with the bacteria by tapping gently. The cells were incubated on ice for 30 min, then heated at 42°C for exactly 30 sec and finally placed on ice to cool for 2 min. Rich SOC medium, provided together with the competent cells, was added and transformed bacteria were plated onto LB medium agar plates with the appropriate selection antibiotic (Table 3.1). Plates were placed into the bacterial incubator overnight at 37°C. Since the antibiotic zeocin is light sensitive and its activity is inhibited by high salt concentrations, plates for bacteria transformed with pZeoSV2+/huTyr contained low-salt LB agar medium and were stored in the dark.

Table 3.1 Plasmid information. Listed are: plasmid names, cDNA inserts, plasmid concentrations used in transformation, plasmid volumes used in transformation, antibiotic resistance encoded by the plasmids, antibiotic concentrations in culture media for transformed bacteria and restriction enzymes used for plasmid linearisation.

plasmid	cDNA insert	transf. conc.	transf. volume	resistance to antibiotic	antibiotic conc.	lin. restr. enzyme
pGEM4Z/GFP/A64	EGFP	n.d.	2 μ L	ampicillin	100 μ g/mL	SpeI
pZeoSV2+/huTyr	tyrosinase	10 ng/ μ L	3 μ L	zeocin	50 μ g/mL	PstI
pcDNA1/Amp/Aa1.2	Melan-A	50 ng/ μ L	2 μ L	ampicillin	100 μ g/mL	XbaI
pcDNA1/Amp/C11.1	CDK4-R24C	720 ng/ μ L	2 μ L	ampicillin	100 μ g/mL	XbaI

3.4.2 Selection and expansion of transformed bacteria

Only bacteria transformed with pDNA, encoding resistance to an antibiotic, were able to grow and form colonies on selection plates despite the presence of the corresponding antibiotic in the agar medium. After overnight growth, colonies were plucked from the plates using sterile tooth-picks. Each individual colony was inoculated into 5 mL of LB medium containing the appropriate antibiotic (Table 3.1) in a 15 mL Falcon tube. If previously selected and frozen transformed bacteria were to be expanded, frozen vials were transferred from the -80°C freezer onto melting ice. Approximately 5 μ L of the partially thawed bacterial suspension were then transferred into a 15 mL Falcon tube containing 5 mL of LB medium with the appropriate antibiotic. The tubes were incubated overnight (approximately 12 hr) at 37°C with vigorous shaking at 150 rpm for efficient growth of transformed bacteria.

3.4.3 Freezing of transformed bacteria

Bacteria are the least harmed by the freezing process if the freezing medium contains 15% of glycerin. Therefore, 400 μ L of the overnight bacterial suspension were added to 84 μ L of autoclaved 87% glycerin, vortexed, quickly frozen in liquid nitrogen and transferred to -80°C .

3.4.4 Plasmid DNA extraction from transformed bacteria

After overnight culture, bacterial suspensions were centrifuged at 5300×g and 4°C for 10 min. Plasmid DNA extraction from bacterial cells was performed using the QIAwell® 8 Ultra Plasmid Kit, according to manufacturer's instructions. Briefly, pelleted cells were lysed. The salt and pH conditions in the lysates ensured exclusive binding of DNA to the membrane, while degraded RNA and cellular proteins were not retained. The membrane was then washed with a buffer which disrupts any DNA-protein interactions allowing the removal of any nucleic acid-binding proteins and other residual contaminants from the pDNA. Additional washing steps removed salts and other non-DNA constituents. Purified pDNA was finally eluted in Tris buffer. The yield of extracted pDNA was 4-8 µg per 5 mL of overnight bacterial culture, depending on the plasmid.

3.4.5 *In vitro* transcription of single-species cDNA into cRNA

Each plasmid was linearised with a restriction enzyme (Table 3.1) in order to produce a template suitable for *in vitro* transcription. Since all plasmids contained the T7 promoter at the 5' end of cDNA encoding the desired protein, transcription was performed using the T7 RNA polymerase from the mMESSAGING mMACHINE™ T7 kit according to manufacturer's instructions. Stability of an RNA molecule and its efficient use as a template for translation into protein depend on the presence of a cap at its 5' end and a poly(A) tail at the 3' end. A poly(A) tail is always part of a mRNA molecule synthesised by a cell. Therefore, the total cellular mRNA amplification procedure, described above, included only the addition of a cap analogue in the *in vitro* transcription reaction. However, single-species cRNA produced using cDNA in a plasmid may or may not contain a poly(A) tail, depending on whether the tail is encoded in the construct or not. Whereas the EGFP plasmid had a poly(dT) sequence at the 3' end of the cDNA, the other three plasmids did not. Therefore, in addition to integrating a cap analogue at the 5' end in the *in vitro* transcription reaction, tyrosinase, Melan-A and CDK4-R24C cRNAs were polyadenylated at the 3' end using the Poly(A) Tailing Kit. Both reactions were performed under conditions suggested by the manufacturer. These are described in Figure 3.8. After *in vitro* transcription and cRNA purification (described below), the measured yield of EGFP cRNA was approximately 30 µg per 20 µL of the *in vitro* transcription reaction

mixture. After *in vitro* transcription, polyadenylation and cRNA purification (described below), the measured yield of tyrosinase, Melan-A and CDK4-R24C cRNA was 60-70 μg per 100 μL of the polyadenylation reaction mixture.

<i>In vitro</i> transcription		
6 μL	pDNA (1 μg) + Nuclease-free water	
10 μL	NTP/Cap (2 \times)	= 1 \times
2 μL	Reaction Buffer (10 \times)	= 1 \times
2 μL	Enzyme Mix	
<hr/>		
20 μL	total	
Incubation at 37°C for 2 hr, followed by DNA digestion by DNase (1 μL) at 37°C for 30 min.		
Polyadenylation		
21 μL	<i>In vitro</i> transcription reaction mixture	
35 μL	Nuclease-free water	
30 μL	E-PAP Buffer (5 \times)	= 1 \times
10 μL	MnCl ₂ (25 mM)	= 2.5 mM
10 μL	ATP (10 mM)	= 1 mM
4 μL	E-PAP enzyme (2 U/ μL)	= 8 U
<hr/>		
100 μL	total	
Incubation at 37°C for 1 hr.		

Figure 3.8 Contents of the *in vitro* transcription and polyadenylation reaction mixtures and reaction conditions.

3.4.6 Purification of cRNA

Purification of cRNA, obtained in *in vitro* transcription reactions using as a template either amplified total cellular cDNA or single-species cDNA in a plasmid, was performed using the RNeasy® Mini Kit according to manufacturer's instructions. The procedure, which included RNA binding to a silica-gel membrane, washing and elution, is described above in the chapter 3.3.1 (Total cellular RNA isolation). For purification, the cell lysis and homogenisation steps were omitted and the procedure started with the transfer of the *in vitro* transcription reaction mixture onto an RNeasy® column. RNA was eluted in DEPC water and aliquots were stored at -80°C .

3.5 Electrophoresis

3.5.1 DNA agarose gel electrophoresis

Separation of DNA fragments was performed in 0.8-1.2% agarose gels with 0.4 $\mu\text{g}/\text{mL}$ of ethidium bromide in the running buffer at 5-10 V/cm. Composition of the DNA containing solution that was loaded into gel slots is shown in Figure 3.9. A 1 Kb DNA ladder was included as a size standard in electrophoresis. For extraction of DNA fragments from agarose gels, the desired fragments were cut from the gel after electrophoresis and purified using the QIAquick® Gel Extraction Kit according to manufacturer's instructions.

8 μL	DNA (0.5 μg) + dist. water	= 0.4 μg
1 μL	TAE Buffer (10 \times)	= 1 \times
1 μL	Blue Juice Loading Buffer (10 \times)	= 1 \times
<hr/>		
10 μL	total per slot	

Figure 3.9 Composition of the DNA containing solution loaded into an agarose gel for electrophoretic separation of DNA fragments.

3.5.2 RNA denaturing-agarose gel electrophoresis

For separation of RNA fragments in agarose gel electrophoresis, DEPC water was used in preparation of the gel, running buffer and the RNA sample. Composition of the RNA containing solution that was loaded into gel slots is shown in Figure 3.10. Prior to adding the loading buffer, the solution was incubated at 65°C for 10 min. The high temperature and formamide denatured RNA. Electrophoresis was performed in 0.8-1.2% agarose gels with ethidium bromide (0.4 $\mu\text{g}/\text{mL}$) in the running buffer and 5-10 V/cm. A 0.24-9.5 kb RNA ladder was included as a size standard.

3 μL	RNA (0.5 μg) + DEPC water	
5 μL	formamide (100%)	= 50%
1 μL	TBE Buffer (10 \times)	= 1 \times
1 μL	Blue Juice Loading Buffer (10 \times)	= 1 \times
<hr/>		
10 μL	total per slot	

Figure 3.10 Composition of the RNA containing solution loaded into an agarose gel for electrophoretic separation of RNA fragments.

3.6 RNA transfection into DCs

The cellular plasma membrane serves the vital function of separating the molecular contents of the cell from its external environment. The membranes are largely composed of amphiphilic lipids which self-assemble into a highly insulating bilayer. On their quest to capture as much antigen as possible, immature DCs are well known to take up various structures (ranging in size from small molecules to apoptotic bodies) from their surroundings, including RNA. They do so through macropinocytosis and endocytosis. Even though simple DC co-incubation with RNA has been shown to achieve T-cell priming, more aggressive methods such as lipofection and electroporation proved to be better transfection methods. Lipofection was performed only with EGFP single-species cRNA. In electroporation, both single-species (EGFP, tyrosinase, Melan-A, CDK4-R24) and total cellular (A375 MEL, SK23 MEL, SK29 MEL and 624.38 MEL) cRNAs were used. Irrespective of the transfection method, either immature DCs after 6 days in culture or mature DCs after 8 days in culture were used.

3.6.1 Lipofection

Lipofection reagents usually consist of cationic lipid and neutral lipid components. The positively charged group of the cationic lipid component electrostatically binds to the negatively charged RNA. This interaction results in the formation of bundle-like RNA-lipid complexes. The hydrophilic negative charge of the nucleic acid is neutralized inside the complex. The mainly hydrophobic complex with surplus positive charge associates with the slightly negatively charged cellular plasma membrane. Entry of the complex into the cytoplasm occurs either via endocytosis or fusion with the plasma membrane. The role of the neutral lipid component is endosomal disruption through which the complex is released into the cytoplasm.

To form RNA-cationic lipid complexes, 24 μL of the lipofection reagent TransFast™ were mixed with 8 μg of EGFP cRNA (volume to mass ratio 4:1) in a total volume of 200 μL of OptiMEM I medium. This mixture was incubated at room temperature for 15 min in a 15 mL polystyrene Falcon tube. Polystyrene does not bind nucleic acids thereby minimising the loss of RNA. At the same time, 2×10^6 DCs were resuspended in 200 μL OptiMEM I

medium. For transfection, 200 μL of the DC suspension were added to the 200 μL of the RNA-lipid complexes solution (total of 400 μL) in the polystyrene Falcon tube and mixed gently by pipetting. The transfection reaction mixture was incubated at 37°C and 5% CO_2 for 1 hr with occasional agitation. After transfection, the solution was washed once with PBS and the cells were resuspended in the dendritic cell medium supplemented with 2% autologous plasma, 800 U/mL GM-CSF and 800 U/mL IL-4.

3.6.2 Electroporation

Electroporation induces reversible permeability of plasma membranes when cells are exposed to short pulses of strong external electric fields. The formation of hydrophilic pores is a result of reorientation of lipids in the bilayer membrane. The molecular mechanism of this phenomenon is still not well understood. The number of pores and their diameter increases with the product of the pulse amplitude and the pulse duration. Whereas small molecules simply diffuse through the pores into the cytoplasm, larger molecules, like nucleic acids, are driven into the cell by electrophoretic forces. It has also been shown that the presence of nucleic acids facilitates pore formation. Pores appear within a microsecond of exposure to the electric field, but it takes minutes for them to reseal.

First, $2\text{-}3 \times 10^6$ DCs, resuspended in at least 170 μL OptiMEM I medium, were put into a 0.4 cm electroporation cuvette and incubated on ice for approximately 3 min. Cooling the suspension before electroporation was advantageous because it slowed down the cellular metabolism. Thereby, overheating due to electricity was prevented. Furthermore, damage caused by the electric shock and by molecules released from dead cells was minimised. Subsequently, RNA, resuspended in no more than 100 μL of DEPC water (depending on RNA concentration and mass, listed in Table 3.2), was added, giving a total electroporation suspension volume of 270 μL . The suspension was shortly mixed by pipetting and then quickly electroporated. Electroporation was performed with 250 V and 150 μF . Immediately after electroporation, cells were transferred into the dendritic cell medium supplemented with 2% autologous plasma, 10 mM HEPES, 800 U/mL GM-CSF and 800 U/mL IL-4. The cells were counted and the suspension was quickly aliquoted for either

FACS™ analyses, RNA isolation or functional assays and placed into the incubator at 37°C and 5% CO₂.

In one experiment, one half of the aliquots was incubated with 5 µg/mL of RNase in the medium described above and the other half without RNase. These DCs were used for RNA isolation.

Table 3.2 Amounts of various RNA species used in electroporation.

RNA species	RNA mass (µg)
EGFP cRNA	2, 4 and 8
tyrosinase cRNA	6, 12, 24 and 48
Melan-A cRNA	48
CDK4-R24C cRNA	48
A375 MEL amplified total cellular mRNA	75
SK23 MEL amplified total cellular mRNA	80 and 160
SK29 MEL total cellular RNA	75
SK29 MEL amplified total cellular mRNA	37.5 and 75

3.7 Functional assay

In the functional assay, RNA-transfected DCs, peptide-pulsed DCs, tumour cells or peptide pulsed T2 cells served as stimulators. Antigen-specific CTL clones served as effectors. In order to measure the stimulatory capacities of stimulators, DCs or tumour cells were first co-incubated with CTLs. Unless noted otherwise, CTLs were harvested and used in co-incubation cultures 8 days after thawing and restimulation. The amount of IFN-γ secreted by activated CTLs was measured in the enzyme-linked immunosorbent assay (ELISA).

3.7.1 DC or tumour cell co-incubation with CTLs

Either 2 hr or 25 hr after electroporation, 100 µL of the CTL suspension (2×10^4 cells in CTL co-incubation medium) were added to 100 µL of the transfected-DC suspension (5×10^3 , 1×10^4 , 2×10^4 , 4×10^4 or 8×10^4 cells in dendritic cell medium supplemented with

2% autologous plasma and 800 U/mL GM-CSF and 800 U/mL IL-4), giving a total of 200 μ L per well of a 96-well plate and 1:4, 1:2, 1:1, 2:1 or 4:1 stimulator to effector ratios.

Untransfected DCs were exogenously pulsed with peptides by adding 10 μ L of the peptide solution (100 μ L/mL) to 100 μ L of the DC suspension (4×10^4 cells in dendritic cell medium supplemented with 2% autologous plasma and 800 U/mL GM-CSF and 800 U/mL IL-4). After a 2 hr incubation at 37°C and 5% CO₂, 100 μ L of the CTL suspension (2×10^4 cells in CTL co-incubation medium) were added, giving a 2:1 stimulator to effector ratio.

For co-incubation of T2 cells with CTLs, lower cell numbers were taken. The exogenous pulsing was performed with 10 μ L of the peptide solution and 100 μ L of the T2 suspension (1.5×10^4 cells in dendritic cell medium supplemented with 2% human serum). After a 2 hr incubation at 37°C and 5% CO₂, 100 μ L of the CTL suspension (3×10^3 cells in CTL co-incubation medium) were added, giving a 5:1 stimulator to effector ratio.

After a 24 hr co-incubation of effectors and stimulators, 150 μ L of each supernatant was harvested and stored at -20°C.

3.7.2 IFN- γ ELISA

The measurement of IFN- γ in DC-CTL or tumour-CTL co-culture supernatants was performed in ELISA using the OptEIA™ Human IFN- γ Set according to manufacturer's instructions. Briefly, the ELISA plates were coated with a mouse anti-IFN- γ capture antibody and then blocked with an FBS-containing solution. In some cases, supernatants were diluted 1:2.5 in the DC-CTL co-incubation medium. The same medium was used to make serial dilutions of the IFN- γ standard. After IFN- γ from cell culture supernatants or standard solutions bound to the capture antibodies in the plates, the biotinylated mouse anti-IFN- γ detection antibody was added together with avidin conjugated to horseradish-peroxidase. To visualise the complexes consisting of capture antibody, IFN- γ , detection antibody, biotin, avidin and horseradish-peroxidase, H₂O₂ (a substrate for peroxidase) in combination with tetramethylbenzidine (substrate reagents A and B mixed) was added, changing the solution colour into blue. The enzymatic reaction was stopped with 1 M ortho-phosphoric acid. Thereby, the colour of the solution turned yellow, its intensity

being directly proportional to the amount of substrate processed, i.e. indirectly proportional to the amount of IFN- γ captured. Light absorption in the reaction solution was measured at 450 nm. Unknown IFN- γ concentrations were calculated with the help of a standard curve which was drawn based on known concentration of the IFN- γ standard and corresponding measured absorbances.

3.8 RNA quantitation

Since different samples were to be compared in highly sensitive quantitation experiments, great care was given to handling all samples the same way. RNA from samples prepared for transfection and RNA isolated from transfected DCs were first reverse transcribed into cDNA. Amounts of EGFP, tyrosinase, Melan-A and CDK4 message contained in these cDNA samples were then precisely determined with the help of real-time PCR using sequence-specific primers.

3.8.1 Total cellular RNA isolation from transfected DCs

Before RNA isolation, transfected DCs were washed twice with PBS and transferred into 1.5 mL Eppendorf tubes. Not many transfected DCs (as few as 1×10^4 cells) were available for RNA isolation, as opposed to unlimited amounts of tumour cells (as many as 10×10^6). To avoid RNA loss in the procedure, the RNeasy® Mini Kit was substituted with the Tri Reagent method. After cells were pelleted, 200 μ L of Tri Reagent (containing phenol and thiocyanate) were vigorously mixed with the cells to disrupt plasma membranes, inactivate released RNases and homogenise the suspension. In the following step, 20 μ g of yeast tRNA were added to later enhance RNA pelleting and visualisation. Incubation at room temperature for 5 min allowed the dissociation of nucleoprotein-complexes. After 40 μ L of chloroform were added, the suspensions were vortexed for exactly 15 sec, incubated at room temperature for 10 min and then centrifuged at $1.2 \times 10^4 \times g$ for 15 min. The upper colourless aqueous phase was transferred into new 1.5 mL Eppendorf tubes. Subsequently, 100 μ L of isopropanol were added. The solutions were vortexed, incubated at room temperature for 10 min and then centrifuged at $1.2 \times 10^4 \times g$ for 12 min. Supernatants were removed and 500 μ L of 75% ethanol were mixed with the solutions by pipetting. After

centrifugation at $1.2 \times 10^4 \times g$ for 10 min, supernatants were quantitatively removed and the RNA pellets were air-dried at room temperature for 5 min. RNA was resuspended in 20 μL of DEPC water.

3.8.2 Reverse transcription of *in vitro* transcribed cRNA and dendritic cell-derived RNA into cDNA

In the case of *in vitro* transcribed amplified total cellular mRNAs and single-species cRNAs, stock aliquots were diluted in DEPC water so that all samples had the final concentration of 0.093 $\mu\text{g}/\mu\text{L}$. Reverse transcription reaction mixtures contained 5 μL of each diluted sample. Therefore, in all reaction mixtures cDNA was synthesised using 0.47 μg *in vitro* transcribed RNA as a template.

The transfected DC suspension was aliquoted for RNA isolation at different time points and the number of transfected DCs in the suspension was determined. Since all samples contained the same amount of DCs, it was not necessary to measure and normalise the concentration of isolated total cellular RNA for reverse transcription or the concentration of cDNA for real-time PCR (described below).

Reverse transcription of *in vitro* transcribed cRNAs and isolated total cellular RNA was performed using the 1st Strand cDNA Synthesis Kit for RT-PCR (AMV) according to manufacturer's instructions described in Figure 3.11. The use of this kit was suggested by the manufacturer of solutions used in the following step, real-time PCR.

RNA denaturation at 60°C for 10 min followed by the addition of kit reagents.		
5 μL	RNA	
3.2 μL	Sterile water	
2 μL	Reaction Buffer (10 \times)	= 1 \times
4 μL	MgCl ₂ (25 mM)	= 5 mM
2 μL	Deoxynucleotide Mix (10 mM)	= 1 mM
2 μL	Oligo-p(dT) ₁₅ Primer (0.8 $\mu\text{g}/\mu\text{L}$)	= 1.6 μg
1 μL	RNase Inhibitor (50 U/ μL)	= 50 U
0.8 μL	AMV Reverse Transcriptase (25 U/ μL)	= 20 U
<hr/>		
20 μL	total	
Annealing at 25°C for 10 min. Reverse transcription at 42°C for 60 min. AMV RT denaturation at 99°C for 5 min. Cooling at 4°C.		

Figure 3.11 Contents of the reverse transcription reaction mixture and reaction conditions

3.8.3 Real-time PCR

The real-time PCR system used SYBR Green I, a fluorescent dye which emitted light only when bound to dsDNA. Therefore, the intensity of fluorescence was proportional to the number of dsDNA molecules, i.e. PCR product. This fluorescence was measured by the LightCycler® instrument and recorded after each PCR cycle, in real time. After the PCR run, LightCycler® software drew a typical PCR curve for every sample measured. As shown in Figure 3.12 and Table 3.3, the samples were then compared based on the same fluorescence (crossing line) but different cycles numbers (crossing points). Samples with more PCR template reached the same fluorescence "sooner" (lower cycle number) than samples with less template (higher cycle number).

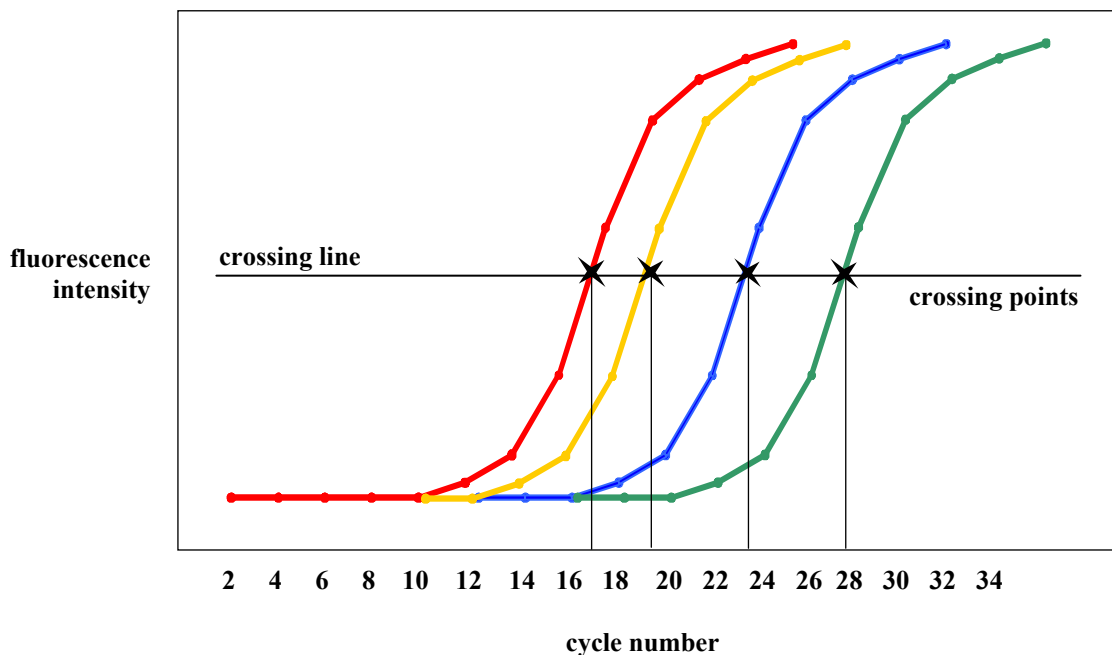


Figure 3.12 Real-time PCR curves. The LightCycler® instrument simultaneously measures fluorescence intensities of all samples at the end of each cycle during a PCR run. Fluorescent light is emitted by the SYBR Green I dye which fluoresces only when bound to dsDNA, i.e. the PCR product. Therefore, the intensity of fluorescence is directly proportional to the amount of the PCR product. A typical PCR curve is drawn for each sample by LightCycler® software after simultaneous PCR runs are recorded by the software in real time. Precise quantitative comparison of samples is possible only in the logarithmic phase of a PCR reaction. Therefore, in analysis, a crossing line is drawn so that it crosses logarithmic sections of all PCR curves. The crossing points between the crossing line and the curves reveal at which point i.e. cycle number during the PCR run a sample reached the fluorescence intensity marked by the crossing line. Samples containing more PCR template at the beginning of the run reach the chosen fluorescence intensity "sooner" (lower cycle number) than samples with less template (higher cycle number).

Compositions of PCR reaction mixtures and LightCycler® instrument settings depended on the primer pair. These are listed in Tables 3.3 and 3.4. The 20 μL of a typical reaction mixture were composed of: 2 μL of cDNA, 2 μL of the forward and reverse primer solution, 2 μL of the SYBR Green I fluorescent dye and enzyme containing solution, sterile PCR grade water and MgCl_2 . Volumes of the water and the MgCl_2 solution depended on the desired final MgCl_2 concentration that was optimal for the primer pair. All components listed above, except for cDNA and primers, were part of the LightCycler® – FastStart DNA Master SYBR Green I kit. Primer pairs for EGFP, Melan-A, CDK4 and α -enolase were designed at the institute. The solution containing tyrosinase primers and MgCl_2 as well as the tyrosinase standard were part of the kit LightCycler® – Primer Set for Human Tyrosinase. Sequences of the tyrosinase primers and the exact compositions of the solutions in the kit were not disclosed by the manufacturer.

Table 3.3 Real-time PCR conditions optimised for individual primer pairs.

primer pair	final MgCl_2 concentration	primer concentration	annealing temperature	annealing duration	elongation duration
EGFP	3 mM	0.50 μM	63°C	3 sec	20 sec
tyrosinase	unknown	unknown	68°C	10 sec	16 sec
Melan-A	3 mM	0.50 μM	59°C	5 sec	20 sec
CDK4	4 mM	0.50 μM	55°C	10 sec	15 sec
α -enolase	5 mM	0.38 μM	60°C	10 sec	25 sec

Melting curves plotted by the LightCycler® software were used to control primer specificities. Each peak of the melting curve corresponded to one PCR product of a certain size. More peaks would have indicated lower specificity of primers resulting in amplification and quantitation of irrelevant sequences in addition to the targeted sequence. With all primer pairs described above, only one peak in the melting curve was observed confirming the high primer specificity.

Quantitation was performed with the help of LightCycler® software and its Fit Points algorithm. This algorithm calculated cycle numbers corresponding to the crossing points between the crossing line and PCR curves of individual samples (Figure 3.12).

Table 3.4 LightCycler® instrument settings for a typical real-time PCR run.

	cycles	analysis mode	temperature	temp. trans. rate	duration	acquisition mode
denaturation	1	none	95°C	20°C/sec	600 sec	none
amplification	40	quantification	95°C	20°C/sec	10 sec	none
			Table 3.3	20°C/sec	Table 3.3	none
			72°C	20°C/sec	Table 3.3	single
melting	1	melting curves	95°C	20°C/sec	0 sec	none
			58°C	20°C/sec	10 sec	none
			99°C	0.1°C/sec	0 sec	continuous
cooling	1	none	40°C	20°C/sec	30 sec	none

As shown in Table 3.5, relative amounts of PCR templates, i.e. molecules detected by the sequence-specific primers, were calculated based on these cycle numbers. The sample with the largest measured amount of the PCR template was taken as a reference. Template quantities detected in other samples were calculated relative to this reference. The n cycle difference between a sample and the reference meant a 2^n -fold difference in the number of template molecules present in the two samples. For example, when sample 2 (cycle number 19.8) was compared with the reference, sample 1 (cycle number 17.2), the cycle difference $n=2.6$ was used to calculate the 6-fold difference ($2^n=2^{2.6}=6$) in the number of PCR template molecules between the reference and sample 2 (Table 3.5). This meant that sample 2 contained 6-fold less template than the reference. This fold-difference was then expressed as either per cent of the reference or in relative units. If the amount of PCR template in the reference was expressed as 100% ($1/1 \times 100 = 100\%$), then sample 2 contained the amount of the PCR template that was 16.67% of the reference ($1/6 \times 100 = 16.67\%$). Similarly, if the reference was expressed as 10^6 relative units ($1/1 \times 10^6 = 10^6$ relative units), then sample 2 could be depicted as 1.66×10^5 relative units ($1/6 \times 10^6 = 1.66 \times 10^5$ relative units).

The LightCycler® – Primer Set for Human Tyrosinase contained a standard for tyrosinase. The standard was included in the real-time PCR run in addition to the samples with unknown tyrosinase cDNA quantities. Based on a standard curve, absolute copy numbers of the tyrosinase PCR template in analysed samples were calculated. These were then

multiplied by dilution factors (from the reverse transcription and real-time PCR steps) and divided by the number of cells from which the RNA had been isolated to express the quantity as copy number from 1×10^4 cells.

Table 3.5 Relative quantitation of PCR template molecules in different samples. Based on crossing points calculated by LightCycler® software as shown in Figure 3.12, amounts of the PCR template in different samples are calculated relative to the reference (sample 1) and expressed either as fold-decrease from the reference, as % of the reference or in relative units.

	cycle number	relative quantity	cycle difference	calculation	quant. difference (fold)	quant. difference (%)	quant. difference (relative units)
sample 1	17.2	high	0.0	$2^0=1$	1	100.00	1 000 000
sample 2	19.8	middle	2.6	$2^{2.6}=6$	6	16.67	166 666
sample 3	23.9	middle	6.7	$2^{6.7}=104$	104	0.96	9 615
sample 4	28.1	low	10.9	$2^{10.9}=1 911$	1 911	0.05	523

Different RNA samples contained different copy numbers of tyrosinase mRNA (total cellular RNA) or cRNA (amplified total cellular mRNA or single-species tyrosinase cRNA), i.e. different amounts of the tyrosinase message. Furthermore, different quantities of these RNA samples were used in electroporation experiments. In order to define how much message for tyrosinase had been introduced into DCs in electroporation with various RNA samples, relative units calculated as described above were recalculated to take different RNA masses into account.

Table 3.6 Relative quantities of PCR template molecules recalculated taking masses of RNA samples into account. Relative units (ru) proportional to different numbers of PCR template molecules in different RNA samples of the same mass (0.46 µg) are calculated as shown in Table 3.5. These relative units are multiplied by the corresponding RNA mass used in electroporation (elp.) and expressed once again relative to the 1×10^6 units of the sample 1 reference.

	ru in 0.46 µg RNA (relative to sample 1)	RNA mass in elp.	calculation	ru in elp. RNA	calculation	ru in elp. RNA (relative to sample 1)
sample 1	1 000 000	48 µg	$48 \times 1 000 000$	48 000 000	$48.00 \times 10^6 / 48 \times 10^6 \times 10^6$	1 000 000
sample 2	166 666	24 µg	$24 \times 166 666$	3 999 984	$3.99 \times 10^6 / 48 \times 10^6 \times 10^6$	83 333
sample 3	9 615	160 µg	$160 \times 9 615$	1 538 400	$1.53 \times 10^6 / 48 \times 10^6 \times 10^6$	32 050
sample 4	523	160 µg	160×523	83 680	$8.36 \times 10^4 / 48 \times 10^6 \times 10^6$	1 743

As shown in the example in Table 3.6, relative units (ru) contained in a sample were multiplied by the mass of that RNA sample used in electroporation (elp.). For better overview and easier understanding, the recalculated relative units were once again expressed relative to the 1×10^6 relative units of the sample 1 reference containing the most tyrosinase message.

4. Results

4.1 Transfection of DCs with RNA encoding EGFP

While the ultimate goal of this project was to investigate the functionality of DCs transfected with tumour-derived RNA, the complexity of an experimental system including RNA-pulsed DCs and CTLs (DC-RNA-CTL system) was first reduced to an analysis of DCs and RNA in order to find the most efficient method of transferring RNA into DCs and to define optimal transfection conditions. Instead of tumour RNA, *in vitro* transcribed cRNA coding for EGFP was used for these experiments. The size of EGFP cRNA does not differ drastically from that of single-species tumour-antigen cRNAs that were to be used in subsequent experiments, allowing the assumption that these single-species cRNAs would behave similarly in transfection. Because of hydrogen peroxide release during chromophore formation, EGFP might be toxic, but only when produced in extremely large quantities. Therefore, cells are known to tolerate EGFP well.

EGFP emits green light (507-509 nm) when excited with blue light (488 nm). The word "enhanced" in its name refers to the changes that were introduced into the wild type green fluorescence protein (GFP): codon-optimisation and two amino acid mutations. Optimised codon usage means that codons more often found in the genome of jellyfish *Aequorea victoria* (from which wild type GFP was isolated) were replaced by triplets coding for the same amino acids, but preferred by mammalian cells. The consequence of such engineering is that the enhanced protein is synthesised quicker in human cells (Yang TT *et al.* 1996). The F64L mutation helps EGFP fold more easily at 37°C. The S65T mutation affects chromophore formation by accelerating oxidation, and makes EGFP 35-times brighter than wild type GFP. Intracellular formation of the wild type GFP chromophore takes up to 95 minutes. EGFP is ready to emit green light upon excitation within no more than 35 minutes (Tsien RY 1998). Despite the enhanced properties of EGFP, additional time is still required after translation for proper folding of the native protein and chromophore maturation. Only then can this molecule be induced to emit green light. The intensity of green fluorescence is proportional to the amount of EGFP. Therefore, EGFP expression upon RNA transfection into DCs was measured in FACS™. In quantitative experiments, amounts of transfected EGFP message were determined by the method of real-time PCR using designed EGFP-specific primers.

The EGFP system was used to address the following questions:

- Which transfection method is more efficient, electroporation or lipofection?
- Which cells take up more RNA, immature or mature DCs?
- Which cells produce more protein after transfection, immature or mature DCs?
- Does electroporation change the phenotype of mature DCs?
- How much single-species RNA should be used for efficient transfection?
- How quickly is transfected RNA degraded inside the DCs?
- Is there a correlation between the kinetics of RNA degradation and protein production inside the DCs?

4.1.1 Generation of DCs

Culture with the cytokines IL-4 and GM-CSF is used to differentiate monocytes into DCs within approximately six days. At this time, the monocyte-derived DCs are in an immature state, characterised by intensified antigen uptake. Maturation of DCs requires the presence of additional cytokines, TNF- α , IL-1 β , IL-6 and PGE₂, also known as the maturation cytokine cocktail, for one to two days. Mature DCs concentrate on exposing processed antigens to T-cells. The transition from antigen-sampling immature to antigen-presenting mature DCs can be observed through changes in the expression of several surface molecules, comprising what is called the phenotype of DCs. The typical expression profile of *in vitro* generated DCs consists of the following surface markers: CD14 (receptor for the complex of LPS and LPS-binding protein, expressed on monocytes but not on DCs), CD1a (involved in presentation of non-peptide lipid and glycolipid antigens), CD206 (mannose receptor), CD11c (myeloid DC marker, as opposed to plasmacytoid DCs, involved in adhesion and signalling), CD83 (DC maturation marker of unknown function), CD40 (co-stimulatory molecule), CD80 (or B7.1, co-stimulatory molecule), CD86 (or B7.2, co-stimulatory molecule), MHC class I (or HLA-A,B,C, antigen-presenting molecules) and MHC class II (or HLA-DP,DQ,DR, antigen-presenting molecules).

The phenotypes of 6-day old immature and 8-day old mature DCs were assessed in FACS™ after staining with FITC or PE-conjugated antibodies specific for the listed surface markers (Figure 4.1). Measured changes in the percentage of positive cells and/or mean fluorescence intensity (MFI), indicating how many cells were expressing the marker

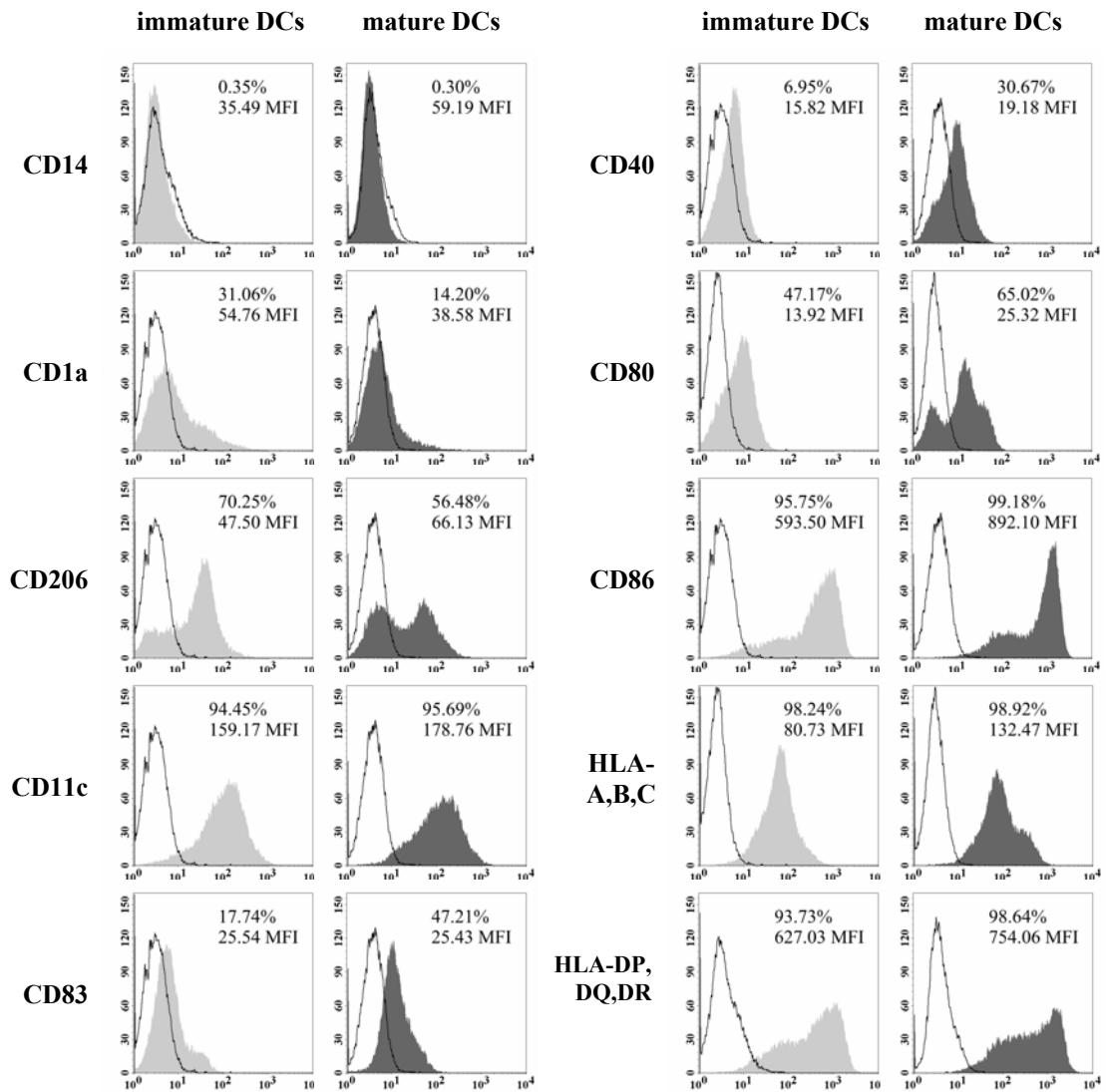


Figure 4.1 Phenotype of immature and mature monocyte-derived DCs. Immature DCs were harvested after 6 days in culture with GM-CSF and IL-4 and stained. Mature DCs were generated from immature DCs in the presence of the maturation cytokine cocktail. They were harvested after a total of 8 days in culture and stained. FACS™ overlay histograms show fluorescence intensities of DCs stained with FITC or PE-conjugated antibodies specific for molecules expressed on the cell surface (filled curves) and corresponding isotype controls (black curves). In analysis, a gate was set around isotype controls. Fluorescence of DCs placed outside the gate was considered specific and those DCs positive for the stained surface marker. Histogram statistics were used to calculate the percentage of positive cells and their mean fluorescence intensity (MFI).

and how much of it on average, were in accordance with published observations. DCs were generally CD14-negative. The relatively high expression of CD1a and CD206 on immature DCs was down-regulated upon addition of the maturation cocktail, whereas the expression of CD11c remained unchanged. CD83, CD40, CD80, CD86, MHC class I and MHC class II, which were already present on immature DCs, were all up-regulated as part of the maturation process.

Monocytes used for generating DCs were isolated from PBMCs through plastic adherence. In preliminary experiments, PBMCs were obtained from buffy coats or fresh blood of different donors. This resulted in unstable yields of morphologically, phenotypically and functionally different DCs and, as a consequence, a low degree of reproducibility in experiments. Keeping in mind that DCs would play an important role in precise quantitation experiments, this variability in the system had to be reduced. Therefore, one HLA-A*0201 donor (donor PH) was subjected to leukapheresis in order to obtain large numbers of PBMCs. These cells were aliquoted and frozen. For each subsequent experiment, ampoules from the same stock of PBMCs were thawed, monocytes isolated and DCs generated according to the same protocol (unless noted otherwise). The standardisation of DC culture proved to be the right solution, since DCs from donor PH, generated on different occasions, displayed the same phenotype (Figure 4.1).

4.1.2 Lipofection vs. electroporation and immature DCs vs. mature DCs

It was postulated that in addition to priming CD8⁺ CTLs, RNA-pulsed DCs could prime CD4⁺ T-helper cells if the transfected RNA was protected by cationic lipids, used as a transfection reagent, and was therefore present inside the cells for a longer time (Su Z *et al.* 2001). For this reason, lipofection was the preferred transfection method in preliminary experiments. A comparison of different cationic lipids revealed that TransFast™ was most efficient (Strobel I *et al.* 2000). Electroporation was then reported to be superior to lipofection and passive pulsing (van Tendeloo VF *et al.* 2001). Electroporation parameters in the following experiments were composed of those suggested in personal communication (Steinkasserer A) and found in several publications (Kalady MF *et al.* 2002, Milazzo C *et al.* 2003).

In order to determine which transfection method was more efficient in the standardised DC system, and which cells were more susceptible to forced RNA uptake, lipofection and electroporation of immature and mature DCs were compared in the same experiment. Immature DCs were harvested after 6 days in culture. One half of these cells was used for transfection with EGFP cRNA on the same day, whereas the other half was placed back into culture with the cytokine maturation cocktail for an additional two days to produce mature DCs. These mature DCs were then transfected under the same conditions as the

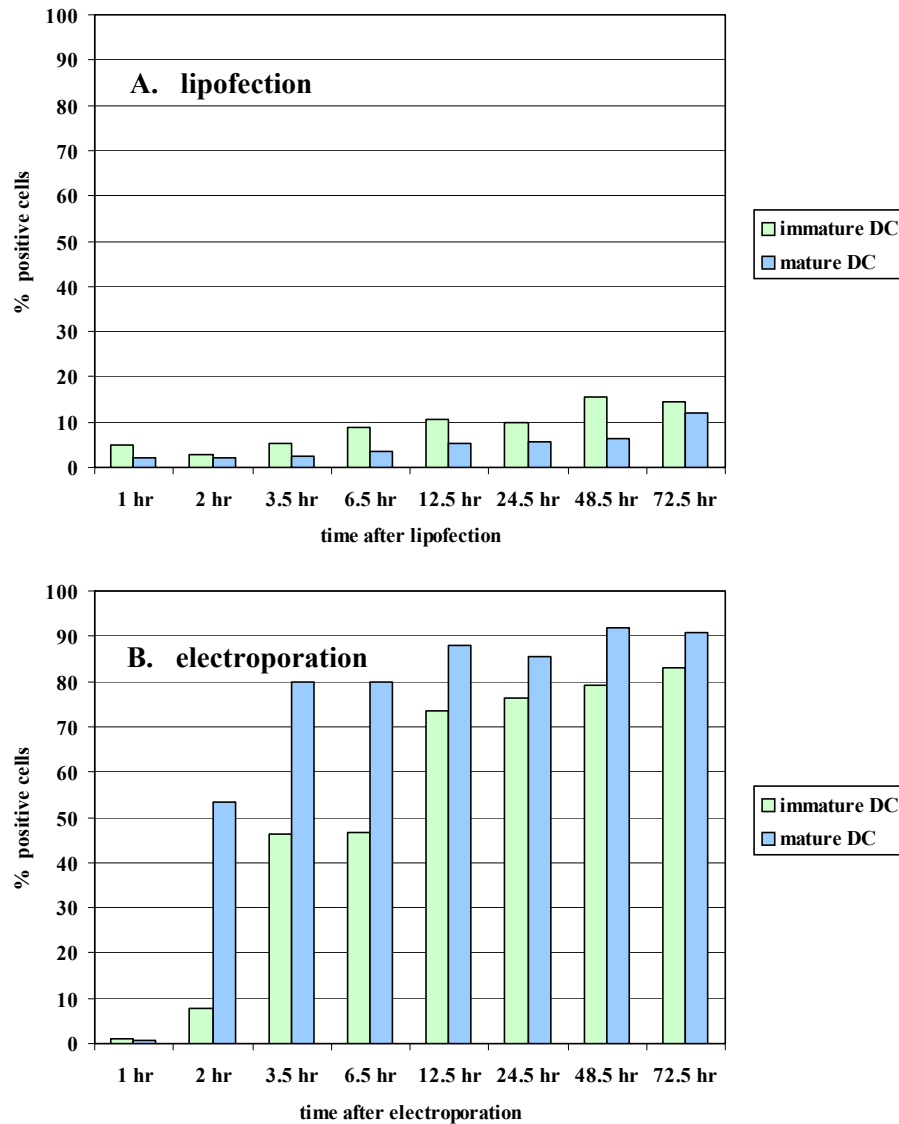


Figure 4.2 Efficiencies of lipofection and electroporation with EGFP cRNA. Same transfection conditions were used for both immature DCs and mature DCs. Lipofection (A) and electroporation (B) were performed with 8 μg of EGFP cRNA. The fluorescence of untransfected or EGFP cRNA-transfected DCs was measured in FACSTM at different time points after transfection. Diagrams show percentages of EGFP-positive DCs from FACSTM overlay histograms in which a gate was set around untransfected DCs. Fluorescence of DCs placed outside the gate was considered to be of EGFP origin and those DCs positive for EGFP.

immature DCs. Eight μg of EGFP cRNA were either lipofected or electroporated into 2×10^6 DCs. The percentage of EGFP-positive cells and the mean intensity of green fluorescence were measured by flow cytometry in all samples 1, 2, 3.5, 6.5, 12.5, 24.5, 48.5 and 72.5 hr after transfection. This kinetics analysis was done to determine how quickly protein expression occurred and how stable the transfectants were following introduction of RNA by both methods.

The two transfection methods are best compared by assessment of how many cells successfully received the RNA, i.e. by determining of the percentages of EGFP-positive cells (Figure 4.2). The development of green fluorescence seemed to take different courses in lipofected and electroporated DCs. At 48 hr after lipofection, the highest percentage (only 15%) of EGFP-positive immature DCs was observed (Figure 4.2A). This suggested that, even though RNA had entered the cytoplasm, it did not immediately make contact with the ribosomes on which protein production takes place. RNA molecules were probably gradually released from the complexes with lipids and the amount of EGFP in the cells increased at a relatively slow pace, allowing detection of positive cells with a certain delay. At all time points, not as many mature DCs were positive, compared to the immature DCs, suggesting that these cells must have taken up fewer RNA-lipid complexes. This observation is consistent with the down-regulation of antigen (in this case RNA-lipid complexes) capture which is known to occur upon DC maturation.

In electroporated cells, RNA was not slowed down by attached lipids. Therefore, RNA was ready for translation once it arrived in the cytoplasm. Already within the first 3.5 hr after transfection, the percentage of EGFP-positive mature DCs rapidly increased, reached a maximum at 12.5 hr and then remained stable at 85-91% for at least two days (Figure 4.2B). Similar kinetics were observed with immature DCs. Nevertheless, electroporated RNA seemed to reach fewer immature DCs (73-83%) compared to the mature ones.

MFI is a direct measure of how much EGFP is produced in the cells. Twenty-four hr after either lipofection or electroporation, the MFI of mature DCs was approximately two-fold higher than the MFI of immature DCs (Figure 4.3). Upon DC maturation, internalisation of extracellular molecules is reduced, and antigen processing becomes the main task. One can assume that intensified protein synthesis in mature DCs contributes to antigen presentation by providing more starting material for peptide production. This makes particular sense if the antigen is introduced into the DC in the form of DNA or RNA. Since internalising antigen is primarily a function of immature cells, it is not likely that under the same transfection conditions mature DCs would take up more RNA than immature DCs. This observation may indicate that mature DCs synthesised more protein than immature DCs transfected with the same amount of RNA.

Surprisingly, even though only a few lipofected cells were detected as EGFP-positive (Figure 4.3), they fluoresced with a convincingly higher intensity (MFI 147 for immature and 299 for mature) compared to their electroporated counterparts (MFI 88 for immature and 202 for mature). It is possible that single cells take up extremely large amounts of RNA through lipofection, whereas the RNA is distributed more evenly among the cells following electroporation.

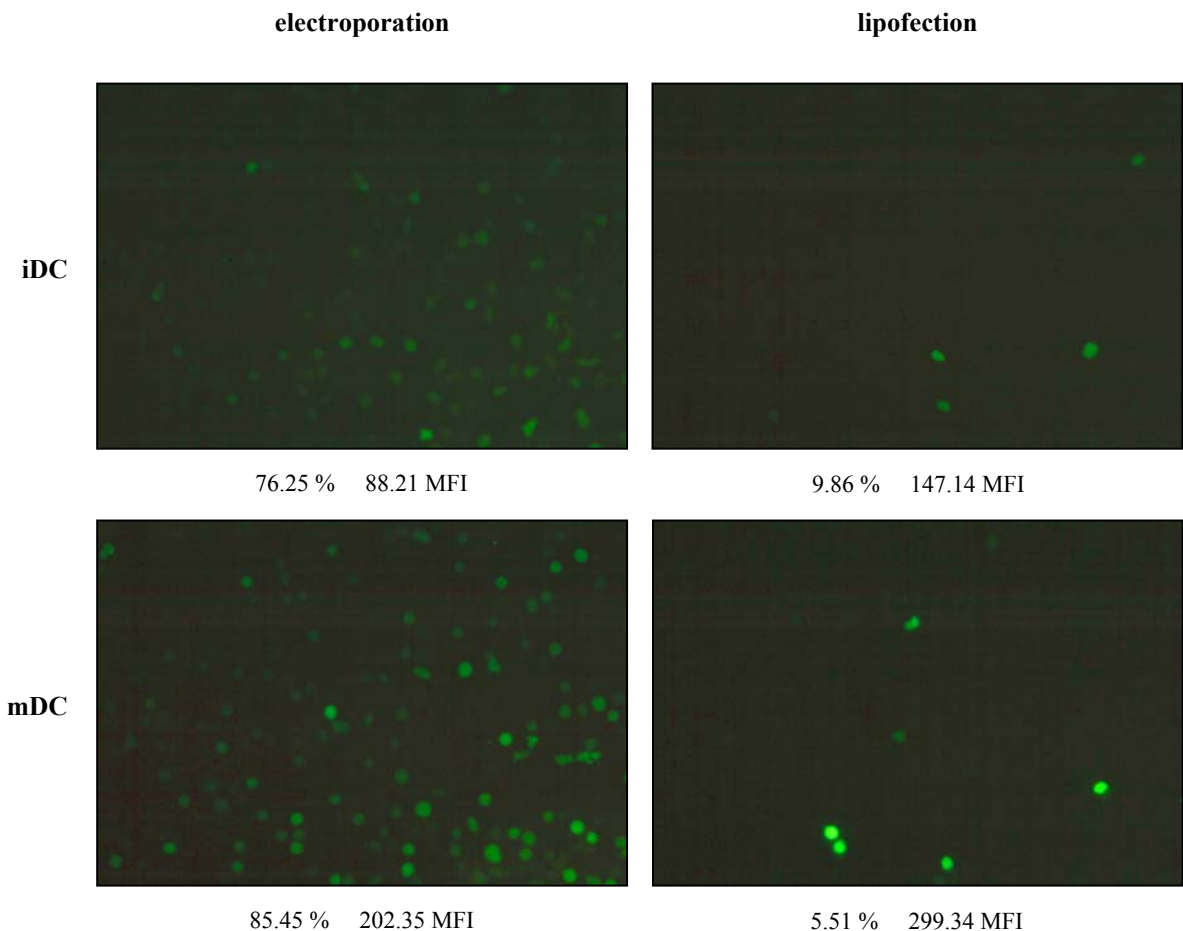


Figure 4.3 Immature and mature DCs after lipofection and electroporation with EGFP cRNA. Same transfection conditions were used for both immature DCs (iDC) and mature DCs (mDC). Lipofection and electroporation were performed with 8 μ g of EGFP cRNA. Fluorescence microscopy photographs show EGFP cRNA-transfected DCs 27 hr after transfection. The corresponding percentages of EGFP-positive cells and EGFP mean fluorescence intensities (MFI) were calculated in overlay histograms based on FACS™ data that were obtained 24.5 hr after transfection. For definition of EGFP-specific fluorescence and EGFP-positive cells see Figure 4.2.

In a separate experiment performed under the same conditions, even 5 days after electroporation, 38% of mature DCs were still EGFP-positive (Figure 4.4). This represented a decrease of only 49% from the maximum, with the intensity of their green fluorescence relatively low (down 85% from the maximum). The compact structure of the

EGFP molecule, which resembles a barrel, makes it very stable under a variety of different conditions, including treatment with proteases (Tsien RY *et al.* 1998), and gives it a half-life of more than 24 hr (Li X *et al.* 1998). Whereas the stability of EGFP surely is largely responsible for this observation, it is also possible that the transfected RNA survived inside the cell for longer periods of time despite the presence of aggressive intracellular RNases.

These experiments showed that the efficiency of electroporation was undoubtedly superior to the efficiency of lipofection. An advantage was also found in using mature DCs, since they produced more protein, based on a given amount of electroporated RNA.

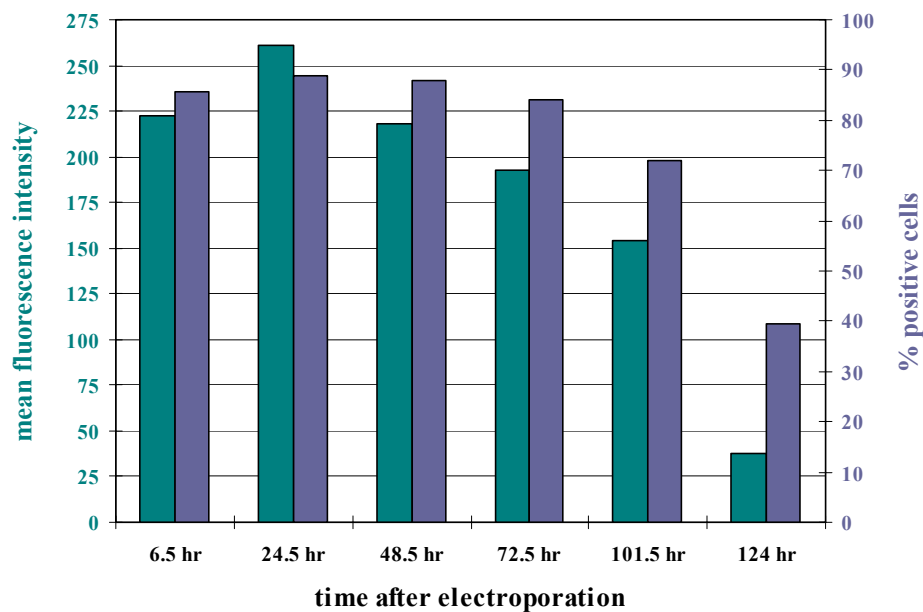


Figure 4.4 Late kinetics of EGFP expression. Mature DCs were electroporated with 8 μg of EGFP cRNA. The fluorescence of EGFP cRNA-transfected DCs was measured in FACS™ at different time points after electroporation, including the relatively late time points 101.5 hr and 124 hr. In the diagram with two Y-axes, mean fluorescence intensities of EGFP cRNA-transfected DCs are depicted on the left Y-axis and corresponding percentages of EGFP-positive cells on the right Y-axis. These were calculated in overlay histograms based on FACS data. For definition of EGFP-specific fluorescence and EGFP-positive cells see Figure 4.2.

4.1.3 Phenotype of electroporated DCs

It was important to assure that placing mature DCs into an electric field and forcing foreign RNA into them did not change their surface phenotype, comprised of important molecules

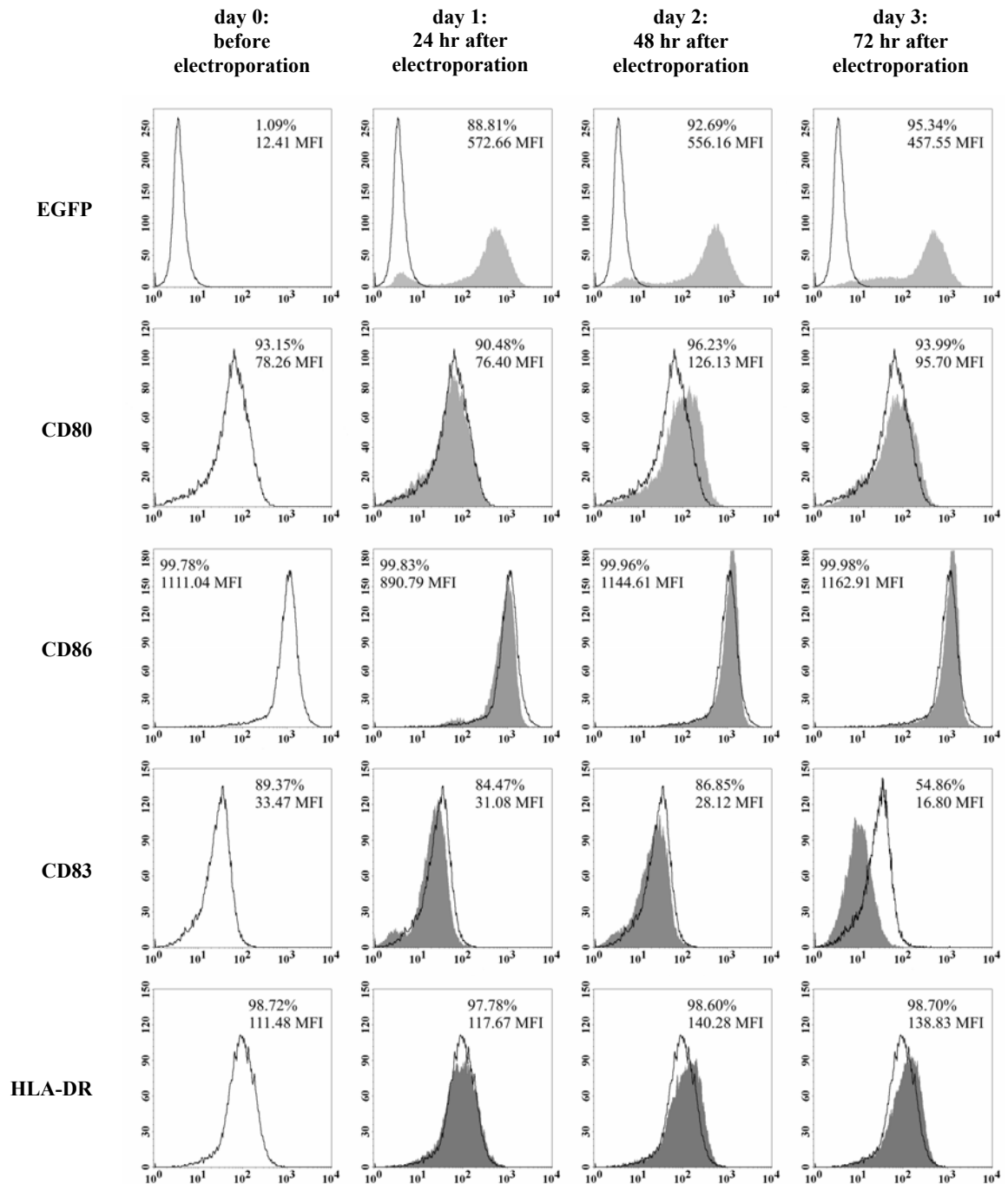


Figure 4.5 DC phenotypes before and after electroporation. Mature DCs were stained before and at several time points after electroporation with 12 μ g of EGFP cRNA. FACSTM histograms for day 0 show only fluorescence intensities of stained untransfected DCs. FACSTM overlay histograms for days 1, 2 and 3 show fluorescence intensities of both stained untransfected DCs (black curves) and stained EGFP cRNA-transfected DCs (filled curves). Staining was performed with PE-conjugated antibodies specific for molecules expressed on the cell surface. Staining with unspecific PE-conjugated antibodies was included as an isotype control (not shown). For definition of surface marker-specific PE fluorescence and surface marker-positive cells see Figure 4.1.

necessary for interaction with lymphocytes. Therefore, after 8 days in culture, one aliquot of mature DCs was stained with PE-conjugated antibodies for CD80, CD86, CD83 and

HLA-DR in order to define their phenotype before electroporation. The other aliquot, containing 3×10^6 cells, was electroporated with 12 μg of EGFP cRNA. Transfected cells were divided into three aliquots and put back into culture with IL-4 and GM-CSF. Aliquots were harvested 24, 48 or 72 hr after electroporation. Expression of EGFP, CD80, CD86, CD83 and HLA-DR was analysed in FACS™ for each time point.

All transfected aliquots showed stable expression of EGFP (Figure 4.5). No significant shifts in the percentages of CD80, CD86 and HLA-DR-positive cells were observed at any of the three time points after electroporation. The number of CD83-positive cells decreased from 89% on day 0 to 55% on day 3, which is most probably an effect caused by the lack of maturation cytokines in the medium and not by electroporation. The only MFI shift was observed in the case of CD86 (MFI down from 1111 before electroporation to 890 a day later), if significant at all, possibly indicating that on average single cells expressed somewhat less of this co-stimulatory molecule. On days 2 and 3, MFI of CD86 returned to the higher range (MFI 1144 and 1162). It could be concluded from these experiments that electroporation did not alter the expression of several important antigen-presenting and co-stimulatory molecules on the surface of mature DCs and therefore should not be detrimental for their interaction with T-cells.

4.1.4 Electroporation with increasing amounts of EGFP cRNA

Since an important goal of these studies was to optimise antigen processing and presentation by the DCs following RNA transfer, it was important to determine whether changing the RNA concentration would have an impact on the efficiency of transfection and the amount of protein produced by the DCs. Therefore, varying amounts of EGFP cRNA (2, 4 or 8 μg) were transfected into 2×10^6 mature DCs, which were then analysed by fluorescence microscopy and flow cytometry at different time points.

More RNA indeed meant more green cells (Figure 4.6). This difference was detected early, only 6.5 hr after electroporation. Only a few DCs transfected with 2 or 4 μg of EGFP cRNA were slightly positive in FACS™, but under a UV-microscope they were either not seen to emit green light at all, or only very weakly. At the same time, many DCs

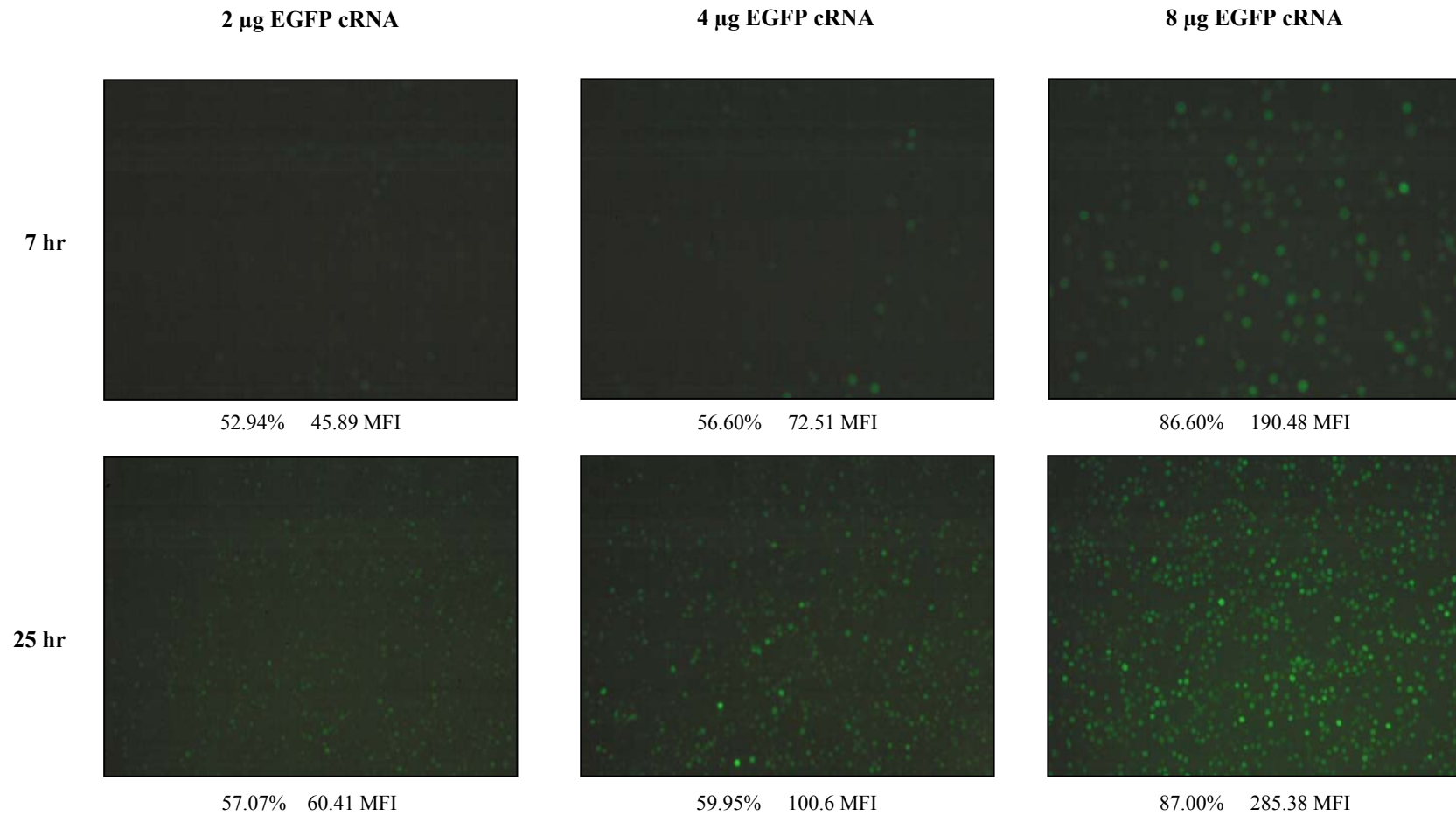


Figure 4.6 DCs after electroporation with increasing amounts of EGFP cRNA. Mature DCs were electroporated with 2, 4 or 8 μg of EGFP cRNA. Fluorescence microscopy photographs show EGFP cRNA-transfected DCs 7 hr and 25 hr after electroporation. The corresponding percentages of EGFP-positive cells and EGFP mean fluorescence intensities (MFI) were calculated in overlay histograms based on FACS™ data that were obtained 6.5 hr and 24.5 hr after transfection. For definition of EGFP-specific fluorescence and EGFP-positive cells see Figure 4.2.

transfected with 8 μg were visibly green. Precise FACSTM analysis at all time points confirmed that the difference between 2 and 4 μg was minimal, as in both cases 55-60% of the cells measured positive for EGFP. Doubling the amount to 8 μg resulted in a convincingly higher number of cells reached by the RNA, yielding approximately 90% positive cells. As expected, protein levels were also influenced by the amount of transfected RNA. The mean fluorescence intensity at 24.5 hr showed only a 1.6-fold difference between 2 and 4 μg (MFI 60 vs. 101), whereas a 2.8-fold difference was found between 4 and 8 μg (MFI 101 vs. 285).

The kinetics of EGFP synthesis was the same in the three electroporated samples with the maximum MFI reached 24.5 hr after transfection and only a slight decrease over the following two days (Figure 4.7). At all time points, the MFI of DCs transfected with 8 μg remained higher than the MFI of DCs transfected with either 4 or 2 μg of EGFP cRNA.

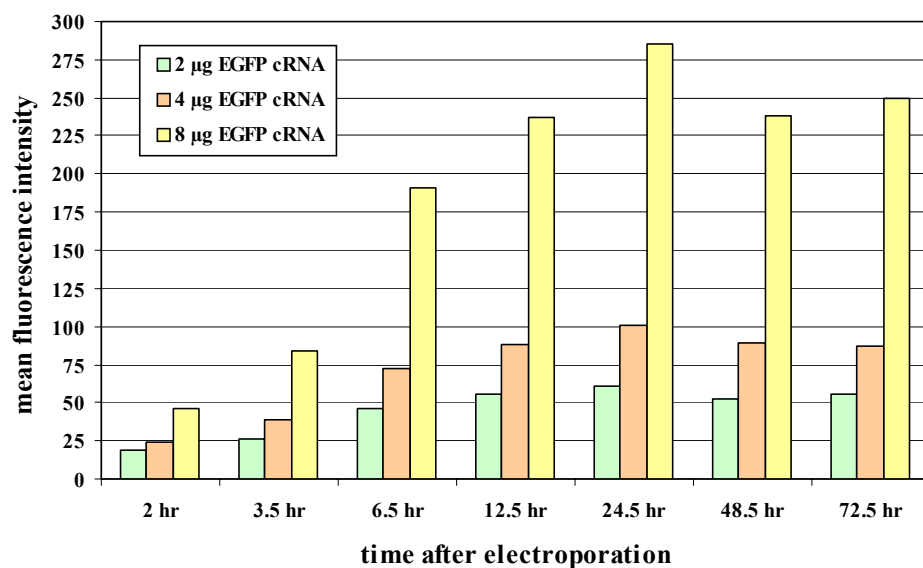


Figure 4.7 EGFP expression in DCs transfected with increasing amounts of EGFP cRNA. Mature DCs were electroporated with 2, 4 or 8 μg of EGFP cRNA. The fluorescence of EGFP cRNA-transfected DCs was measured in FACSTM at different time points after electroporation. In the diagram, mean fluorescence intensities of EGFP cRNA-transfected DCs are depicted. These were calculated in overlay histograms based on FACSTM data. For definition of EGFP-specific fluorescence and EGFP-positive cells see Figure 4.2.

In order to achieve better antigen presentation, through generation of more DCs containing more transferred RNA, thereby providing more peptides for presentation within their MHC molecules, RNA dose-finding seemed to be the right method for enhancing the function of

DCs. After this experiment it remained to be seen if T-cells would really react more strongly to the DCs that were pulsed with higher amounts of tumour RNA. DCs needed some time to recover from the electric shock, and to produce, process and present the antigen. In the case of EGFP, the time needed to recuperate and express the highest amount of the protein summed up to approximately 24 hr.

4.1.5 Kinetics of EGFP cRNA degradation and EGFP expression

The next issue that was addressed was how transfected RNA behaved inside the cell. Most importantly, how long after electroporation or lipofection could transfected RNA be detected and did the kinetics of its degradation correlate with the kinetics of protein expression?

To examine these parameters, DCs were aliquoted immediately after electroporation with 8 μg of EGFP cRNA. From these aliquots, total cellular RNA, also containing the transfected EGFP cRNA, was isolated at 0.5, 1.5, 3, 6, 12, 24, 48 and 72 hr after electroporation. Isolated RNA was reverse transcribed into cDNA. The quantity of cRNA, i.e. cDNA coding for EGFP, was then assessed in all samples using the highly sensitive and precise method of real-time PCR. If samples are compared with a standard, the amount of measured RNA can be expressed as the number of molecules. Unfortunately, a standard for EGFP RNA was not available. Since in an experimental setup without a standard a good reference is important, RNA was isolated from the transfected DCs only 10 and 30 min after electroporation.

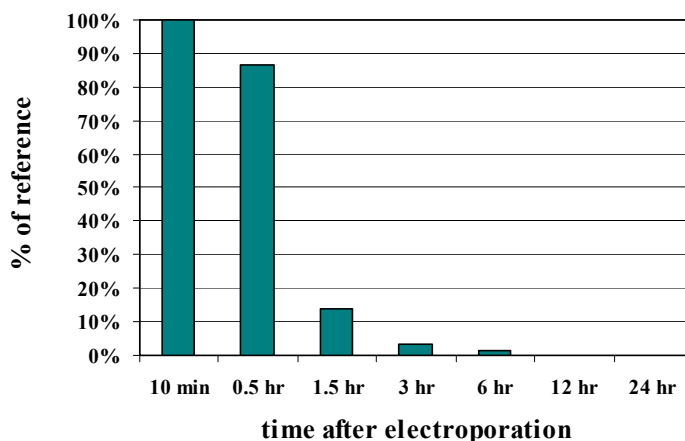


Figure 4.8 Kinetics of EGFP cRNA degradation. Total cellular RNA was isolated from DCs transfected with 8 μg of EGFP cRNA at different time points after electroporation. Isolated RNA was reverse transcribed into cDNA and the amount of EGFP message was assessed by real-time PCR using EGFP-specific primers. The diagram shows the amounts of EGFP message expressed relative to the 10 min value which was taken as the 100% reference.

The comparison of the 10 min and the 30 min values (Figure 4.8) revealed that within those 20 min the amount of EGFP cRNA decreased from 100% (10 min) to 86% (30 min). Therefore, the 30 min value was judged to be a suitable reference, since it still encompassed most of the RNA that made contact with the cells and provided a time period that allowed appropriate technical handling of the samples.

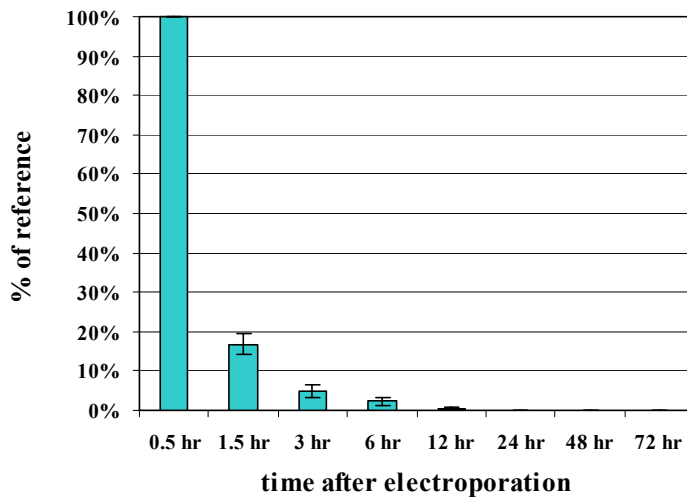


Figure 4.9 Kinetics of EGFP cRNA degradation – mean values. Total cellular RNA was isolated from EGFP cRNA transfected-DCs at different time points after electroporation. Isolated RNA was reverse transcribed into cDNA and the amount of EGFP message was assessed by real-time PCR using EGFP-specific primers. The diagram shows the amounts of EGFP message expressed relative to the 0.5 hr value which was taken as the 100% reference. Mean values and their standard deviations represent seven experiments.

Small standard deviations showed that RNA had similar degradation kinetics in all samples, irrespective of the amount used for transfection (Figure 4.9). The value at 0.5 hr, depicted as the 100% reference, was less than what was put into the electroporation cuvette because not all RNA was transported into the cells during transfection. The value at 1.5 hr

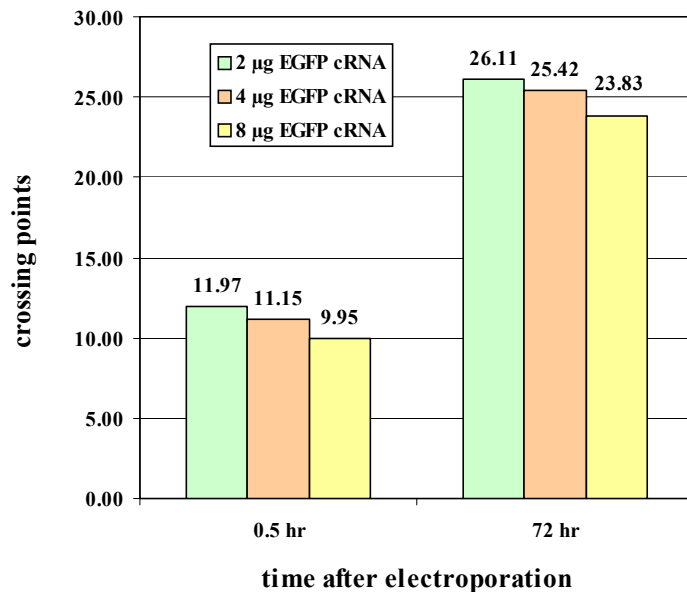


Figure 4.10 Detection of transfected EGFP cRNA 72 hr after electroporation Total cellular RNA was isolated from DCs transfected with 2, 4 or 8 µg of EGFP cRNA at different time points after electroporation. Isolated RNA was reverse transcribed into cDNA and the amount of EGFP message was assessed by real-time PCR using EGFP-specific primers. The diagram shows crossing points (real-time PCR raw data) which can be used to calculate relative or absolute amounts of analysed genetic message – the higher the crossing point, the less message detected.

was stunningly low, indicating that within only an hour the amount of RNA rapidly decreased to approximately 17% of that which was associated with the cells in the first place. It seems that a lot of RNA was lost due to the transfection method and to the presence of extracellular and intracellular RNases. The value at 3 hr showed that within the following hour and a half another 12% of the RNA was lost, and then between 6 and 72 hr less than 1% could be detected. Keeping in mind that all these values were calculated relative to the highest amount measured only 30 min after electroporation, it is clear that <1% did not necessarily mean that extremely little or no RNA could be found. Real-time PCR raw data (crossing points between 23 and 27) proved that even 72 hr after electroporation, EGFP cRNA could still be detected inside the transfected cells (Figure 4.10). Higher crossing points do mean less RNA, but only the analysis of those above 35 is critical because of the technical limitations imposed by the LightCycler® instrument in which real-time PCR is performed.

Interestingly, plotting the kinetics of EGFP cRNA degradation against the kinetics of EGFP expression showed that RNA and protein behaved very differently (Figure 4.11). This raised the question of how protein production could increase while RNA degradation eliminated most of the translation substrate from the cell.

In mature electroporated DCs, green fluorescence peaked at 12 hr (Figure 4.11A). At the same time, EGFP cRNA could still be detected, but less than 1% of the amount that had been found at 0.5 hr. The same RNA and protein kinetics experiment was performed with lipofected immature DCs (Figure 4.11B). In these cells, EGFP cRNA degradation took place at a slower pace, with 40% of the maximum amount still detectable 12 hr after lipofection. Since lipofected RNA entered the cell as part of an RNA-lipid complex, this most likely meant that RNA was better protected from RNases by the lipids used as the transfection reagent. Also with lipofection, the question remained whether the real-time PCR studies were detecting extracellular RNA in addition to the intracellular transfected RNA.

In order to eliminate the RNA that had not entered the cells and was left floating in the culture medium, all cell samples were washed twice before RNA isolation. Nevertheless, it was still possible that the negatively charged RNA remained electrostatically attached to the slightly negatively charged cell surface. Therefore, it was not certain whether the RNA

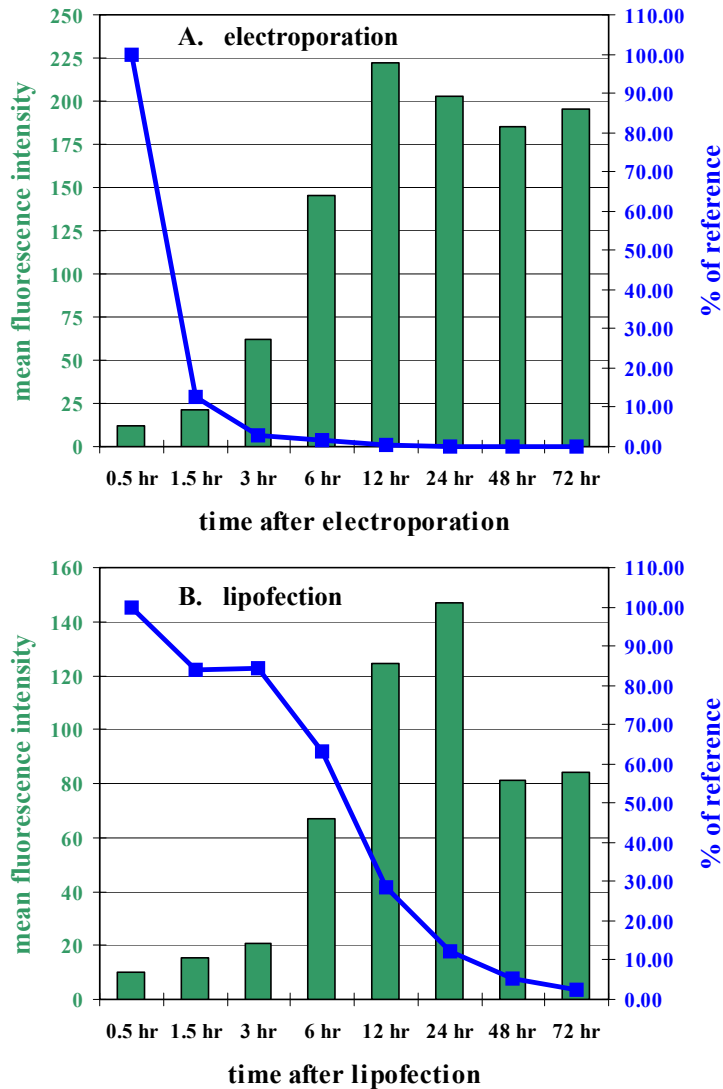


Figure 4.11 Kinetics of EGFP cRNA degradation and kinetics of EGFP expression. Mature DCs were electroporated (A) and immature DCs were lipofected (B) with 8 μg of EGFP cRNA. At different time points after transfection, the fluorescence of EGFP cRNA-transfected DCs was measured in FACS™ and total cellular RNA was isolated from the cells. Isolated RNA was reverse transcribed into cDNA and the amount of EGFP message was assessed by real-time PCR using EGFP-specific primers. In the diagram with two Y-axes, the kinetics of RNA degradation is plotted against the kinetics of EGFP expression. On the right Y-axis, the amounts of EGFP message are shown (curve). These were expressed relative to the 0.5 hr value which was taken as the 100% reference. On the left Y-axis, corresponding mean fluorescence intensities are shown (columns). These were calculated in overlay histograms based on FACS™ data. For definition of EGFP-specific fluorescence and EGFP-positive cells see Figure 4.2.

detected by real-time PCR derived only from inside the cells or may also have included RNA associated with the cell surface. Even though extracellular RNA could still be internalised by the DC, the origin of RNA is important because most of the potentially measured extracellular RNA is not functional and could not contribute to the synthesis of EGFP. The rapid RNA degradation effect that was observed may be an artefact due to large amounts of extracellular RNA that are aggressively degraded by RNases in the serum containing culture medium.

Contradictory kinetics of RNA degradation and protein synthesis may, to a certain extent, be explained by the delayed development of green fluorescence due to the time needed for proper folding of the EGFP molecule and its chromophore formation. While RNA was being degraded, EGFP was being produced, but could not be detected. At the moment

when it seemed the electroporated RNA levels were extremely low compared to what had been measured at the beginning, EGFP started fluorescing.

4.1.6 Summary of the data obtained in the EGFP system

If DCs were generated from identical stocks of frozen PBMCs and according to same protocol, they displayed an unchanged phenotype. Standardization of the DC system was important for the reproducibility of results in precise quantitation experiments. The highest efficiency of EGFP cRNA transfection into DCs was achieved with electroporation. Lipofection yielded significantly fewer EGFP-positive cells, but individual lipofected cells expressed more EGFP based on transfected RNA than individual electroporated cells. Mature DCs expressed more EGFP than immature DCs, the maximum being reached 12 hr after electroporation. DCs remained EGFP-positive for at least 5 days. Expression of important antigen-presenting and co-stimulatory molecules on the surface of DCs did not change after electroporation with EGFP cRNA. EGFP cRNA dose-finding showed that more RNA used in electroporation would indeed result in higher EGFP expression. Even though the expression of EGFP in transfected DCs increased over the first 12 hr after electroporation, the kinetics of EGFP cRNA degradation revealed that the amount of transfected RNA rapidly decreased shortly after electroporation. EGFP cRNA could still be found in transfected DCs 3 days after electroporation. It was unclear whether EGFP cRNA detected in quantitation experiments was of intracellular origin or also derived from the cell surface.

Experimental model for the study of TAA expression in RNA-transfected DCs

Identification of multiple melanoma-associated antigens was a major achievement in tumour immunology within the last decade (reviewed by Castelli *et al.* 2000). The biochemical approach (peptide extraction from MHC molecules and their mass spectrometric analysis) and/or the genetic approach (screening of tumour cDNA libraries by anti-tumour T-cells) were used to define twenty different MAAs to date and, at least, one MHC epitope has been identified for most of these tumour-associated antigens. Based on their expression patterns in malignant and normal tissues, the antigens have been classified into three groups: melanocyte differentiation antigens, tumour/testis-specific antigens and melanoma-specific antigens.

For these studies, the melanoma model was chosen to quantitatively analyse antigen transfection, processing and presentation in DCs because it is well characterised at the cellular and molecular levels. Tyrosinase, Melan-A and CDK4-R24C antigens were selected for these experiments.

Tyrosinase is a transmembrane protein of 529 amino acids. This enzyme is critical for the synthesis of melanin in melanocytes and retina cells. In the case of melanoma, it belongs to the melanocyte differentiation antigens group of tumour-associated antigens. The following reagents were available for tyrosinase:

- cDNA in a plasmid vector (1888 bp insert in pZeoSV2+/huTyr)
- two HLA-A*0201-restricted peptides (tyrosinase₃₆₉₋₃₇₇ epitope YMNGTMSQV that was predicted based on the cDNA sequence and tyrosinase₃₆₉₋₃₇₇ epitope YMDGTMSQV that was later found to be naturally presented by the cells)
- two CTL clones specific for these epitopes (TyrF8 CTL and IVS B CTL)

Melan-A, also known as MART-1 (melanoma antigen recognised by T-cells 1), is a transmembrane protein of 118 amino acids. Like tyrosinase, it is expressed in melanocytes and retina cells, but its function is still unknown. It belongs to the melanocyte differentiation antigens group of melanoma-associated antigens. The following reagents were available for Melan-A:

- cDNA in a plasmid vector (656 bp insert in pcDNA1/Amp/Aa1.2)
- one HLA-A*0201-restricted peptide (Melan-A₂₆₋₃₅ epitope ELAGIGILTV)

- two CTL clones specific for this epitope (A42 CTL and 11/33 CTL)

CDK4-R24C is a mutated form of CDK4, a protein of 301 amino acids that serves as a stimulator in cell cycle progression. This particular mutation renders CDK4 insensitive to its inhibitor, resulting in cell cycle dysregulation and, as a consequence, uncontrolled cell growth. CDK4-R24C is unique to melanomas and belongs to the melanoma-specific antigens group. The following reagents were available for CDK4-R24C:

- cDNA in a plasmid vector (1331 bp insert in pcDNA1/Amp/C11.1)
- one HLA-A*0201-restricted peptide (CDK4-R24C₂₃₋₃₂ epitope ACDPHSGHFV)
- one CTL clone specific for this epitope (14/35 CTL)

Furthermore, five different melanoma cell lines were used in these studies:

- 623.38 MEL
- A375 MEL
- IL-2 MEL
- SK23 MEL
- SK29 MEL

4.2 Transfection of DCs with RNA encoding tyrosinase

CTLs are activated through their TCRs that recognise MHC class I molecules presenting antigenic peptides. Activated CTLs secrete IFN- γ , among other cytokines. In a natural situation, IFN- γ directly inhibits viral replication in infected cells, activates macrophages, increases expression of MHC class I and other molecules involved in peptide processing and presentation, and also increases or even induces MHC class II expression. In immunotherapy against tumours, viruses or other pathogens are not always present, but the CTLs react in the same manner after specifically recognising pMHC on tumour cells. They can also recognise their pMHC ligands on other cell types, such as APCs, if the APCs are provided with either synthetic peptides or genetic information encoding the peptide in the form of DNA or RNA.

In functional assays, DCs pulsed with cRNA coding for tyrosinase were co-incubated with the tyrosinase-specific TyrF8 CTL clone recognising the tyrosinase₃₆₉₋₃₇₇ peptide. IFN- γ

secretion by these CTLs was taken as a measure of DC stimulatory capacity and was assessed by ELISA. In quantitative experiments, amounts of tyrosinase message were determined in real-time PCR using published tyrosinase-specific primers.

The tyrosinase system was used to address the following questions:

- How long after their last restimulation should CTLs be added to the transfected DCs for efficient stimulation?
- How much time after electroporation should elapse before the DCs show efficient antigen production, processing and presentation?
- Does exposure of DCs to the electroporation procedure alter their function so that they activate CTLs independent of pMHC expression?
- How much single-species tumour-antigen cRNA must be used for efficient CTL stimulation?
- How many transfected DCs are needed in order to fully engage TCRs on CTLs?
- How reproducible are the results in a standardised DC-RNA-CTL system?
- Which RNA concentration is important for electroporation?
- How quickly is transfected single-species tumour-antigen cRNA degraded inside the DCs?
- How does treatment of transfected DCs with RNase influence RNA degradation kinetics?

4.2.1 Time in culture needed for CTLs to most efficiently react to antigen presentation

It was observed that the TyrF8 CTL clone was extremely sensitive to cell culture conditions and that it had an individual rhythm of proliferation and reactivity, depending on how often it had already been restimulated. Standardising the DC-RNA-CTL system meant expanding the TyrF8 CTLs and freezing them in such a quantity that for each of the subsequent experiments ampoules from the same stock could be utilised. Using the same source of frozen cells, the same restimulation conditions and the same culture conditions provided a hypothetical guarantee that once these CTLs were applied in an assay, they would show similar or even identical reactivities against the antigen-presenting cell.

According to experience, TyrF8 CTLs needed to be restimulated every two weeks in order to survive and proliferate. If CTLs required time to recover after thawing, and if after two weeks they would no longer proliferate, it was essential to determine the optimal time to harvest them from restimulation cultures so that their function could be assessed after co-incubation with test APCs.

To address this point, one ampoule of TyrF8 CTLs was thawed and restimulated. The same was done once again five days later. On the day of co-incubation with the test DCs, one set of the CTLs had already been in culture for thirteen days and the other set for only eight days. Whereas the maximum amount of EGFP cRNA used for transfection had been 8 μg , the decision was made to use more tyrosinase cRNA. RNA coding for tyrosinase is approximately twice as long as RNA coding for EGFP, therefore a sample of the same mass contains less message for tyrosinase than message for EGFP. Electroporation was performed with 12 μg of tyrosinase cRNA and 3×10^6 DCs. Twenty-five hours later, either 13-day or 8-day TyrF8 CTLs were mixed with the transfected DCs. The number of DCs per well was 4×10^4 , 2×10^4 , 1×10^4 or 5×10^3 . The number of 2×10^4 CTLs per well was constant, giving stimulator to effector ratios of 2:1, 1:1, 1:2 and 1:4.

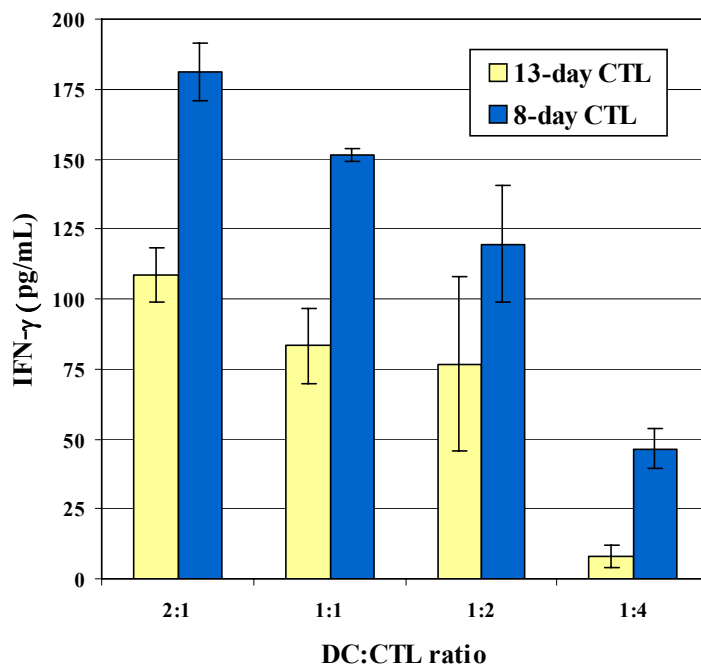


Figure 4.12 Reactivities of 8-day old and 13-day old TyrF8 CTLs. Mature DCs were electroporated with 12 μg of tyrosinase cRNA. On the day of mixing with transfected DCs, TyrF8 CTLs, specific for tyrosinase pMHC, had been in culture for 8 or 13 days after the last restimulation. The diagram shows the amount of IFN- γ secreted by 2×10^4 activated CTLs during the 24 hr co-incubation with 4×10^4 , 2×10^4 , 1×10^4 or 5×10^3 transfected DCs. IFN- γ was measured in supernatants by ELISA. Mean values and their standard deviations represent co-incubation triplicates.

TyrF8 CTLs that had spent only eight days in culture between the last restimulation and co-incubation with the test DCs reacted stronger than the thirteen-day old CTLs, producing

almost twice as much IFN- γ (e.g. 181 pg/mL IFN- γ vs. 109 pg/mL IFN- γ at 2:1) in response to the presented tyrosinase antigen (Figure 4.12). Better effector cell stimulation was also observed with higher numbers of stimulator cells (181 pg/mL IFN- γ at 2:1 vs. 46 pg/mL IFN- γ at 1:4 when compared using 8-day CTLs). This showed that taking more DCs ensured better engagement of CTLs, resulting in stronger activation.

4.2.2 Time needed for transfected DCs to most effectively present the antigen

Data obtained in transfection experiments with EGFP cRNA showed that the maximum expression of protein was reached approximately 24 hr after electroporation. In the EGFP system, green fluorescence served as a measure of protein expression. The tyrosinase system was not completely comparable because it was based on RNA coding for a protein with different properties and because the measurement of protein expression was indirect and required antigen presentation to be assessed in a functional assay. Nevertheless, it seemed fair to assume that electroporated DCs would need time to recover from the electric shock and to produce, process and present the antigen on the surface. The question remained whether CTLs would react better if they were present throughout the production and the processing phase, or whether they would respond better if they first came into contact with the DCs after the pMHC complexes had already been generated.

A kinetic experiment was performed to address this question. Here, 24 μ g of tyrosinase cRNA were used in electroporation of 3×10^6 DCs. Transfected DCs were divided into two aliquots. One aliquot was used 2 hr later for antigen presentation to the 8-day TyrF8 CTLs. The other aliquot was mixed with 9-day CTLs 25 hours after electroporation. Once again 4×10^4 , 2×10^4 , 1×10^4 or 5×10^3 DCs and 2×10^4 CTLs gave the DC:CTL ratios of 2:1, 1:1, 1:2 and 1:4.

As shown in Figure 4.13, more efficient CTL stimulation was observed with the DCs that were given 25 hr to process the transfected RNA before addition of CTLs, compared to 2 hr (e.g. 499 pg/mL IFN- γ vs. 246 pg/mL IFN- γ at 2:1). As expected, the highest DC:CTL ratio again resulted in the strongest CTL stimulation (499 pg/mL IFN- γ at 2:1 vs. 84 pg/mL IFN- γ at 1:4 when compared using CTLs stimulated by DCs 25 hr after electroporation). This meant that 4×10^4 DCs induced the maximum IFN- γ secretion by 2×10^4 CTLs.

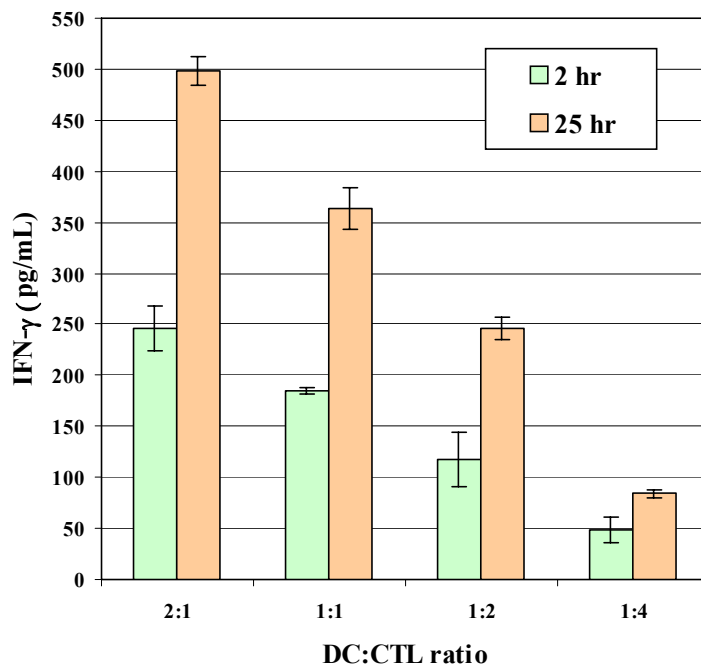


Figure 4.13 Stimulatory capacities of tyrosinase cRNA-transfected DCs 2 hr and 25 hr after electroporation. Mature DCs were electroporated with 24 μ g of tyrosinase cRNA. At the moment of mixing with TyrF8 CTLs, specific for the tyrosinase pMHC, transfected DCs had been in culture for 2 or 25 hr after electroporation. The diagram shows the amount of IFN- γ secreted by 2×10^4 activated CTLs during the 24 hr co-incubation with 4×10^4 , 2×10^4 , 1×10^4 or 5×10^3 transfected DCs. IFN- γ was measured in supernatants by ELISA. Mean values and their standard deviations represent co-incubation triplicates.

In the previous experiment, 12 μ g of tyrosinase cRNA were used in electroporation and TyrF8 CTLs produced 181 pg/mL IFN- γ when stimulated by the transfected DCs. In this experiment 24 μ g of tyrosinase cRNA were introduced into the DCs and they stimulated the same CTLs to produce 499 pg/mL IFN- γ . This comparison indicated that better stimulation of an antigen-specific CTL clone could be achieved by transfecting more antigen RNA into the DCs. DCs would in turn express more tyrosinase protein and more pMHC at the cell surface.

In general, these experiments showed that TyrF8 CTLs should be used in co-stimulation experiments after only 8 days in culture following thawing and restimulation. After transfection and before contact with the TyrF8 CTLs, DCs should also be allowed approximately 24 hr to generate pMHC before contact with the TyrF8 CTLs.

4.2.3 Controls in the DC-RNA-CTL system

In assessing function in the DC-RNA-CTL system, a number of controls were important. Two-hour incubation of PBMCs in plastic cell culture dishes resulted in generation of monocyte monolayers adhering to the plastic surface. Non-adherent PMBCs were

carefully washed away and the remaining monocytes were differentiated into DCs within approximately one week. Despite washing, 10-30% lymphocytes were detected within the enriched monocyte population. These lymphocytes were also present among the mature DCs after 8 days of culture and were always part of the cell suspension used in electroporation. Therefore, it was possible that after transfection the contaminating lymphocytes could produce IFN- γ in response to the pulsed DCs or even in response to their own contact with extremely high amounts of RNA. If such a response occurred, IFN- γ would have been produced in the electroporated suspension without the addition of antigen-specific TyrF8 CTLs. This would have required subtraction of the background IFN- γ secretion from the reactivity attributed to the TyrF8 CTLs.

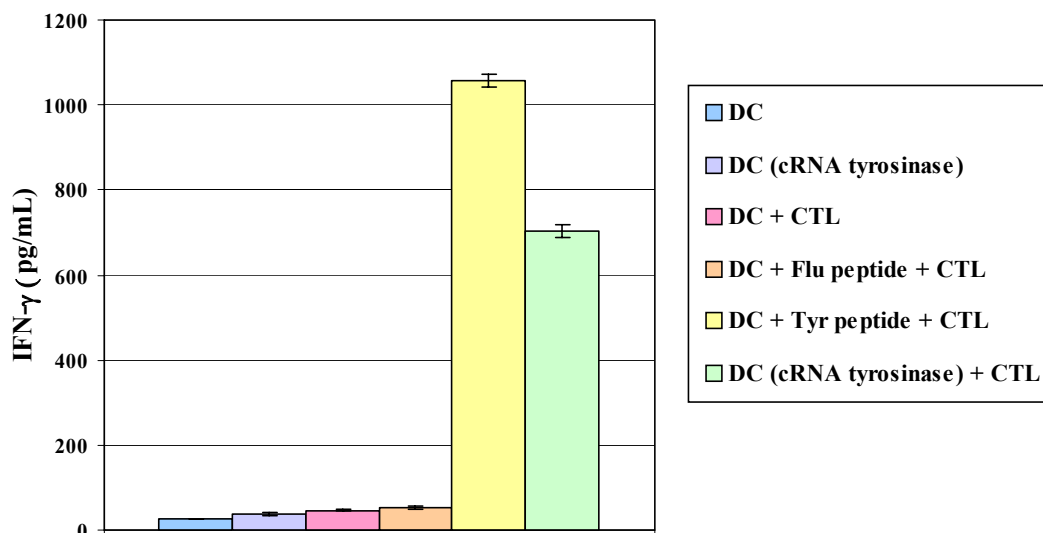


Figure 4.14 Controls in the DC-RNA-CTL system. Mature DCs were electroporated with 24 μg of tyrosinase cRNA. One day later, transfected and untransfected DCs were either incubated alone or mixed with TyrF8 CTLs, specific for the tyrosinase pMHC. Untransfected DCs were also pulsed exogenously with 10 $\mu\text{g}/\text{mL}$ of Tyr peptide YMNGTMSQV or irrelevant Flu peptide GILGFVTL for 2 hr prior to the addition of TyrF8 CTLs. The diagram shows the amount of IFN- γ secreted by 2×10^4 activated CTLs during the 24 hr co-incubation with 4×10^4 DCs. IFN- γ was measured in supernatants by ELISA. Mean values and their standard deviations represent co-incubation triplicates.

It also had to be determined whether TyrF8 CTLs were activated to unspecific IFN- γ secretion through their experimental manipulation. This was assessed after incubation of TyrF8 CTLs for 24 hr either alone or with peptide-pulsed DCs or with unpulsed DCs. Mature DCs pulsed with exogenous peptides through a simple two-hour co-incubation, prior to the addition of CTLs, were generally included in experiments as positive (Tyr

peptide YMNGTMSQV) or negative (Flu peptide GILGFVTL) controls for the antigen-presenting capacity of the DCs and the specificity of the CTLs.

As shown in Figure 4.14, untransfected and transfected DCs alone secreted small amounts of IFN- γ (27 pg/mL and 38 pg/mL respectively). The addition of TyrF8 CTLs to the untransfected DCs did not increase IFN- γ production significantly (46 pg/mL). The irrelevant Flu peptide presented within MHC class I molecules on the surface of DCs was not recognised by TyrF8 CTLs (53 pg/mL). As expected, TyrF8 CTLs were stimulated to secrete high amounts of IFN- γ only by specific recognition of the synthetic Tyr peptide exogenously pulsed onto the DCs or the natural Tyr peptide produced by the DCs themselves after transfection of tyrosinase cRNA (1056 pg/mL and 703 pg/mL, respectively).

4.2.4 Electroporation with increasing amounts of tyrosinase cRNA

In terms of triggering CTLs through antigen presentation by the DCs, it remained to be seen how much RNA should be transfected and how many pulsed DCs should be used in order to generate the highest possible stimulatory capacity.

Therefore, 48 μ g of tyrosinase cRNA were transfected into 3×10^6 mature DCs, in addition to the previously tested 24 μ g and 12 μ g. One day later, DCs presenting the tyrosinase antigen were exposed to the TyrF8 CTLs. The number of DCs per well was increased to 8×10^4 , but 4×10^4 and 1×10^4 were also taken as a control. With 2×10^4 CTLs per well, the stimulator to effector ratios were 4:1, 2:1 and 1:2.

As shown in Figure 4.15, with the 4:1 DC to CTL ratio, CTLs were not stimulated above the level reached with the 2:1 ratio (e.g. 1036 pg/mL IFN- γ at 4:1 vs. 1039 pg/mL IFN- γ at 2:1 for 48 μ g cRNA). It can be hypothesised that more DCs did not make a difference, since 4×10^4 DCs were enough to achieve the maximum engagement of TCRs on the 2×10^4 CTLs. The highest tyrosinase cRNA amount of 48 μ g indeed resulted in the highest stimulatory capacity of DCs (1036 pg/mL IFN- γ for 48 μ g vs. 602 pg/mL IFN- γ for 24 μ g vs. 181 pg/mL IFN- γ for 12 μ g at 2:1). With 48 μ g of transfected tyrosinase cRNA, 43% more IFN- γ secretion was induced than with 24 μ g, and 83% more than with 12 μ g.

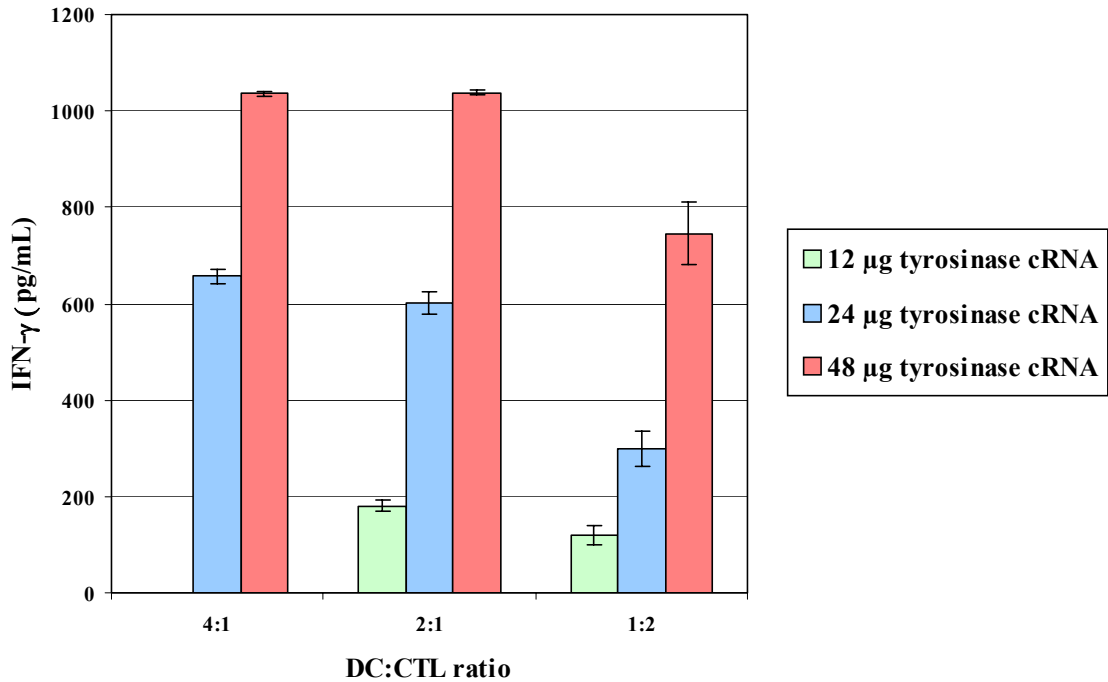


Figure 4.15 Stimulatory capacity of DCs transfected with increasing amounts of tyrosinase cRNA. Mature DCs were electroporated with 12, 24 or 48 μg of tyrosinase cRNA. One day later, transfected DCs were mixed with TyrF8 CTLs, specific for the tyrosinase pMHC. The diagram shows the amount of IFN-γ secreted by 2×10^4 activated CTLs during the 24 hr co-incubation with 8×10^4 , 4×10^4 or 1×10^4 DCs. IFN-γ was measured in supernatants by ELISA. Mean values and their standard deviations represent co-incubation triplicates.

Based on the results of this experiment the decision was made to electroporate DCs with 48 μg of single-species tumour-antigen cRNA and then to stimulate CTLs with those DCs in a stimulator to effector ratio of 2:1, i.e. 4×10^4 DCs and 2×10^4 CTLs.

4.2.5 RNA and DC concentrations in electroporation

In published studies of RNA electroporation into DCs and in the experiments performed here, not only were different amounts of RNA used, but also different cell numbers. The quantity of DCs available for an experiment was usually the limiting factor. It was possible that using fewer DCs would require taking proportionally less RNA in order to achieve levels of antigen presentation comparable to those in other experiments. Therefore, it was determined whether the number of DCs could be varied in electroporation without changing their stimulatory capacity.

The amount of tyrosinase cRNA was kept constant at 48 μg , but either 2×10^6 or 3×10^6 mature DCs were taken for electroporation, which was performed in a total suspension volume of 280 μL . Therefore, the RNA concentration per volume was the same in both cases (17 μg RNA per 100 μL), but the RNA concentration per number of DCs was different (24 μg RNA per 1×10^6 DCs and 16 μg RNA per 1×10^6 DCs).

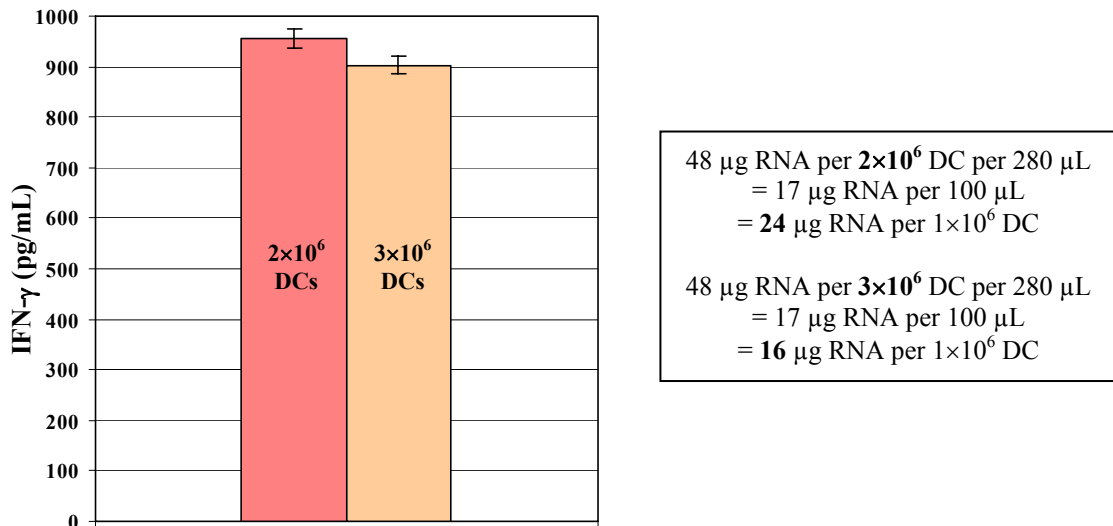


Figure 4.16 Stimulatory capacities of DCs electroporated in different concentrations. The same amount of tyrosinase cRNA, 48 μg , was transfected into either 2×10^6 or 3×10^6 mature DCs. One day later, transfected DCs were mixed with TyrF8 CTLs, specific for the tyrosinase pMHC. The diagram shows the amount of IFN- γ secreted by 2×10^4 activated CTLs during the 24 hr co-incubation with 4×10^4 DCs. IFN- γ was measured in supernatants by ELISA. Mean values and their standard deviations represent co-incubation triplicates.

As shown in Figure 4.16, co-incubation of TyrF8 CTLs with DCs electroporated under both conditions did not result in distinct IFN- γ levels (903 pg/mL and 956 pg/mL). This indicated that the important criterion for RNA entry into DCs was the amount of RNA present in the suspension volume, and less the number of DCs exposed to this concentration of RNA.

4.2.6 Reproducibility of results in a standardised system

As noted before, substantial time and effort were made to standardise the complicated DC-RNA-CTL system so that the results of different fine-tuned quantitation experiments could be compared. In Figure 4.17, IFN- γ secretion by TyrF8 CTLs in three separate

experiments was compared in order to assess the reproducibility of results. As described, mature DCs were electroporated with 48 μg of tyrosinase cRNA 24 hr before they were mixed with the CTLs. For comparison, mature DCs were pulsed with the Tyr peptide before addition of the CTLs.

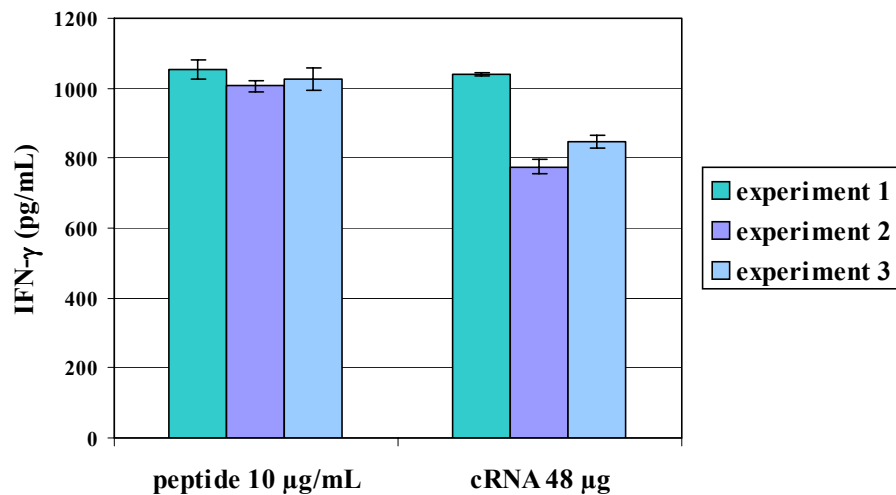


Figure 4.17 Stimulatory capacities of DCs electroporated in different experiments under the same conditions. In all three experiments, mature DCs were electroporated with 24 μg of tyrosinase cRNA. One day later, transfected DCs were mixed with TyrF8 CTLs, specific for the tyrosinase pMHC. Untransfected DCs were pulsed with 10 $\mu\text{g/mL}$ of Tyr peptide YMNGTMSQV for 2 hr prior to the addition of TyrF8 CTLs. The diagram shows the amount of IFN- γ secreted by 2×10^4 activated CTLs during the 24 hr co-incubation with 4×10^4 DCs. IFN- γ was measured in supernatants by ELISA. Mean values and their standard deviations represent co-incubation triplicates.

The comparison showed that if the same conditions were applied in the generation of DCs from stock PBMCs, if CTLs were restimulated the same number of times and cultured under the same conditions and if the same RNA was used every time in electroporation according to the same protocol, then the results of separate experiments displayed a good degree of reproducibility (with up to 20% variability).

4.2.7 Kinetics of tyrosinase cRNA degradation

The tyrosinase cRNA dose-finding experiment showed that the amount of RNA applied in electroporation influenced antigen presentation and CTL stimulation by DCs. Since the presence of transfected RNA in DCs is the prerequisite for antigen expression, it was of

interest to know how long after electroporation and in what quantities tyrosinase cRNA could be detected in the DCs. Furthermore, in comparison to EGFP cRNA, it was of interest to determine whether two different RNA species would display distinct characteristics in the same experimental setup.

After transfection of 6 μg , 12 μg , 24 μg or 48 μg of tyrosinase cRNA into 3×10^6 DCs in a volume of 270 μL , electroporated cells were aliquoted and incubated until total cellular RNA, containing the transfected tyrosinase cRNA, was isolated 0.5, 1.5, 3, 6, 12, 24, 48 or 72 hr later. This RNA was reverse-transcribed into cDNA, which was then quantitatively analysed in real-time PCR for the presence of tyrosinase message.

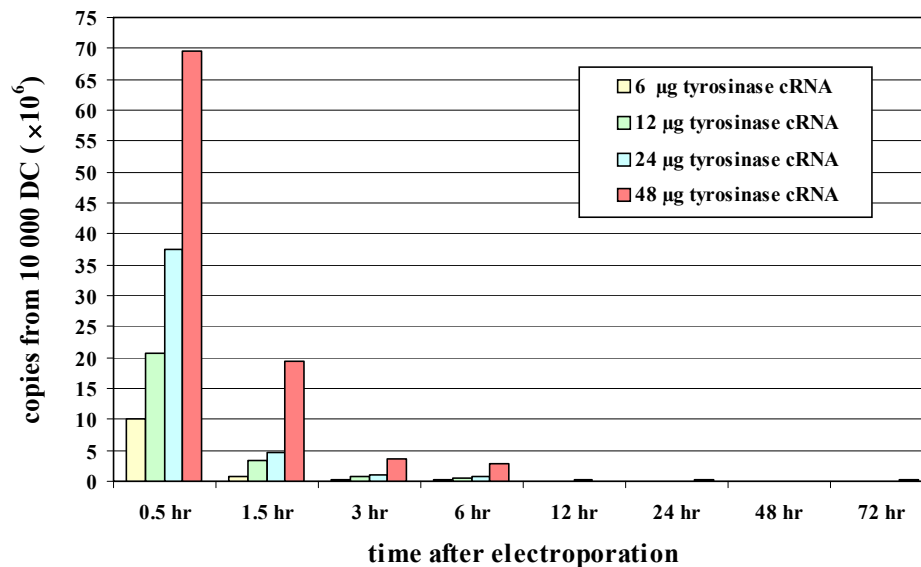


Figure 4.18 Kinetics of tyrosinase cRNA degradation – absolute values. Total cellular RNA was isolated from mature DCs transfected with 6, 12, 24 or 48 μg of tyrosinase cRNA at different time points after electroporation. Isolated RNA was reverse transcribed into cDNA and the amount of tyrosinase message was assessed by real-time PCR using tyrosinase-specific primers. The diagram shows the amounts of tyrosinase message expressed in absolute numbers of copies detected in samples originating from 1×10^4 cells. These were calculated from a real-time PCR tyrosinase standard curve.

A tyrosinase cDNA standard was available, making absolute quantitation possible (Figure 4.19). The amount of tyrosinase message was calculated as the number of copies of tyrosinase cRNA molecules found in association with a given number of cells. The most interesting observation at the 0.5 hr time point was that the two-fold differences in amount of applied tyrosinase cRNA remained almost unchanged after electroporation, incubation,

RNA isolation and reverse transcription (69.6 vs. 37.6 vs. 20.7 vs. 9.9 million copies). Considering the time the cells were given to process the transfected RNA, it was also interesting that the two-fold differences changed slightly, but were still detectable one hour later, at 1.5 hr (19.3 vs. 11.6 vs. 3.5 vs. 0.9 million copies). These studies demonstrated that through the transfection of DCs it was possible to establish a precise foundation for antigen-presentation, which had been established via functional assays, and was hereby confirmed at the molecular level.

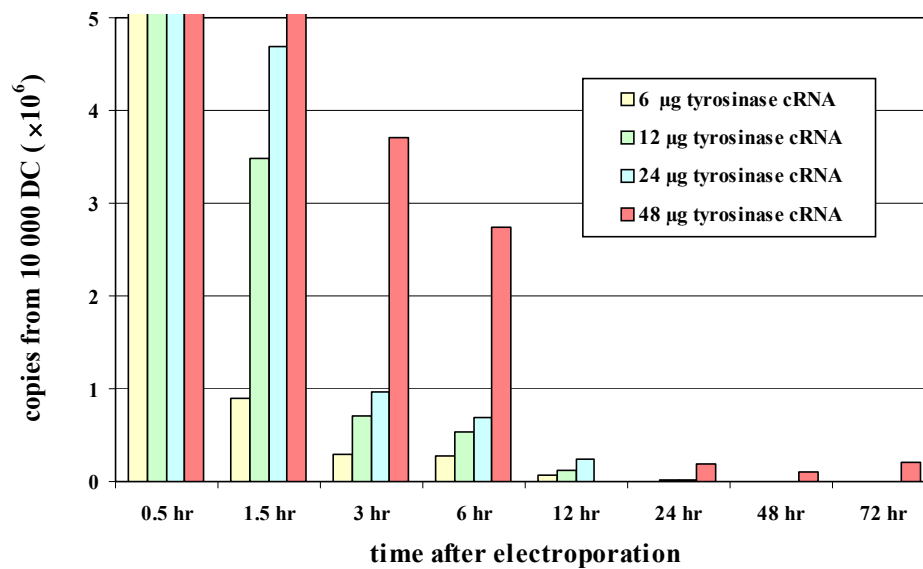


Figure 4.19 Kinetics of tyrosinase cRNA degradation – absolute values. Same diagram as in Figure 4.17, showing only the lower range of the Y-axis ($0-5 \times 10^6$ copies from 1×10^4 DCs).

The kinetics of tyrosinase cRNA degradation offered a possible explanation as to why the DCs pulsed with higher amounts of RNA developed higher stimulatory capacities. At all measured time points, the most tyrosinase message was detected in the cells that had received the most tyrosinase cRNA through electroporation (Figure 4.19). These data indicated that the large quantity of RNA provided not only ample starting material for antigen production within a short period of time, but also showed a prolonged presence in the DCs.

If the value measured at 0.5 hr was taken as a 100% reference and all other values were expressed relatively, it became obvious that tyrosinase cRNA had similar degradation kinetics to EGFP cRNA (Figure 4.20). Already between the 0.5 hr and the 1.5 hr time

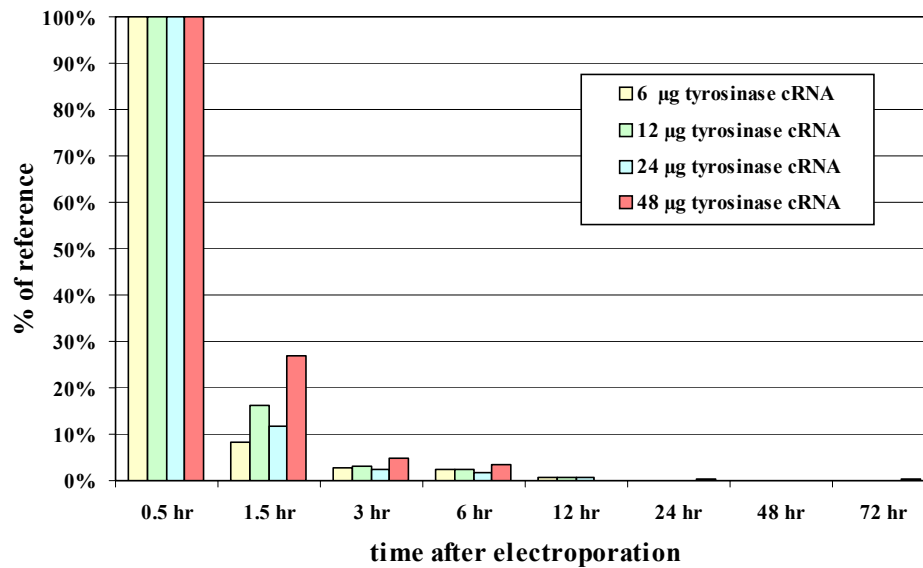


Figure 4.20 Kinetics of tyrosinase cRNA degradation – relative values. Total cellular RNA was isolated from mature DCs transfected with 6, 12, 24 or 48 µg of tyrosinase cRNA at different time points after electroporation. Isolated RNA was reverse transcribed into cDNA and the amount of tyrosinase message was assessed by real-time PCR using tyrosinase-specific primers. The diagram shows the amounts of tyrosinase message expressed relative to the 0.5 hr value which was taken as the 100% reference.

points, a strong decrease from 100% down to 8-27% was observed, depending on how much RNA had been used in electroporation. Even though the highest amount of electroporated RNA (48 µg) ensured the smallest decrease (73%), once again it was obvious that much of the applied RNA would not make contact with the DCs during electroporation or would be degraded by extracellular and intracellular RNases after association with the cells. Nevertheless, small amounts of tyrosinase cRNA could still be detected 72 hr after electroporation and the transfected DCs could activate antigen-specific CTLs within 48 hr after receiving the antigenic RNA.

It remained unclear whether RNA detected by the method of real-time PCR had come only from inside the cells or was also partly derived from the DC surface, the difference being important because extracellular RNA would not be functional in terms of antigen expression in the DCs. After electroporation, one half of tyrosinase cRNA-transfected DCs was incubated in the presence of RNase and the other half without RNase. Aliquots were taken from both suspensions to isolate total cellular RNA immediately after electroporation and 0.5 hr, 1.5 and 3 hr later. RNA was reverse transcribed into cDNA. The tyrosinase message was then quantitated in all cDNA samples. A house-keeping gene, α -enolase, was quantitated in real-time PCR as an internal control in order to differentiate

between extracellular and possible intracellular actions of added RNase. If indeed a substantial amount of tyrosinase cRNA amplified in the PCR had originated from outside the DCs, then the extracellular activity of RNase should result in different kinetics, i.e. a larger RNA decrease, compared to the samples incubated without RNase.

Table 4.1 Degradation of DC-associated tyrosinase cRNA and α -enolase mRNA in the presence or absence of RNase in the culture medium.

	without RNase		with RNase	
	tyrosinase	α -enolase	tyrosinase	α -enolase
0 hr	15.18	28.04	18.45	28.93
0.5 hr	15.02	28.35	22.96	33.51
1.5 hr	18.70	28.77	24.81	33.66
3 hr	19.89	29.11	26.60	35.76

Immediately after electroporation with 48 μ g of tyrosinase cRNA, mature DCs were resuspended in culture medium containing 5 μ g/mL or no RNase A. At different time points after electroporation, tyrosinase cRNA transfected-DCs were washed twice and then their total cellular RNA was isolated. Isolated RNA was reverse transcribed into cDNA and the amounts of transfected tyrosinase message and cell-expressed α -enolase message were assessed by real-time PCR, using tyrosinase-specific and α -enolase-specific primers. The table shows crossing points (real-time PCR raw data) which can be used to calculate relative or absolute amounts of analysed genetic message – the higher the crossing point, the less message detected.

Table 4.1 shows real-time PCR raw data - the higher the crossing point, the less RNA detected. In the presence of RNase, a strong decrease of tyrosinase message was observed between 0 hr and 0.5 hr. Such changes were not seen in the absence of RNase, suggesting that real-time PCR was indeed detecting extracellular tyrosinase cRNA, in addition to the intracellular tyrosinase cRNA. On the other hand, a similar behaviour between 0 hr and 0.5 hr was observed for α -enolase. This may indicate that RNase acted not only on the tyrosinase RNA sticking to the cell surface, but also on the intracellular RNA since α -enolase was undoubtedly of intracellular origin. It is not likely that RNase molecules crossed the membrane barrier and degraded α -enolase RNA in the cytoplasm. Even though all suspensions were washed twice between incubation with RNase and RNA isolation, it is possible that RNase was not fully eliminated and, as a consequence, was still present during cell lysis and RNA isolation. This may have resulted in an artefact seen as a decreased amount of α -enolase message. This problem might be circumvented by inactivating RNase with a protease, but on the other hand a protease may influence

receptors on the cell surface, sending signals into the cell and resulting in yet another artefact. Unfortunately, adding RNase to the transfected cells did not provide an unambiguous solution to the problem of differentiating between RNA outside and RNA inside the DCs, leaving this question open for further discussion and research.

4.2.8 Summary of the data obtained in the tyrosinase system

Standardization of the DC-RNA-CTL system showed that good reproducibility of results could be achieved if DCs and CTLs were cultured according to standardised protocols and if electroporation was performed under the same conditions with RNA from identical stocks. The reactivity of tyrosinase-specific CTLs was higher if they had spent not 13 days but only 8 days in restimulation cultures prior to co-incubation with tyrosinase cRNA-transfected DCs. The stimulatory capacity of transfected DCs was higher if they were allowed not only 2 hr but 25 hr to recuperate from electroporation and to produce the tyrosinase pMHCs. In contact with DCs, CTLs reacted by secreting IFN- γ only upon recognition of the synthetic peptide or the natural peptide produced by the DCs based on transfected RNA. Contaminating lymphocytes in electroporation DC suspensions did not produce IFN- γ above background. In electroporation, the important criterion for RNA entry into DCs seemed to be the amount of RNA present in the suspension volume, and less the number of DCs exposed to a certain concentration of RNA. Tyrosinase cRNA dose-finding showed that more RNA used in electroporation would indeed result in higher stimulatory capacities of transfected DCs. Kinetics of tyrosinase cRNA degradation, similar to kinetics of EGFP cRNA degradation, revealed that the amount of transfected RNA rapidly decreased within only 1.5 hr after electroporation. The smallest decrease was observed with the highest amount of RNA applied in electroporation. Tyrosinase cRNA could still be found in transfected DCs 3 days after electroporation. It remained unclear whether tyrosinase cRNA detected in quantitation experiments was of intracellular origin or also derived from the cell surface.

4.3 Transfection of DCs with RNA encoding a combination of antigens

In the tyrosinase system, conditions were investigated for optimal transfer of single-species RNA into DCs and the subsequent recognition by CTLs. Nevertheless, only one antigen was scrutinised. A combination of several antigens represents a situation that occurs naturally in which peptides have to compete for MHC molecules in order to be presented as pMHC ligands on the surface of DCs. To characterise the parameters for using multiple RNA species, three MAAs were studied. The tyrosinase, Melan-A and CDK4-R24C antigens were examined for their individual and combined use in DC-based immunotherapy. These three antigens were compared at the molecular level as single-species antigen RNA and as components of total cellular melanoma RNA. In quantitative experiments, amounts of tyrosinase, Melan-A and CDK4-R24C message in different RNA samples were determined by real-time PCR using published tyrosinase-specific primers and designed Melan-A-specific and CDK4-R24C-specific primers. Expressed genetic message being a basis for antigen presentation, the three antigens were further compared on the cellular level of presentation as pMHC by melanoma cells and RNA-transfected DCs. Stimulatory capacities of these cells were assessed by IFN- γ ELISA after co-incubation with antigen-specific CTLs. This data provided insight into the possibility of developing a generic vaccine based on DCs pulsed either with pooled single-species cRNAs or amplified RNA derived from malignant cells.

The three-antigen system (tyrosinase, Melan-A and CDK4-R24C) was used to address the following questions:

- How much more antigen message does an RNA sample contain after RT-PCR and *in vitro* transcription of total cellular tumour RNA?
- How much more antigen message does a single-species tumour-antigen cRNA sample contain, compared to total cellular tumour RNA samples?
- Do different CTL clones specific for the same antigen have different affinities for corresponding pMHC?
- How does the amount of antigen message in tumour cells correlate with the recognition of pMHC by antigen-specific CTLs?
- How efficient is electroporation with single-species tumour-antigen cRNA?
- How high is the stimulatory capacity of DCs pulsed with total cellular tumour RNA, compared to single-species tumour-antigen cRNA?

- Is it possible to stimulate CTLs of different specificities with DCs that were pulsed with pooled single-species tumour-antigen cRNAs?
- How does the amount of antigen message transfected into DCs correlate with the recognition of pMHC by antigen-specific CTLs?

4.3.1 Amount of antigen message in different RNA samples

The whole repertoire of proteins expressed by a malignant cell is encoded in its RNA. If that RNA is isolated from tumour cells and transfected into antigen-presenting cells, a basis is established for the expression of a wide variety of tumour-antigens in a non-tumour environment. DCs not only present these antigens more efficiently, but also interact better with T-cells due to their high expression of co-stimulatory and adhesion molecules. The strategy of pulsing DCs with total cellular tumour RNA offers a possible solution to the problem of insufficient information regarding TAAs. Relying on the fact that RNA from tumour cells likely contains message for several TAAs, the choice of the antigen and its presented epitope is left solely to the DC, and the need to know precise peptide sequences is eliminated. Furthermore, total cellular tumour RNA can be isolated from a relatively small amount of tumour tissue and then amplified through RT-PCR and *in vitro* transcription, providing enough working material for multiple experiments or vaccine production.

As noted before, several TAAs have been identified in the melanoma system and immune responses directed against them have been well characterised. Thereby, it was possible to compare total cellular RNA derived from five melanoma cell lines with single-species cRNA coding for three different MAAs. The studies using single-species tyrosinase cRNA described above showed that the amount of RNA electroporated into DCs influenced their stimulatory capacity. This raised the question of how much antigen message could be found in RNA samples isolated from tumour cells, which had already been used or were to be used for transfection into DCs.

To address this issue, various total cellular RNA samples were studied. These included isolated RNA and mRNA amplified after isolation from melanoma cell lines SK29 MEL, 624.38 MEL, SK23 MEL and IL-2 MEL (melanoma cells transfected with cDNA encoding

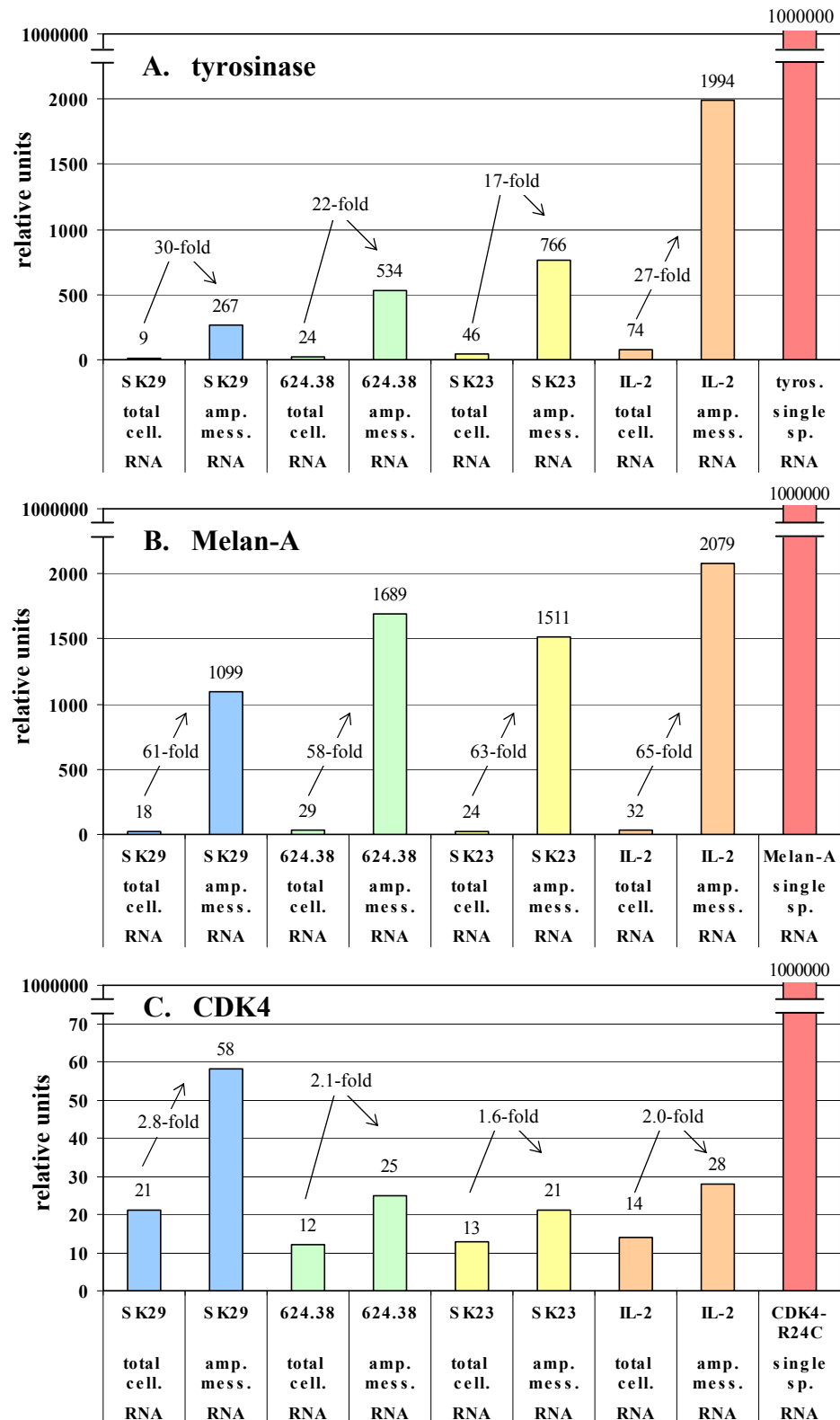


Figure 4.21 Amounts of antigen message in different RNA samples. The same mass, 0.46 μg , of single-species tumour-antigen cRNAs (tyrosinase, Melan-A and CDK4-R24C), total cellular melanoma RNAs and amplified total cellular melanoma mRNAs was used for reverse transcription into cDNA. The amounts of tyrosinase (A), Melan-A (B) and CDK4/CDK4-R24C (C) message were assessed in these cDNA samples by real-time PCR using tyrosinase, Melan-A and CDK4-specific primers. Only SK29 MEL cells were positive (heterozygous) for CDK4-R24C. CDK4-specific primers did not differentiate between CDK4 and CDK4-R24C. The diagram shows the amounts of antigen message expressed relative to the single-species tumour-antigen value which was taken as the 1×10^6 relative units reference.

IL-2). RNAs from A375 MEL and RCC26, a renal cell carcinoma cell line, were used as negative controls. Single-species RNA samples included cRNA coding for tyrosinase, Melan-A and CDK4-R24C. The concentration of all samples was adjusted so that the amount of RNA in each reverse transcription reaction was 0.46 µg. The same volume, 2 µL, of each cDNA sample was then quantitatively analysed in real-time PCR to determine the relative amounts of tyrosinase, Melan-A or CDK4-R24C message.

As expected, the highest amount of antigen message was found in the single-species samples (Figure 4.21). These values were expressed as 1×10^6 relative units and taken as a reference. The least amount of tyrosinase and Melan-A message was detected in total cellular RNA isolated from the melanoma cell line SK29 MEL. IL-2 MEL was found to be the cell line producing the most antigenic RNA. Compared to SK29 MEL, 8-fold more tyrosinase RNA and almost 2-fold more Melan-A RNA was found in the IL-2 MEL sample. A375 MEL and RCC26 cells were confirmed to be negative for tyrosinase and Melan-A RNA (data not shown).

Primers used to detect the CDK4-R24C message were specific for both the wild type protein, CDK4, and its mutated form, CDK4-R24C. The real-time PCR product, synthesised with this primer pair, included the point-mutation site (substitution of C with T) in the 24. codon. Since it was unclear which melanoma cell lines expressed the mutated protein, the real-time PCR products were separated in agarose gel electrophoresis, extracted from the gel, purified and sequenced. Sequencing revealed that the only cell line positive for CDK4-R24C message was SK29 MEL. However, these cells were heterozygous resulting in co-expression of CDK4 and CDK4-R24C proteins.

The RT-PCR used only poly(A)-positive RNA as a template. This meant that mRNA was amplified whereas rRNA, tRNA and other RNA species were not. As a consequence, an RNA sample obtained after RT-PCR and *in vitro* transcription was supposed to contain higher proportions of message for individual proteins. Indeed, processing of total cellular tumour RNA proved to be advantageous not only because it increased the mass of RNA, but also because it resulted in amplification of RNA coding for tumour-antigens (Figure 4.21 and Table 4.2). Amplification of total cellular mRNA from all four inspected melanoma lines increased the amount of tyrosinase message in the range 17 to 30-fold, with the mean fold increase of 24. RNA coding for Melan-A was amplified differently, the

mean fold-increase of 62 was calculated from the range 58 to 65. CDK4 RNA was the least amplified with a 2.1-fold increase calculated from the range 1.6 to 2.8.

Table 4.2 Differential RT-PCR amplification of the tyrosinase, Melan-A and CDK4 message in the same melanoma RNA samples.

Antigen	Cell line	Total cellular RNA (relative units)	Amplified mRNA (relative units)	fold increase	mean fold increase ± stand. deviation
tyrosinase	SK29 MEL	9	267	29.67	23.88 ± 5.71
	624.38 MEL	24	534	22.25	
	SK23 MEL	46	766	16.65	
	IL-2 MEL	74	1994	26.95	
Melan-A	SK29 MEL	18	1099	61.06	61.81 ± 2.86
	624.38 MEL	29	1689	58.24	
	SK23 MEL	24	1511	62.96	
	IL-2 MEL	32	2079	64.97	
CDK4	SK29 MEL	21	58	2.76	2.12 ± 0.47
	624.38 MEL	12	25	2.08	
	SK23 MEL	13	21	1.62	
	IL-2 MEL	14	28	2.00	

Single-species tyrosinase and Melan-A cRNA samples were best compared with the IL-2 MEL amplified mRNA sample because it contained more antigen message than all other analysed melanoma RNAs. The CDK4-R24C cRNA sample was compared with the SK29 MEL amplified mRNA sample because only this melanoma cell line expressed CDK4-R24C and the amplified mRNA sample contained more antigen message than the total cellular RNA sample. If the same masses of these RNAs were taken for an experiment, a single-species sample would contain 502-fold more message for tyrosinase and 481-fold more message for Melan-A when compared with an amplified mRNA sample from the optimal tumour cell line (Figure 4.21). Since CDK4-specific real-time PCR primers did not differentiate between wild type CDK4 and its mutated form, CDK4-R24C, co-expressed in SK29 MEL cells, it was not possible to precisely quantitate the CDK4-R24C message. However, electropherogram of the CDK4 real-time PCR product showed that the mutated form had a higher proportion in the sequenced SK29 MEL total cellular RNA sample than the wild type form. Taking these facts into account, it could only be concluded that the single-species CDK4-R24C cRNA sample contained <17241-fold more

message for CDK4-R24C than the same mass of the SK23 MEL amplified mRNA sample (Figure 4.21).

4.3.2 Different CTL reactivities upon exposure to synthetic peptides

In order to evaluate the cellular expression of the three antigens, additional CTL clones specific for Melan-A and CDK4-R24C had to be integrated into the DC-RNA-CTL system. Two CTL lines, 11/33 and A42 CTLs, were included which recognised Melan-A pMHC ligands. The CTLs 14/35 were used as CDK4-R24C-specific T-cells. The tyrosinase pMHC ligand was recognised by both IVS B CTLs and the previously described TyrF8 CTLs. The use of all five CTL clones was standardised by expanding them to produce large batches which were then frozen in aliquots. For each experiment, cells from identical stocks were thawed and cultured according to the standardised protocol.

In order to investigate the affinities of the different CTL clones for their pMHC ligands, synthetic peptides were loaded onto T2 cells that express only empty HLA-A2 molecules at the cell surface due to a defect in the TAP transporter. If T2 cells are cultured in the presence of exogenous peptides they will express homogenous pMHC ligands comprised of HLA-A2 molecules and the provided peptide. TyrF8 CTLs and IVS B CTLs were exposed to two different peptides, representing the same tyrosinase epitope. YMNGTMSQV is an HLA-A2-binding peptide sequence predicted from the primary structure of the tyrosinase protein. This peptide was used for *in vitro* generation of the TyrF8 CTL clone. However, mass spectroscopy of peptides eluted from an HLA-A*0201 melanoma cell line revealed that the actual sequence of the naturally-presented peptide was YMDGTMSQV. 11/33 CTLs and A42 CTLs were tested against the ELAGIGILTV peptide from Melan-A and 14/35 CTLs against the ACDPHSGHFV peptide from CDK4-R24C. These peptides, at a relatively low concentration of 0.1 µg/mL, were allowed to form complexes with MHC molecules on 1.5×10^4 T2 cells 2 hr before the addition of 3×10^3 CTLs (stimulator to effector ratio 5:1). After 24 hr of co-incubation, supernatants were harvested and the amount of IFN-γ secreted by activated CTLs was determined in ELISA.

As shown in Figure 4.22, TyrF8 CTLs recognised both the predicted and the natural tyrosinase peptide, but reacted stronger with the predicted peptide against which it was primed (3386 pg/mL vs. 2037 pg/mL). In contrast, IVS B CTLs secreted significantly less IFN- γ than TyrF8 CTLs and seemed to recognise only the natural form of the peptide (338 pg/mL), the reactivity against the predicted peptide being slightly above background (43 pg/mL). These results demonstrated that T-cells were activated only upon highly specific recognition of pMHC motifs and that selection of an alternative but highly similar peptide resulted in loss of T-cell activation. 11/33 CTLs and A42 CTLs both reacted against the Melan-A peptide, but also displayed very different degrees of reactivity. 11/33 CTLs produced more IFN- γ than A42 CTLs (2933 pg/mL vs. 280 pg/mL). The amount of IFN- γ secreted by 14/35 CTL upon exposure to the CDK4-R24C peptide fell in the lower range (419 pg/mL). All CTL clones tested with the same peptides in unspecific combinations (e.g. TyrF8 CTL with Melan-A peptide) showed no reactivity (data not shown).

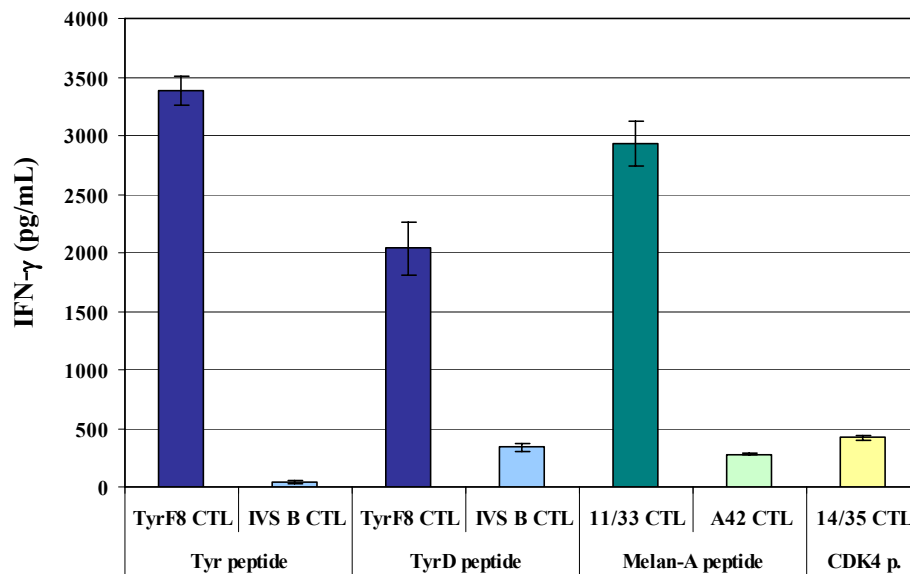


Figure 4.22 Reactivities of different CTL clones upon presentation of synthetic peptides. T2 cells with empty HLA-A2 molecules at the surface were pulsed exogenously with 10 μ g/mL of Tyr peptide YMNGTMSQV, TyrD peptide YMDGTMSQV, Melan-A peptide ELAGIGILTV or CDK4-R24C peptide ACDPHSGHFV for 2 hr prior to the addition of corresponding antigen-specific CTLs. The diagram shows the amount of IFN- γ secreted by 3×10^3 activated CTLs during the 24 hr co-incubation with 1.5×10^4 peptide-pulsed T2 cells. IFN- γ was measured in supernatants by ELISA. Mean values and their standard deviations represent co-incubation triplicates. Background IFN- γ secreted by CTLs in response to unpulsed T2 cells was subtracted from the values shown.

At the level of recognition between stimulator and effector cells, TCR structures defined different T-cell affinities for pMHC ligands. At the intracellular level, distinct signalling patterns caused T-cells to secrete different amounts of IFN- γ , which was detected with an ELISA experiment. Therefore, in subsequent experiments, the reactivities of CTL clones were taken as a measure of antigen-presenting capacities of other cells. Even though some of the CTLs recognised the same epitope, their reactivities were not directly compared because the differences in response to peptides were so great. Each tumour cell or DC co-incubation with a CTL clone was perceived as a separate system and a direct comparison of antigen-presenting capacities was only allowed within that system.

4.3.3 Correlation between amount of antigen message and epitope recognition by CTLs

Taking the complicated process of antigen presentation out of the natural context and dividing it into separate components was necessary in order to better characterise the molecular basis underlying epitope generation, on the one hand, and CTL activation upon exposure to pMHC ligands, on the other. Returning to a more natural environment, the antigen processing and presentation machinery of a tumour cell was added as an important component of the system. Here, reactivity of antigen-specific CTLs was no longer directed against synthetic peptides bound to MHC molecules, but instead was directed against pMHC produced naturally, based on antigen mRNA present in the total cellular RNA pool. This raised the question of whether differences in amounts of tyrosinase, Melan-A and CDK4-R24C message would influence the pMHC ligand-induced activation of the CTLs.

To address this issue, melanoma cells SK29 MEL, 624.38 MEL, SK23 MEL and IL-2 MEL were co-incubated with CTLs TyrF8 and IVS B specific for tyrosinase, 11/33 and A42 specific for Melan-A, and 14/35 specific for CDK4-R24C for 24 hr at a 5:1 ratio (1.5×10^4 stimulators and 3×10^3 effectors per well). A375 MEL and RCC26 were included as negative controls. IFN- γ secreted by activated CTLs was quantitated in ELISA. These values were plotted against the relative amounts of antigen RNA present in the corresponding tumour cells (Figure 4.21).

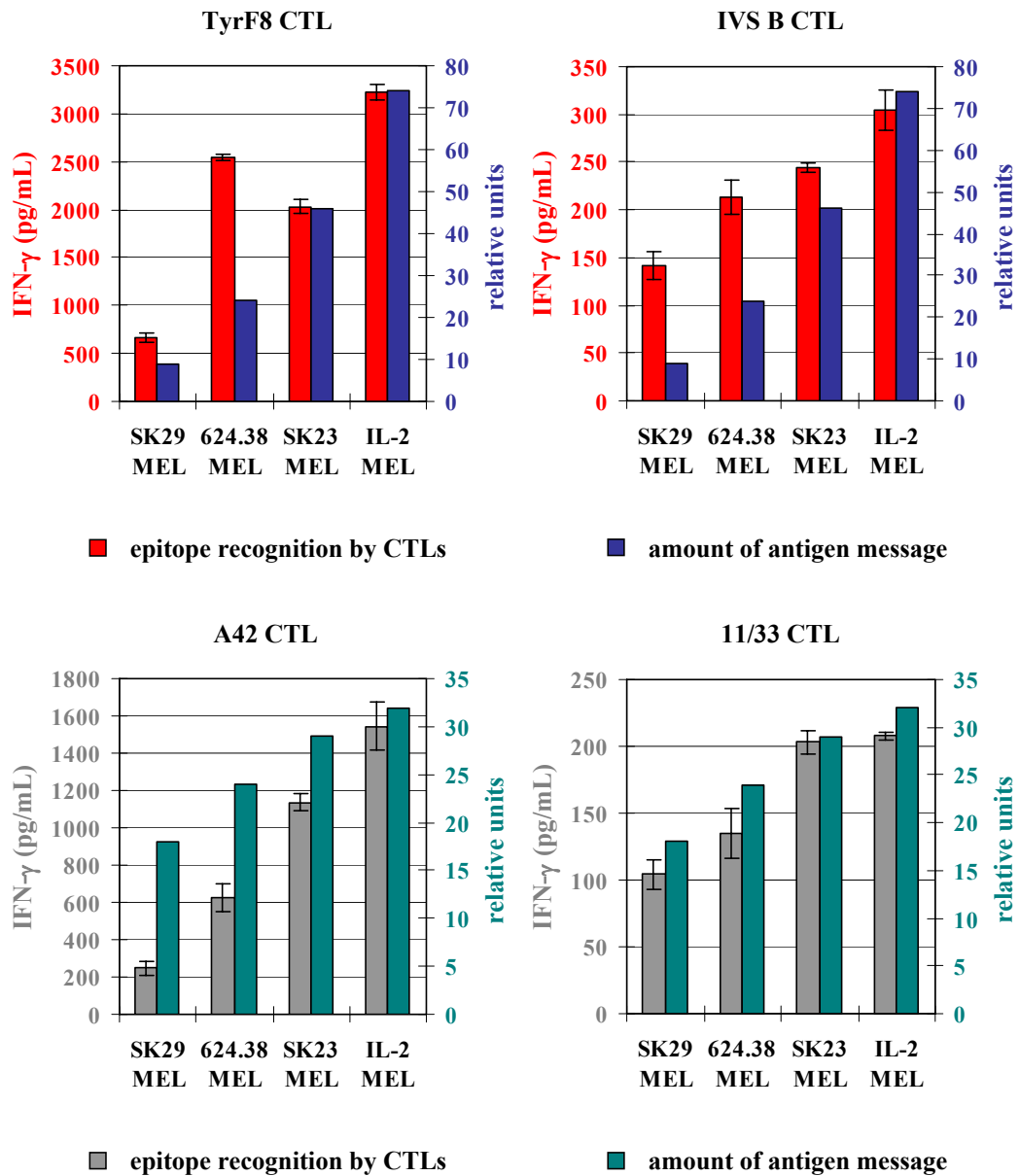


Figure 4.23 Amounts of antigen message in melanoma cells and epitope recognition by antigen-specific CTLs. Different melanoma cells were mixed with tyrosinase-specific TyrF8 and IVS B CTLs (upper row) and Melan-A-specific A42 and 11/33 CTLs (lower row). In the diagrams with two Y-axes, epitope recognition by CTLs is plotted against the amount of antigen message in tumour cells. On the left Y-axis of each diagram, the amounts of IFN- γ secreted by 3×10^3 activated CTLs during the 24 hr co-incubation with 1.5×10^4 melanoma cells are shown. IFN- γ was measured in supernatants by ELISA. Mean values and their standard deviations represent co-incubation triplicates. Background IFN- γ secreted by CTLs alone was subtracted from the values shown. IFN- γ secretion by CTLs in response to negative controls A375 MEL (0-25 pg/mL) and RCC26 (0-21 pg/mL) is not shown. On the right Y-axis of each diagram, the amounts of antigen message are shown. These were expressed in relative units as explained in Figure 4.21.

A generally good correlation between the amount of antigen message and the degree of IFN- γ secretion, representing the pMHC recognition by the CTLs, was consistently

observed with the various CTLs (Figure 4.23). More RNA coding for tyrosinase or Melan-A present in melanoma cells secured better antigen presentation and CTL activation. The only exception was 624.38 MEL, which stimulated TyrF8 CTLs to produce more IFN- γ than SK23 MEL (2566 pg/mL vs. 2050 pg/mL) even though these cells contained less RNA coding for tyrosinase (24 relative units vs. 46 relative units). IL-2 MEL cells were found to be the best stimulators, possibly due to the high amounts of antigen RNA. Nevertheless, part of their superiority can also be attributed to their capacity to secrete IL-2, which is well known to support T-cell proliferation and secretion of IFN- γ . The negative controls, A375 MEL and RCC26, did not stimulate CTLs above background levels (data not shown). Interestingly, A42 CTLs displayed a clearly different behaviour following contact with the naturally-produced and presented antigenic peptide. Co-incubation with melanoma cells resulted in A42 CTLs secreting significantly more IFN- γ than 11/33 CTLs (e.g. 1544 pg/mL vs. 220 pg/mL stimulated by IL-2 MEL), the opposite of what was observed with the synthetic peptide loaded onto T2 cells (3047 pg/mL vs. 291 pg/mL). This once again confirmed the importance of a naturally-selected epitope for efficient T-cell stimulation.

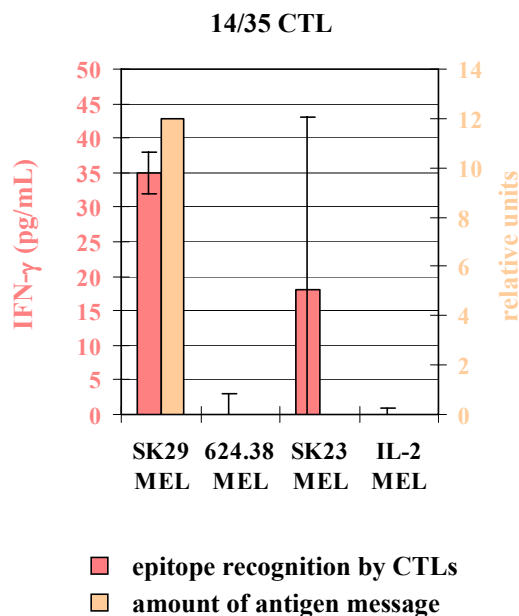


Figure 4.24 Amounts of CDK4-R24C message in melanoma cells and epitope recognition by CDK4-R24C-specific CTLs. Different melanoma cells were mixed with CDK4-R24C-specific 14/35CTLs. In the diagram with two Y-axes, epitope recognition by CTLs is plotted against the amount of antigen message in tumour cells. On the left Y-axis of the diagram, the amounts of IFN- γ secreted by 3×10^3 activated CTLs during the 24 hr co-incubation with 1.5×10^4 melanoma cells are shown. IFN- γ was measured in supernatants by ELISA. Mean values and their standard deviations represent co-incubation triplicates. Background IFN- γ secreted by CTLs alone was subtracted from the values shown. IFN- γ secretion by CTLs in response to A375 MEL (3 pg/mL) and RCC26 (0 pg/mL) is not shown. Unlike other melanoma cells that express only wild type CDK4, SK29 MEL cells also express CDK4-R24C, the mutated form of the protein. Therefore, on the right Y-axis of the diagram, only the amount of antigen message in SK29 MEL cells is shown. This amount was expressed in relative units as explained in Figure 4.20.

Since SK29 MEL cells are the only ones expressing the CDK4-R24C antigen, 14/35 CTLs were activated solely by this cell line. In Figure 4.24, the amount of CK4/CDK4-R24C message in SK29 MEL cells is shown not for comparison with CDK4 amounts in other

melanoma cells but to indicate that SK29 MEL cells are the only ones expressing the mutated form of the CDK4 protein.

4.3.4 Efficiency of electroporation with single-species tumour-antigen cRNA

Electroporation of cRNA EGFP into DCs proved to be very efficient, with the percentage of EGFP-positive cells reaching the maximum of 90% within only 12 hr after transfection. The efficiency of electroporation with a different cRNA species was investigated in two experiments. Electroporation was performed with 48 μg of Melan-A cRNA and either 1.6×10^6 mature DCs from donor PH or 2×10^6 mature DCs from donor RZ. Transfected DCs and untransfected DCs, which served as a control, were harvested either 7 hr or 25 hr later. The relatively early 7 hr time point was chosen because the Melan-A protein has a half-life of approximately 3 hr (de Mazière AM *et al.* 2002) and the 25 hr time point was analysed in order to ascertain whether the antigen was still detectable in the DCs at the time when CTLs were added in functional assays. Harvested DCs were fixed, permeabilised and stained intracellularly with an antibody specific for Melan-A. The percentages of Melan-A-positive DCs were then assessed in FACS™.

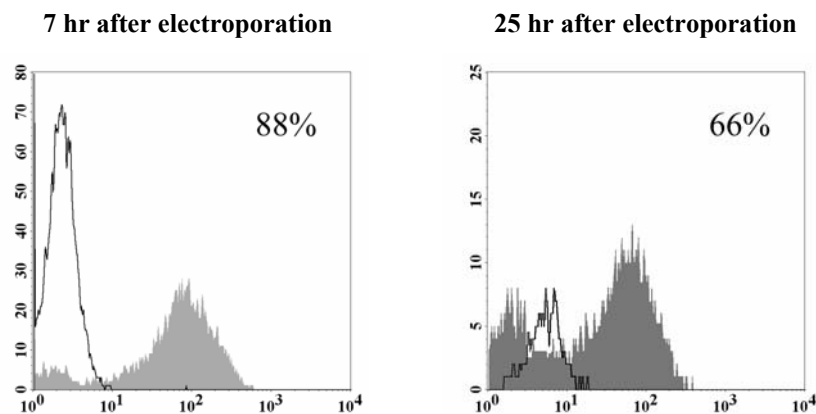


Figure 4.25 Efficiency of electroporation with Melan-A cRNA. Mature DCs were stained 7 hr and 25 hr after electroporation with 48 μg of Melan-A cRNA. FACS™ overlay histograms show fluorescence intensities of both stained untransfected DCs (black curves), that served as an isotype control, and stained Melan-A cRNA-transfected DCs (filled curves). Intracellular staining was performed after fixation and permeabilisation of the cells. The primary antibody bound to Melan-A. The secondary FITC-conjugated antibody was used to detect the primary antibody. For definition of Melan-A-specific FITC fluorescence and Melan-A-positive cells see Figure 4.1.

Melan-A was present in 88% of transfected DCs 7 hr after electroporation (Figure 4.25). When protein expression was measured 25 hr after electroporation, 66% of the DCs expressed Melan-A, clearly showing that transfected RNA was still functional inside the cells, allowing high levels of protein to be produced.

4.3.5 Stimulatory capacity of DCs pulsed with single-species tumour-antigen RNA and total cellular tumour RNA

Tumour cells are known to often down-regulate their antigen processing and presentation machinery in order to escape immune recognition. The variability in epitope producing machineries of melanoma cells was eliminated by transfecting either total cellular tumour RNA or single-species antigen RNA into professional APCs. These experiments were performed to determine how efficiently DCs pulsed with a variety of RNA species in different amounts would stimulate CTLs. They were also designed to provide additional quantitative insight into the process of antigen presentation that occurs following transfer of RNA into DCs.

Single-species cRNAs coding for tyrosinase, Melan-A and CDK4-R24C were electroporated into $1-2 \times 10^6$ mature DCs either separately (48 μg and 24 μg) or pooled (3 \times 48 μg and 3 \times 24 μg). Total cellular RNA (75 μg) and amplified mRNA (75 μg and 37.5 μg) from SK29 MEL cells were chosen because they contained the message for all three tumour-antigens. Electroporation with A375 MEL amplified mRNA (70 μg) was also performed as a negative control. The same DCs, loaded with exogenous peptides (YMNGTMSQV from tyrosinase, ELAGIGILTV from Melan-A and ACDPHSGHFV from CDK4-R24C) at a high concentration of 10 $\mu\text{g}/\text{mL}$, were included as positive controls. One day after electroporation or 2 hr after loading with peptides, 2×10^4 TyrF8, IVS B, A42, 11/33 or 14/35 CTLs were co-incubated with 4×10^4 DCs. Supernatants were harvested 24 hr later and the amount of IFN- γ secreted by activated CTLs was assessed in ELISA (Figures 4.26, 4.27 and 4.28).

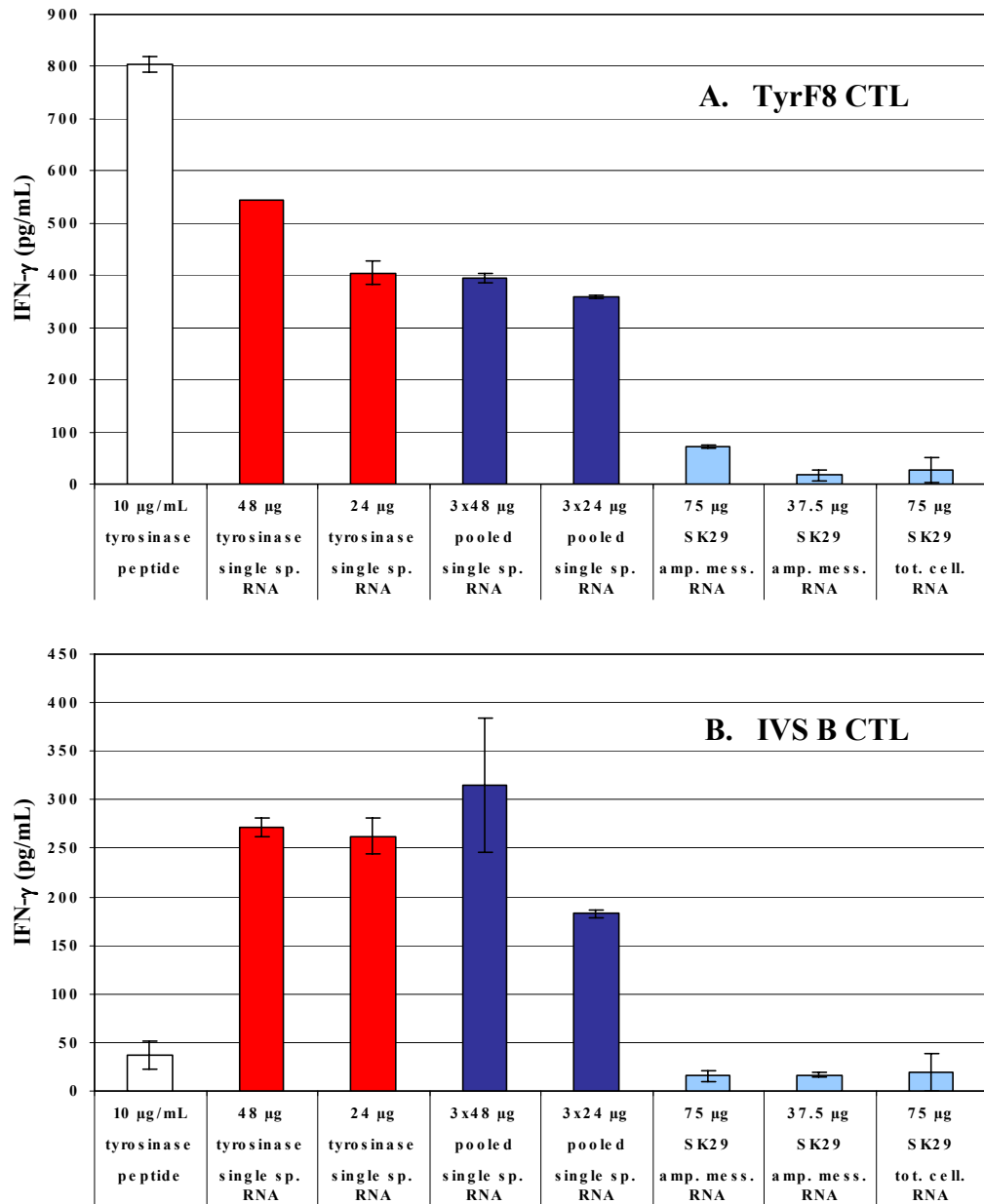


Figure 4.26 Stimulatory capacities of tyrosinase-pulsed DCs. Mature DCs were electroporated with different amounts of various RNA species. One day later, transfected and untransfected DCs were mixed with TyrF8 CTLs (A) or IVS B CTLs (B), specific for the tyrosinase pMHC. Untransfected DCs were also pulsed exogenously with 10 μ g/mL of Tyr peptide YMNGTMSQV for 2 hr prior to the addition of CTLs. The diagram shows the amount of IFN- γ secreted by 2×10^4 activated CTLs during the 24 hr co-incubation with 4×10^4 DCs. IFN- γ was measured in supernatants by ELISA. Mean values and their standard deviations represent co-incubation triplicates. Background IFN- γ secreted by CTLs in response to unpulsed DCs was subtracted from the values shown. IFN- γ secretion by TyrF8 CTLs (17 ± 10 pg/mL) and by IVS B CTLs (18 ± 12 pg/mL) in response to the negative control A375 MEL amplified mRNA-pulsed DCs is not shown.

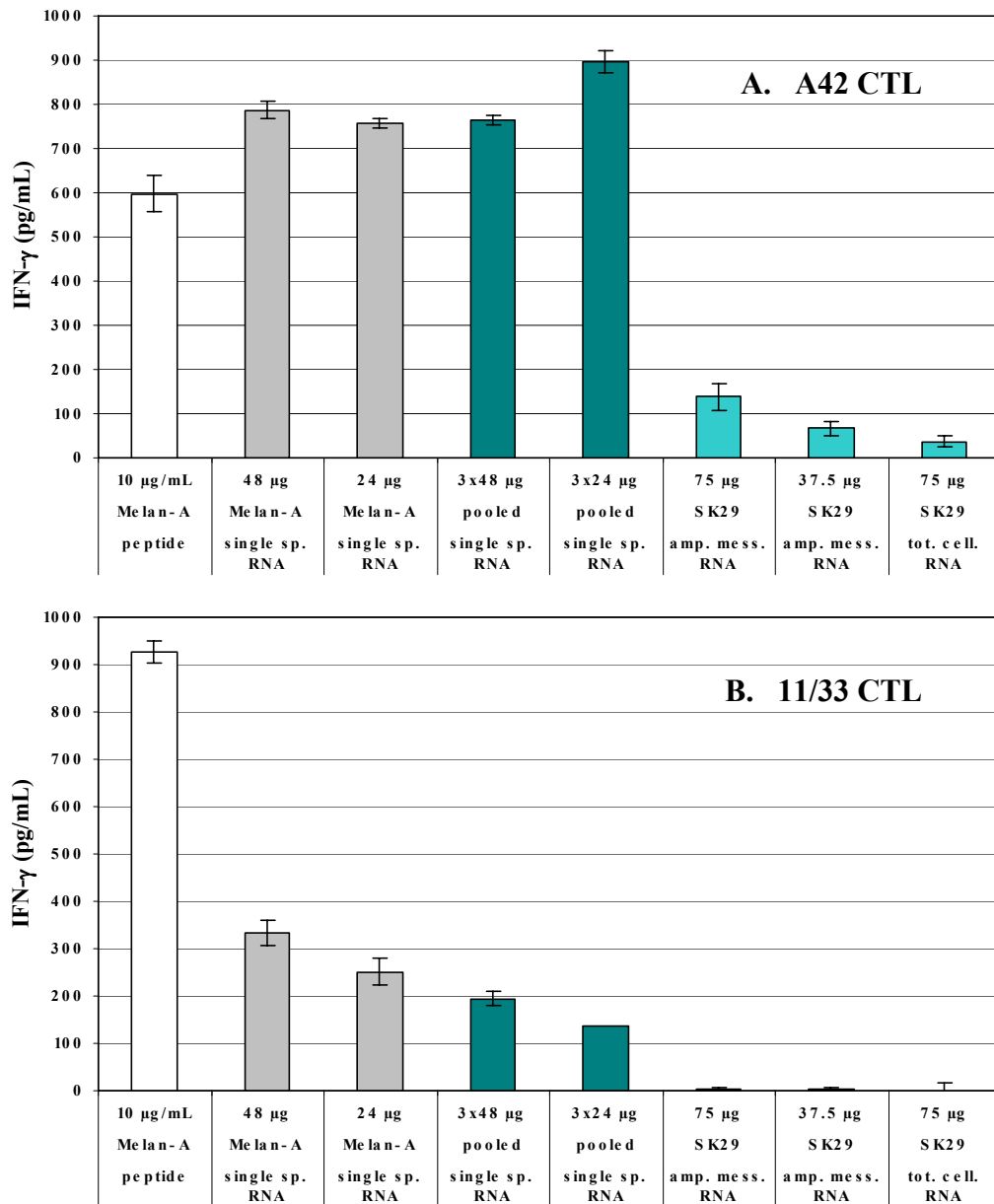


Figure 4.27 Stimulatory capacities of Melan-A-pulsed DCs. Mature DCs were electroporated with different amounts of various RNA species. One day later, transfected and untransfected DCs were mixed with A42 CTLs or 11/33 CTLs, specific for the Melan-A pMHC. Untransfected DCs were also pulsed exogenously with 10 μ g/mL of Melan-A peptide ELAGIGILTV for 2 hr prior to the addition of CTLs. The diagram shows the amount of IFN- γ secreted by 2×10^4 activated CTLs during the 24 hr co-incubation with 4×10^4 DCs. IFN- γ was measured in supernatants by ELISA. Mean values and their standard deviations represent co-incubation triplicates. Background IFN- γ secreted by CTLs in response to unpulsed DCs was subtracted from the values shown. IFN- γ secretion by A42 CTLs (35 ± 95 pg/mL) and by 11/33 CTLs (10 pg/mL, single value) in response to the negative control A375 MEL amplified mRNA-pulsed DCs is not shown.

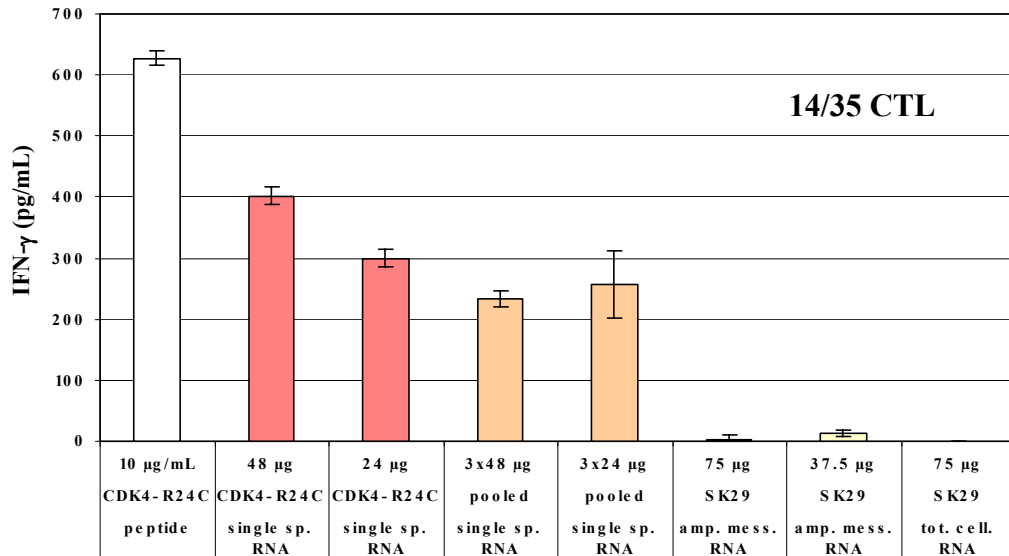


Figure 4.28 Stimulatory capacities of CDK4-R24C-pulsed DCs. Mature DCs were electroporated with different amounts of various RNA species. One day later, transfected and untransfected DCs were mixed with 14/35 CTLs, specific for the CDK4-R24C pMHC. Untransfected DCs were also pulsed exogenously with 10 μ g/mL of CDK4-R24C peptide ACDPHSGHFV for 2 hr prior to the addition of CTLs. The diagram shows the amount of IFN- γ secreted by 2×10^4 activated CTLs during the 24 hr co-incubation with 4×10^4 DCs. IFN- γ was measured in supernatants by ELISA. Mean values and their standard deviations represent co-incubation triplicates. Background IFN- γ secreted by 14/35 CTLs in response to unpulsed DCs was subtracted from the values shown. IFN- γ secretion by CTLs in response to the A375 MEL amplified mRNA-pulsed DCs (19 ± 4 pg/mL) is not shown.

Differential reactivities against the tyrosinase pMHC ligand were observed again with the TyrF8 clone producing generally more IFN- γ than the IVS B clone. As expected based on the results of the experiment using T2 cells, the YMNGTMSQV tyrosinase peptide pulsed onto the DCs stimulated only TyrF8 CTLs (804 pg/mL). An important observation in the tyrosinase system was that IVS B CTLs reacted very weakly (37 pg/mL) upon exposure to the predicted form of the epitope, i.e. synthetic peptide, but strongly recognised the epitope naturally processed by DCs after transfection of RNA coding for tyrosinase. A similar situation was found in the Melan-A system. A42 CTLs reacted less well to the synthetic peptide, ELAGIGILTV, than 11/33 CTLs (598 pg/mL vs. 927 pg/mL), but secreted more IFN- γ when stimulated with RNA-transfected DCs. Despite the common use and occasional success of applying peptide-pulsed APCs in immunotherapy, manipulation of DCs to express antigens and to produce and present their immunogenic peptides, proved to be advantageous with respect to the selection of the correct epitopes for CTL activation. DCs transfected with amplified mRNA from the cell line SK29 MEL also specifically stimulated T-cells. All five CTL clones secreted IFN- γ definitely above, but close to,

background, in a range where the standard deviation of the values was critical for distinguishing between positive and negative results. The expected differences in reactivities were observed only with the more potent clones, TyrF8 and A42 (73 pg/mL vs. 17 pg/mL upon tyrosinase recognition and 138 pg/mL vs. 67 pg/mL upon Melan-A recognition), possibly due to the amount of transfected RNA (70 μ g vs. 37.5 μ g). Total cellular RNA from SK29 MEL did not cause significant T-cell stimulation. Amplified mRNA from A375 MEL induced only very low IFN- γ secretion (data not shown). This was unspecific, since A375 MEL did not express RNA for any of the three antigens.

Most importantly, single-species cRNAs for tyrosinase, Melan-A and CDK4-R24C maintained their functionality after being mixed. DCs electroporated with pooled RNAs were co-incubated separately with each CTL clone, and managed to stimulate all CTLs by simultaneously presenting epitopes from the three antigens. Two different amounts of pooled RNA were used – 3 \times 48 μ g that summed up to 144 μ g and 3 \times 24 μ g that gave a total of 72 μ g. Only small differences were observed using DCs for stimulation that had received either of the two amounts of RNA. This indicated that the multiplicity of antigen message present in the 144 μ g sample exceeded the antigen-presenting capacity of the DCs. In most cases, satisfactory levels of T-cell activation were achieved, similar to or only slightly below those reached with 24 μ g of a single-species cRNA alone. Therefore, it was clear that even though competition for MHC class I molecules may have occurred, CTL responses to pooled RNAs were not inhibited.

In this and other experiments performed under comparable conditions, DCs were transfected with various amounts of different RNA species, all containing RNA coding for tyrosinase. Data from these experiments had to be normalised first and then compared in order to determine if epitope recognition by TyrF8 CTLs correlated with the amount of tyrosinase message transfected into DCs. In Table 4.2, all message amounts were expressed relative to the highest amount used in electroporation, corresponding to 48 μ g of single-species tyrosinase cRNA and depicted as 1×10^6 relative units. Epitope recognition was measured as IFN- γ produced by CTLs and was calculated relative to 100% of the strongest stimulation, achieved after DC transfection with 48 μ g of single-species cRNA. It was found above that IFN- γ secretion during CTL co-incubation with melanoma cells strongly depended on tumour RNA profiles. Except for obvious large differences, no such correlation was observed with RNA isolated from malignant cells and forced into antigen-

presenting cells. The lack of correlation may possibly be due to the variable of electroporation that had to be introduced into the DC system. Nevertheless, this comparison clearly indicated that even small amounts of antigen message were sufficient to develop DC stimulatory capacity that was specific and above background.

Table 4.2 Amounts of transfected antigen messages in electroporated DCs and epitope recognition by TyrF8 CTLs.

RNA	Species	RNA mass transfected (μg)	Tyr. message transfected (ru)	% maximum IFN- γ secretion
tyrosinase	single-species cRNA	48.0	1000000	100.00
tyrosinase	single-species cRNA (part of pool)	48.0	1000000	72.46
tyrosinase	single-species cRNA	24.0	500000	74.46
tyrosinase	single-species cRNA (part of pool)	24.0	500000	65.71
SK23 MEL	amplified mRNA	160.0	2553	6.64
624.38 MEL	amplified mRNA	160.0	1810	6.17
SK23 MEL	amplified mRNA	80.0	1277	5.15
624.38 MEL	amplified mRNA	80.0	905	5.74
SK29 MEL	amplified mRNA	75.0	417	13.39
SK29 MEL	amplified mRNA	37.5	209	3.07
SK29 MEL	total cellular RNA	75.0	14	5.11

The table shows the mass (μg) of RNA samples applied in different DC electroporation experiments, the amount of tyrosinase message (ru) contained in those samples and the level of epitope recognition by TyrF8 CTL (% of maximum IFN- γ secretion) during co-incubation with the transfected DCs. The amount of transfected tyrosinase message was calculated from the relative units shown in Figure 4.20 and the mass of the RNA applied in electroporation. It is expressed relative to the 48 μg sample which contains the largest amount of tyrosinase message and is taken as a 1×10^6 relative units reference. The level of epitope recognition is expressed relative to the maximum IFN- γ secreted which corresponds to the TyrF8 CTL stimulation by DCs transfected with 48 μg of tyrosinase cRNA. This value was taken as a 100% reference.

4.3.6 Summary of the data obtained in the three-antigen system

Quantitation experiments showed that total cellular RNA samples from various melanoma cells contained different amounts of tyrosinase, Melan-A and CDK4/CDK4-R24C message. In RT-PCR of mRNA from these samples, the Melan-A message was amplified more than the tyrosinase message. The CDK4/CDK4-R24C message was amplified the least. Even after amplification of melanoma mRNA in RT-PCR, *in vitro* transcribed tyrosinase, Melan-A and CDK4-R24C cRNA samples still contained significantly more antigen message. After co-incubation of antigen-specific CTLs with melanoma cells, a

generally good correlation was observed between the amounts of antigen message present in tumour cells and epitope recognition by CTLs. In two cases, CTLs displayed higher reactivities in response to peptides naturally-produced by tumour cells than in response to synthetic peptides. The efficiency of electroporation with Melan-A cRNA was just as high as the efficiency of electroporation with cRNA EGFP. Electroporation of single-species tumour-antigen cRNAs into DCs resulted in the highest DC stimulatory capacities. When single-species tyrosinase, Melan-A and CDK4-R24C cRNAs were pooled and then transfected into DCs, satisfactory levels of T-cell stimulation were achieved, indicating that CTL responses to pooled RNAs were not inhibited even though competition for MHC class I molecules may have occurred. Based on transfected amplified melanoma mRNA, DCs also developed stimulatory capacities, but at much lower levels. Two CTL clones once again secreted more IFN- γ upon exposure to epitopes naturally produced by transfected DCs than to synthetic peptides. No correlation was observed between the fine differences in the amounts of transfected antigen message and epitope recognition by CTLs.

5. Discussion

The ultimate goal of these studies is to design a vaccine that can be applied clinically to eradicate malignant cells in cancer patients. The strategy analysed here is based on DCs that are manipulated to present TAAs to effector cells of the immune system. Melanoma is the most suitable tumour model because it is well characterised at both the cellular and the molecular levels. Technological innovation has to be combined with knowledge from the fields of cellular biology and immunology in order to better understand and manipulate biological mechanisms underlying anti-tumour immunity and to ensure the efficiency of antigen presentation. For this reason, in the following text, a relatively new methodology is discussed not so much in the clinical context but more in the context of basic science. Sequential arguments are presented demonstrating why RNA was chosen as an antigen form that is optimal for a DC-based therapy. Two protocols for RNA transfection into DCs of different maturation stages are compared. The stimulatory capacities of DCs are correlated to different amounts of TAA message in various RNA samples that were used for transfection. Furthermore, approaches are considered to improve initiation and maintenance of anti-tumour immune responses. Pooling RNAs encoding several different TAAs is suggested as a strategy to overcome tumour immune escape. Competition between antigens and immunodominance are discussed. Finally, the dangers of autoimmunity that are associated with immunotherapy are evaluated.

5.1 Efficiency of RNA transfection into DCs

If the preferred approach is to generate TAA-expressing DCs using transfer of genetic material, instead of protein, two different antigen forms are available: DNA and RNA. Transfection of RNA was shown to be more efficient than DNA transfection (80% vs. 50% positive cells) when identical amounts of plasmid DNA and cRNA coding for EGFP were used in electroporation. Furthermore, the level of EGFP expression was slightly higher using transfected RNA. However, the duration of EGFP expression was similar after electroporation of either RNA or DNA. It should be noted that DNA electroporation required stronger electric pulsing, since DNA had to cross two membranes in order to reach the nucleus. For this reason, up to 60% mortality was caused by the electric shock (Ponsaerts P *et al.* 2003). Electroporation of RNA was associated with less toxicity

because RNA had to be transferred through only one membrane. Once in the cytoplasm, RNA could be translated directly into protein. Lundqvist and colleagues (Lundqvist A *et al.* 2002) compared RNA transfection with viral transduction of DCs. Even though viral gene-transfer resulted in a higher transfer efficiency (90% vs. 60% positive cells), electroporation of RNA proved to be an adequate alternative, which did not require dealing with safety issues usually associated with viral vectors.

The Gilboa group, which initiated the use of RNA-transfected DCs as a vaccine, relied on passive pulsing (Heiser A *et al.* 2000) and lipofection (Su Z *et al.* 2002) for efficient transfer of RNA into DCs. However, many other groups obtained unsatisfactory results with simple co-incubation of RNA and DCs, and chose electroporation over lipofection because of significantly higher transfection efficiencies. Kalady and colleagues directly compared passive pulsing, lipofection and electroporation of EGFP cRNA into DCs (Kalady MF *et al.* 2002). With passive pulsing of immature DCs, they obtained less than 1% of EGFP-positive cells. Lipofection had an efficiency of 19% and electroporation 50%. In my analysis, 15% immature DCs and 5% mature DCs captured EGFP cRNA-lipid complexes and developed green fluorescence (Figure 4.2). In comparison, van Tendeloo reported only 7.5% EGFP-positive immature DCs and 4% mature DCs after lipofection (van Tendeloo VF *et al.* 2001).

It is difficult to directly compare the efficiency of electroporation in my study with that in other studies because experiments were performed under different conditions and the efficiencies were defined according to different criteria. Not only the type of electric pulse (exponential decay or square-wave) and electroporation parameters (voltage and capacitance) but also the number of DCs, amount of RNA and suspension volume in the electroporation cuvette influenced the outcome of transfection. The maturation status of DCs (immature or mature) also seemed to make a difference. The percentage of EGFP-positive DCs was taken as a measure of electroporation efficiency in all studies, but it was assessed at various time points after transfection. In some cases, total DC populations, including dead cells, were analysed whereas in others only viable DCs were taken into account. In my experiments, only 15% of electroporated DCs were found to be dead and they were not excluded from the population of cells in which green fluorescence was measured. Groups that performed comparable analyses reported electroporation efficiencies with immature DCs in the range of 63%, achieved with 4 µg of EGFP cRNA

and $1-4 \times 10^6$ cells in 100 μL (van Tendeloo VF *et al.* 2001), to 73%, achieved with 10 μg of EGFP cRNA and 5×10^6 cells in 100 μL (Ponsaerts P *et al.* 2002). When 0.7×10^6 immature DCs were electroporated with 3 μg of EGFP cRNA in a suspension volume of 100 μL , I found a transfection efficiency as high as 80% (Figure 4.2B). Up to 90% of mature DCs were EGFP positive. These findings are contrary to the observations of van Tendeloo and colleagues. In their hands, electroporation of DCs matured with LPS and TNF- α , instead of the cytokine cocktail used here, yielded only 33% EGFP-positive cells (van Tendeloo VF *et al.* 2001). When cRNA encoding the Melan-A TAA was transfected into mature DCs instead of the reporter protein EGFP, 88% positive cells were measured (Figure 4.25). This showed that electroporation efficiency was reproducible irrespective of RNA species using the optimal conditions developed in my studies. Therefore, electroporation of RNA into DCs can be characterised as a simple, efficient, quick and low-cost technology with good clinical applicability. Particularly important was also the fact that cryopreserved PBMCs were used as the starting source for DC generation, enabling a further step in standardisation to be achieved.

5.2 Antigen processing in immature and mature DCs

Whether RNA should be transfected into immature or mature DCs depends on many factors. DCs of different maturation stages may display distinct susceptibilities to RNA transfer. Furthermore, immature and mature DCs are responsible for different steps of antigen processing and presentation, meaning that antigen in the form of RNA must be introduced into cells with proper functionality. It is clear that mature DCs most efficiently present antigenic peptides due to their up-regulation of MHC expression, improved rate of peptide loading into MHC molecules and intensified transport of pMHC complexes to the cell surface. However, at exactly which stage before antigen presentation DCs generate the epitope peptides is the matter of considerable controversy.

Peptides are largely produced when cytosolic proteins are degraded by proteasomes. In DCs, changing profiles of MHC-bound peptides are associated with the replacement of active proteasome subunits by the so-called immunosubunits (Gileadi U *et al.* 1999). Both proteasomes and immunoproteasomes seem to have similar efficiencies in degrading proteins, but bioinformatic analysis of experimental degradation data showed that they had

individual cleavage motifs, yielding a different and less diverse pool of peptides produced by immunoproteasomes (Kesmir C *et al.* 2003). A less diverse pool of peptides should enhance the presentation of relevant antigenic peptides, since they do not have to compete for MHC molecules with many other irrelevant peptides. If proteasomes were restricted to immature DCs and immunoproteasomes to mature DCs, the variable quality of generated peptides might even serve to prevent autoimmune reactions. However, data regarding the time point of immunoproteasome assembly and activation are somewhat contradictory and do not yet allow clear conclusions to be drawn. One group reported down-regulation of mRNA encoding the immunoproteasome subunits upon DC maturation (Li J *et al.* 2001). This might contribute to the higher antigen-processing capability of immature DCs. Another group found that immunoproteasomes already represented half of the proteasome population in immature DCs. Quantitative analysis of mRNA showed either very limited or moderate induction of immunoproteasome subunit expression in mature DCs. Given that proteasomes are long-lived complexes with half-lives of several days, it was postulated that their replacement with immunoproteasomes occurs only gradually over an extended period of time. Therefore, the amount of immunoproteasomes may not be significantly different between immature and mature DCs and should not strongly influence antigen processing. However, authors of the study postulated that other, unidentified mechanisms involving regulation of (immuno)proteasome activity are responsible for the marked differences in antigen presentation between immature and mature DCs (Macagno A *et al.* 2001). The DC maturation stage at which such regulatory mechanisms are active remains unclear.

Obviously, the need is to introduce RNA into DCs at a maturation stage that allows the newly synthesised proteins to be degraded by immunoproteasomes and not by proteasomes. Until more precise information is available about when immunoproteasomes are activated inside DCs, the decision of whether to transfect RNA into immature or mature DCs can only be based on transfection and antigen-presenting efficiencies. Unfortunately, relevant data are scarce and also contradictory. Van Tendeloo and colleagues obtained the most potent CTL activation when immature DCs were loaded with Melan-A cRNA by electroporation or lipofection, subsequently matured with LPS and TNF- α , and then co-incubated with the CTLs. They attributed the lower stimulatory capacity of DCs transfected after maturation to a lower degree of transfectability by either lipofection or electroporation (van Tendeloo VF *et al.* 2001). My results contribute to the

controversy by showing that electroporation of EGFP cRNA was more efficient with mature DCs, compared to immature DCs (Figure 4.2B). Furthermore, mature DCs expressed more protein than immature DCs, based on the use of identical amounts of electroporated or lipofected EGFP cRNA (Figure 4.3). This was not a function of transfection efficiency because mature DCs were more difficult to lipofect (Figure 4.2B), but nevertheless expressed more EGFP than their immature counterparts. If mature DCs translate RNA into more protein, they are likely to generate more peptides. Therefore, in my experimental system tumour-antigen RNA was transfected into mature DCs only, resulting in satisfactory levels of CTL stimulation.

As will be discussed below, protein expression decreases relatively quickly after transfection due to degradation of transfected RNA by intracellular RNases, thereby narrowing the time period in which antigens are produced and processed. Different susceptibilities of proteins to digestion by intracellular proteases also have to be taken into account. The half-life of tyrosinase was estimated to be at least 12 hr (Halaban R *et al.* 1997) and that of Melan-A to be approximately 3 hr (de Mazière AM *et al.* 2002). The relative instability of Melan-A was indicated in this study when Melan-A cRNA-transfected DCs were stained with a Melan-A-specific antibody and analysed in FACS™ (Figure 4.25). Melan-A was expressed in 88% of the cells from one donor 7 hr after electroporation. However, 24 hr after electroporation, Melan-A was detected in 66% of transfected DCs from a second donor. Additional staining experiments, to assess precise kinetics and quantify mean fluorescence intensity, are required to confirm the observed decrease in Melan-A expression. In terms of antigen presentation, different stabilities of TAAs could lead to a situation in which peptides originating from one antigen, e.g. Melan-A, are generated and presented sooner than peptides derived from another antigen, e.g. tyrosinase. Considering the fact that an average pMHC class I complex has a half-life of 5-10 hr on the cell surface (Cella M *et al.* 1999), choosing the right time-frame for DC-CTL interaction may be critical for efficient T-cell activation. Whereas selection of an optimal time point may not be possible for all antigens encoded by total cellular RNA, it might prove to be advantageous with single-species tumour-antigen cRNAs. Therefore, an additional argument in favour of electroporating mature DCs might be that the expression of their co-stimulatory, adhesion and antigen-presenting molecules is already up-regulated. This phenotype is not changed by electroporation (Figure 4.5). If mature DCs are transfected, there is no need to wait an additional 1-2 days in order for their maturation to

take place. Theoretically, they can be used for CTL stimulation immediately after transfection. Practically, however, DCs need time to recuperate from the shock of electroporation and to produce, process and present the antigen. This was demonstrated by my finding that tyrosinase cRNA-pulsed DCs developed a higher stimulatory capacity when they were cultured one day before contact with the CTLs, as opposed to only two hours (Figure 4.13). This 24 hr time period might be used for simultaneous maturation, if immature DCs were electroporated, however, if RNA encoding a short-lived antigen is used, it may be necessary to initiate co-incubation of DCs and CTLs sooner, thereby limiting the time available for DC maturation.

Keeping in mind that all steps performed *in vitro* are merely attempts to simulate *in vivo* situations, a strong argument in favour of RNA transfection into immature DCs is made by the Gilboa group (Nair S *et al.* 2003). Instead of maturing DCs *in vitro* through culture with various agents that mimic the conditions encountered at a site of inflammation, immature DCs were electroporated and then injected into adjuvant-pretreated skin. Thereby, transfected DCs were matured *in situ* and displayed migratory capacities, immunostimulatory properties and anti-tumour activity that were comparable to, or even better than, those achieved using DCs matured *ex vivo*. Mature DCs injected into adjuvant-treated sites migrated more efficiently, but their immunostimulatory capacities remained lower than those of immature DCs that matured *in situ*. In the end it will probably be necessary to evaluate these various parameters using labeled DCs in comparative clinical trials in order to define the best clinical strategy.

5.3 Quantitation of antigen presentation on RNA-pulsed DCs

In the vast majority of studies evaluating the ability of RNA-pulsed DCs to prime or activate CTLs, uncloned lines were used in which the CTLs were only one component of a complex pool of lymphocytes. The function of polyclonal CTLs specific for repertoires of unknown tumour epitopes or even for defined individual epitopes was mostly tested in cytotoxicity assays. In my experimental system only antigen-specific CTL clones were analysed because the goal of the study was to detect fine quantitative differences based on DCs pulsed with various amounts of different RNA species. Considering that the efficiency of CTL activation depends on the quantity of pMHC complexes expressed on

the surface of DCs and that the number of peptides generated is proportional to the amount of protein synthesised, it was important to know whether higher protein expression and stronger CTL stimulation could be achieved with increased doses of RNA. The kinetics of transfected RNA degradation and protein expression were investigated to determine the time-frame in which the most antigen was produced. Furthermore, quantitation of RNA samples was performed in order to precisely define how much antigen message was introduced into the DCs. Finally, the correlation between the amount of transfected antigen message and CTL stimulation was analysed.

Varying amounts of RNA transferred into the DCs could indeed be used to manipulate levels of protein expression and subsequent peptide presentation. The dependence of protein expression on the quantity of transfected RNA was demonstrated in the EGFP cRNA dose-finding experiment (Figures 4.6 and 4.7). Pulsing DCs with increased amounts of tyrosinase cRNA resulted in improved stimulation of CTLs (Figure 4.15), indicating that, given more RNA, more proteins were produced in DCs and, consequently, more peptides were processed and presented at the cell surface. Whereas a total of 8 μg (or 3 μg per 100 μL electroporation suspension) was the maximum dose of EGFP cRNA applied in electroporation, 48 μg (or 19 μg per 100 μL) was the highest amount of cRNA used encoding tyrosinase, Melan-A or CDK4-R24C. Total cellular melanoma RNA and amplified melanoma mRNA samples contained less message for individual antigens, therefore, 75 μg (or 30 μg per 100 μL) were used. These amounts were similar to or even exceeded those described in the literature. For comparison, 20 μg per 100 μL of Melan-A cRNA (Kalady MF *et al.* 2002) and 10 μg per 100 μL of myeloma RNA (Milazzo C *et al.* 2003, Grünebach F *et al.* 2003) were among the highest electroporation RNA doses reported by other groups.

The kinetics of EGFP cRNA degradation (Figures 4.8, 4.9 and 4.10) and tyrosinase cRNA degradation (Figures 4.18, 4.19 and 4.20) in the DCs showed that transfected RNA was rapidly lost within the first several hours after electroporation. Nevertheless, RNA could still be detected inside the cells three to five days later. The behaviour of RNA after electroporation was also investigated by Eppler and colleagues. When DCs were electroporated with fluorochrome-labelled RNA and then immediately analysed in FACS™, a pronounced increase of fluorescence was observed, compared to control DCs that were mixed with the RNA, but were not transfected. Four hours after electroporation,

fluorescence decreased to control levels (Eppler E *et al.* 2002). In my analyses, large amounts of RNA applied by electroporation allowed prolonged antigen expression, but most antigen was probably produced within a relatively short time after transfection. The intensity of EGFP fluorescence reached a maximum 24 hr after electroporation and then slowly decreased over the following four days (Figures 4.4 and 4.7). Although EGFP molecules have a long half-life of more than 24 hr (Li X *et al.* 1998), kinetic measurements clearly demonstrated that after the initial surge of EGFP expression, based on high amounts of freshly transfected RNA, the EGFP translation rate was reduced due to elimination of the RNA template. Another group reported similar kinetics in luciferase cRNA-lipofected DCs. Luciferase activity reached a maximum 3-8 hr after transfection and decreased significantly by 24 hr (Weissman D *et al.* 2000).

In the studies of others, it was demonstrated that total cellular tumour RNA could be amplified in RT-PCR without the loss of biological function (Boczkowski D *et al.* 2000). Using this technology, one important advantage is that unlimited RNA stocks can be produced from a limited number of tumour cells. Another advantage is that the proportions of antigen message in amplified RNA were found to be higher than in native RNA. This was due to the fact that only mRNA is reverse transcribed and amplified in RT-PCR whereas rRNA, tRNA and other RNA species are not. Interestingly, in my analysis of melanoma-derived RNA samples, the Melan-A message was amplified 62-fold, the tyrosinase message 24-fold and the CDK4 message only 2-fold (Figure 4.21). These differences may reflect variations in the expression levels of the message for the three antigens in melanoma cells from which the RNA samples were obtained. Whereas CDK4-R24C may have a lower expression level, tyrosinase and Melan-A may have higher expression levels in melanomas. Therefore, the polymerase could associate sooner with tyrosinase and Melan-A cDNA templates and their amplification started in earlier PCR cycles. The amplification of CDK4 molecules may have taken place later during the PCR run because they were not so easily detected by the polymerase. The same approach helped to define quantitative differences between single-species tumour-antigen RNA samples and total cellular melanoma RNA samples. Approximately 17240-fold more CDK4-R24C message, at least 500-fold more tyrosinase message and at least 480-fold more Melan-A message was found in corresponding single-species cRNAs compared to amplified melanoma mRNAs.

A good correlation was observed between the quantity of antigen message in various melanoma cells and the CTL recognition of antigenic epitopes presented on their surfaces. In other words, antigen-specific CTLs consistently reacted better to tumour cells that contained more RNA encoding the specific antigen (Figure 4.23). When RNA was transfected into DCs, such fine quantitative differences in epitope recognition were not detected (Table 4.3). Nevertheless, the elucidation of parameters affecting antigen presentation on RNA-transfected cells (Figure 4.21) made it possible to better understand the stimulatory capacities of differently-pulsed DCs. The amount of CDK4-R24C message remained low in the RNA sample even after RT-PCR. Therefore, DCs developed no stimulatory capacity for CDK4-R24C-specific CTLs when electroporation was performed with either total cellular melanoma RNA or amplified melanoma mRNA (Figure 4.28). In extrapolation, it is likely that total cellular tumour RNA-transfer will not allow DCs displaying a repertoire of mutated peptides to efficiently prime specific CTLs, unless the mutations lead to over-expression of the template message. In contrast, successful amplification of tyrosinase and Melan-A message resulted in the activation of both tyrosinase-specific CTL clones and one of two Melan-A-specific CTL clones by DCs transfected with amplified mRNA (Figures 4.26 and 4.27). DCs pulsed with native tumour RNA did not stimulate CTLs specific for tyrosinase above background. The Melan-A epitope, however, was recognised even on DCs transfected with native tumour RNA when a CTL clone with high avidity was used. As expected, CTLs responded significantly stronger to electroporation with single-species tyrosinase, Melan-A or CDK4-R24C cRNA. Compared to transfection with tyrosinase cRNA, levels of CTL stimulation with amplified melanoma mRNA-pulsed DCs were 8-fold and 18-fold lower, depending on the CTL clone. This means that amplified mRNA yielded 13.4% and 5.5% , respectively, of the stimulation levels found with single-species tyrosinase cRNA. In the case of Melan-A, stimulation with amplified melanoma mRNA was 6-fold lower or 17.5% of the maximum reached with single-species cRNA.

Clearly, it is technically feasible to force extremely large quantities of RNA into many DCs. Whereas this leads to reproducibly high stimulation of antigen-specific CTL clones, it seems that less antigen presented on fewer DCs will suffice for T-cell priming. Theoretically, this may lead to preferential expansion of high-avidity T-cells. Heiser and colleagues observed specific killing when CTLs were stimulated after 1×10^6 DCs were passively pulsed with as little as 10 ng of PSA (prostate-specific antigen) cRNA.

Increasing the dose resulted in augmented responses that reached a plateau at 1.5 μg (Heiser A *et al.* 2000). The Weissman group lipofected only 0.2 μg of HIV (human immunodeficiency virus) gag cRNA into 1×10^5 DCs and induced antigen-specific CTLs when these DCs were co-incubated with PBMCs (Weissman D *et al.* 2000). However, differences between electroporated and passively pulsed or lipofected DCs have been investigated so far only at the functional level of CTL priming or activation. In terms of protein expression, my fluorescence microscopy and corresponding FACS™ data (Figure 4.3) clearly showed that each of the few lipofected DCs produced more EGFP than any of the many electroporated DCs. This observation and other quantitation data now provide the basis for evaluating the efficiency of T-cell priming using only a few or many DCs expressing low, intermediate or high levels of antigen.

5.4 Correct and incorrect peptide sequences

The HLA-A2-restricted tyrosinase₃₆₈₋₃₇₆ epitope YMNGTMSQV, predicted from the amino acid sequence of the protein (Wölfel T *et al.* 1994b), was found to be slightly different from the tyrosinase₃₆₈₋₃₇₆ epitope YMDGTMSQV, identified by mass spectroscopy of peptides eluted from an HLA-A*0201 melanoma cell line (Skipper JC *et al.* 1996). The difference between the primary sequence and the sequence of the presented peptide is due to a posttranslational conversion of asparagine (N) into aspartic acid (D) at position 3. The newly defined peptide was recognised much more efficiently by a CTL clone than the predicted peptide, indicating that the post-translationally modified peptide in fact is the natural epitope. Whereas this difference is of central importance for peptide recognition by melanoma CTLs, it has no impact on peptide binding to the MHC molecule. Based on this discovery, a novel mechanism was suggested for the generation of peptides from transmembrane and secreted proteins. These proteins are associated with the ER as they are synthesised and, thus, they have no physical contact with the proteasome in the cytosol. However, peptides are produced from transmembrane and secreted proteins. It was hypothesised that either their proteolysis takes place in the ER (Lee SP *et al.* 1996) or that such proteins are mistranslated in the cytosol (Wang RF *et al.* 1996). A mechanism responsible for the generation of the tyrosinase peptide was postulated by Engelhard and colleagues (Engelhard VH *et al.* 2002). Tyrosinase is a transmembrane protein and it is, therefore, synthesised on ER-bound ribosomes. Once properly folded, the tyrosinase

molecule, anchored in a lipid-bilayer, is sorted to the melanosomal compartments. The conversion of YMNGTMSQV into YMDGTMSQV is not based on a simple deamination of N into D, but involves constitutive glycosylation of N in the ER during synthesis. After translation and glycosylation, some tyrosinase molecules, possibly the misfolded ones, are reverse translocated into the cytosol where deglycosylation of N is accompanied by its deamination into D. Tyrosinase is then degraded by the proteasome and generated peptides are transferred into the ER by the TAP transporter.

The only epitope displayed on tyrosinase expressing cells was indeed found to be YMDGTMSQV (Skipper JC *et al.* 1996, Mosse CA *et al.* 1998). Even though the sequence YMNGTMSQV does not adequately represent this epitope, it is a good example of a peptide that, in a natural system, is most probably perceived as unnatural, contrary to the best knowledge of scientists at the time. As discussed below, in this case, "unnatural" also means "incorrect". However, heteroclitic peptides demonstrate that in nature "the unnatural" peptide can sometimes be recognised and possibly mount an even stronger immune response than "the natural" epitope (Dyall R *et al.* 1998). Heteroclitic peptides differ from their natural counterparts in amino acids that are responsible for binding to MHC molecules and/or interaction with TCRs on CTLs. The slightly different sequences ensure a higher stability of pMHC complexes and sometimes a higher immunogenicity of the peptides. These peptides should be recognised by the same CTLs that react upon presentation of natural peptides. If heteroclitic peptides are used for priming, it can be expected that the resultant CTLs will react strongly to the naturally-produced peptides during secondary challenge.

In this study, TyrF8 CTLs and IVS B CTLs were used to recognise the tyrosinase₃₆₈₋₃₇₆ epitope presented on RNA-transfected DCs. TyrF8 CTLs were cultured from PBMCs of a healthy donor. After priming and expansion with autologous YMNGTMSQV-pulsed antigen-presenting cells, TyrF8 CTLs were cloned by standard limiting dilution procedures (Visseren MJ *et al.* 1995). Whereas the predicted peptide was used in the generation of TyrF8 CTLs, IVS B CTLs were established from mixed lymphocyte tumour-cell cultures which included autologous melanoma cells, presenting the natural YMDGTMSQV peptide. IVS B CTLs were not cloned, but subsequently produced clones were tested and had lytic activities identical to that of IVS B. This line is, therefore, referred to as a clone (Wölfel T *et al.* 1993). When the two tyrosinase peptides were separately loaded onto T2

cells, TyrF8 CTLs reacted stronger to the predicted epitope, but recognised both peptides (Figure 4.22). IVS B CTLs showed almost no reactivity against the predicted peptide, but did react to presentation of the natural epitope. The specificity of the IVS B clone for the naturally processed peptide was confirmed in co-incubation experiments with different melanoma cells (Figure 4.23). Since tumour cells always present the natural tyrosinase peptide, IVS B CTLs were successfully activated. Most importantly, when DCs were either pulsed exogenously with the predicted peptide or produced the natural peptide based on transfected tyrosinase cRNA, IVS B were stimulated to a significantly higher level by the RNA-pulsed DCs than by the peptide-pulsed DCs (Figure 4.26B).

A similar situation was observed with A42 CTLs recognising the Melan-A₂₆₋₃₅ epitope. A42 CTLs were cloned by limiting dilution of tumour infiltrating lymphocytes from a melanoma patient. Autologous tumour cells, presenting the natural peptide, served as stimulators in the culture of this clone. A42 CTLs were reported to successfully recognise the EAAGIGILTV peptide, among several others (Kawakami Y *et al.* 1994). The 11/33 clone was also used in this study to detect presentation of the Melan-A epitope. Since 11/33 CTLs were obtained by limiting dilution from mixed cultures of PBMCs and autologous melanoma cells, this clone is also specific for the naturally processed peptide (Wölfel T *et al.* 1993). Even though both A42 and 11/33 CTLs were generated against the same Melan-A epitope, avidities of their TCRs for pMHC complexes were likely to be different. This was confirmed by the use of a slightly changed peptide. The heteroclitic peptide ELAGIGILTV, used in this analysis, is an analogue of the peptide with the natural sequence EAAGIGILTV. The substitution of alanin (A) with leucine (L) was shown to result in stable binding of the peptide to MHC molecules and more efficient recognition by CTLs (Valmori D *et al.* 1998). Activation of the 11/33 clone was also positively influenced by this change. 11/33 CTLs reacted stronger to the synthetic peptide exogenously pulsed onto both T2 cells (Figure 4.22) and DCs (Figure 4.27B) than to melanoma cells (Figure 4.23) and Melan-A cRNA-pulsed DCs (Figure 4.27B) which produced the natural peptide. In contrast, the A42 clone was stimulated to much higher levels by tumour cells (Figure 4.23) than by peptide-pulsed T2 cells (Figure 4.22). Furthermore, co-incubation with RNA-transfected DCs resulted in slightly stronger activation of A42 CTLs, compared to peptide-pulsed DCs (Figure 4.27A).

The outcome of loading DCs with a certain peptide strongly depends on the repertoire of CTLs. As was seen with TyrF8, CTLs may recognise unnatural peptides in addition to the natural ones representing the same epitope. The 11/33 example showed that some CTLs can even react significantly stronger to synthetic rather than peptides produced by the cells. On the other hand, peptides with sequences different from those in primary structures of proteins may cause lower reactivity or no immunity at all. Experiments performed with IVS B and A42 CTLs demonstrated the advantage of DC-pulsing with RNA, as opposed to loading with peptides. The use of RNA technology eliminated the need to know the correct sequences of immunogenic peptides. Unfortunately, not even RNA-transfected DCs can be counted on to generate and present the same peptides as tumour cells. For example, virally-infected murine DCs were shown to differentially present the same MHC class I epitopes compared to infected fibroblasts, even though both cell types produced similar levels of infectious virions and individual viral proteins (Butz EA and Bevan MJ 1998). However, in most cases, a DC is likely to better choose antigens and their epitopes for presentation than the scientist. When DCs are loaded with RNA, this choice is not restricted to only one HLA allotype, but takes into consideration all MHC class I and class II molecules expressed by the DC. Immunotherapy based on pulsing with synthetic peptides usually has the disadvantage of restricted presentation by only one HLA allotype, which automatically eliminates the possibility of treating patients whose repertoires do not include the allele in question.

Furthermore, peptides intracellularly associated with MHC molecules may have an advantage over peptides that bind extracellularly to empty MHC molecules expressed on the cell surface. Proteins fused with a cell-penetrating peptide were shown to rapidly and efficiently enter intact cells (Rojas M *et al.* 1998). In a study performed by Wang, DCs were pulsed with a construct consisting of an epitope from TRP-2 and the cell-penetrating peptide, resulting in successful internalisation of the construct (Wang RF and Wang HY 2002). These DCs were observed to present the TRP-2 epitope over longer periods of time *in vitro* and, after injection into mice, a much more efficient elimination of a melanoma challenge occurred *in vivo*, when compared to DCs pulsed with the TRP-2 peptide alone. Even though the mechanism of prolonged antigen presentation is not clear (it may involve gradual release of peptides from endosomes into the cytoplasm), the difference between peptides endogenously bound to MHC molecules and peptides exogenously loaded onto MHC molecules strongly indicates that the endogenous pathway yields higher stimulatory

capacities of antigen-pulsed DCs. Following transfection of RNA, peptides are produced and associated with antigen presenting molecules inside the DCs, again supporting the use of RNA technology to create pMHC complexes on DCs.

5.5 Priming T-helper cells in addition to CTLs

Most tumours express MHC class I molecules on their surface, but are negative for MHC class II. CTLs recognise antigenic peptides presented within class I molecules. They are very effective in terms of lysing malignant cells directly upon recognition of pMHC class I complexes. Therefore, tumour immunotherapy has focussed on the induction of CTL responses. This is exemplified by an increasingly larger list of identified MHC class I-restricted TAA epitopes. Immunisation of patients with antigens known to provide these epitopes and, thereby, to stimulate CTLs, was shown to generate anti-tumour immunity leading to tumour regression. However, in the majority of vaccinated patients, overall immune responses were too weak and short-lasting to eradicate all cancer cells. Fortunately, a growing body of evidence suggests that including T-helper cells in immunotherapeutic strategies can improve initiation and maintenance of CTL responses (Wang RF 2001).

T-helper cells play an important role in priming CTLs. One proposed mechanism is that they recognise antigens presented within MHC class II molecules on the DCs and, in turn, activate antigen-bearing DCs. Molecules responsible for the interaction between T-helper cells and DCs are CD40 and CD40 ligand (CD40L). CD40L is a membrane molecule expressed by antigen-stimulated T-helper cells which triggers CD40, a surface receptor on DCs. CD40 activates DCs, resulting in increased production of cytokines, especially IL-12 that is a well-known CTL activation factor (Cella M *et al.* 1996). Therefore, after interaction with T-helper cells, DCs become competent to prime CTLs. Inflammatory cytokines and bacterial products that up-regulate MHC and co-stimulatory molecules increase the ability of DCs to stimulate CTL responses (Sallusto F and Lanzavecchia A 1994) and may be even sufficient to activate DCs to a state where they can autonomously do so, even in the absence of T-helper cells (Lanzavecchia A 1998). However, T-helper cells are essential for the maintenance of CTL effector functions by secreting cytokines such as IL-2, which are necessary for CTL growth and proliferation (Greenberg PD 1991).

These findings have important implications in cancer therapy because complete tumour elimination requires prolonged anti-tumour immunity (Ossendorp F *et al.* 1998). Furthermore, T-helper cells can also mediate tumour regression in the absence of CTLs (Greenberg PD 1991). Mechanisms underlying this phenomenon are not clear but several studies suggested that IFN- γ , secreted by T-helper cells, might be involved in anti-tumour and anti-angiogenic activities (Qin Z and Blankenstein T 2000, Mumberg D *et al.* 1999). Other studies proposed that T-helper cells eliminate tumours through activation and recruitment of effector cells, including macrophages and eosinophils (Hung K *et al.* 1998 J, Greenberg PD 1991). It was shown that IFN- γ sensitises tumour cells to CTLs via up-regulation of MHC class I molecules (Dighe AS *et al.* 1994). T-helper cells also activate B-cells to become antibody-secreting plasma cells. Tumour-specific antibodies might, in turn, contribute to therapeutic anti-tumour immunity (Glennie MJ and Johnson PW 2000).

The prerequisite of using antigens in the form of RNA is that transfected RNA has to reach the cytoplasm in order for proteins to be synthesised. Endogenously expressed antigens are presented within MHC class I molecules. Consequently, CTLs and not T-helper cells are activated. However, the RNA technology can be modified to prime both CTL and T-helper cell responses. It has been shown that MHC class II presentation of antigens can be greatly enhanced when they are fused with a sorting signal of LAMP-1 (lysosome-associated membrane protein 1), which directs endogenously expressed proteins into lysosomal compartments and, to a lesser extent, into late endosomes (Wu TC *et al.* 1995). The Gilboa group produced cRNAs encoding chimeric proteins, consisting of the LAMP-1 sorting signal and either telomerase or CEA (carcinoembryogenic antigen). When these RNAs were used in T-cell priming, good CTL responses, significantly higher antigen-specific T-helper cell proliferation and higher numbers of IFN- γ secreting T-helper cells were detected, compared to priming with native telomerase or CEA proteins (Nair S *et al.* 1998). The same group tried another approach. A short incubation of cRNA-transfected DCs with invariant chain antisense oligonucleotides suppressed the expression of the invariant chain, resulting in enhanced presentation of class II epitopes, activation of T-helper cells and more potent and longer lasting CTL responses in vaccinated mice (Zhao Y *et al.* 2003). One of the functions of the invariant chain is to block peptide-binding sites of MHC class II molecules while they are being assembled in the ER and transported into endosomal compartments where they are loaded with peptides derived from internalised exogenous proteins. If the invariant chain is not expressed and the class II peptide-binding

sites are unprotected, i.e. open, endogenous peptides can be associated with MHC II molecules in the ER. Thereby, the repertoire of presented endogenous peptides is expanded and corresponding T-helper cells are activated, in addition to CTLs.

5.6 Overcoming tumour immune escape

One of the strategies used by tumours to escape from immune surveillance is to down-regulate TAA expression. This phenomenon has been observed especially in melanoma, where tumour progression is often associated with reduced expression of melanocyte differentiation antigens such as gp100, Melan-A and tyrosinase (de Vries T *et al.* 1997). In most cases, molecular mechanisms involved in the down-regulation of tumour-antigens are unknown. However, Kurnick and colleagues discovered that some melanoma cells produce soluble factors which actively, but reversibly, down-modulate transcription of the Melan-A gene (Kurnick JT *et al.* 2001).

In order to avoid tumour immune escape, immunotherapy can target multiple TAAs simultaneously. Polyclonal responses of CTLs specific for more than one antigen are likely to result in more efficient elimination of malignant cells, and the killing should not be hampered by the down-regulation of one of the targeted molecules. Such an approach is complicated with DNA vectors, but can be easily developed with RNA. Heiser and colleagues transfected DCs with total cellular RNA from renal cell carcinoma (RCC) and used them for *in vitro* priming of CTLs. Unlike the melanoma model, immunogenic antigens associated with RCC have not been identified. Nevertheless, CTLs against telomerase were found to be a component of the CTL pool primed against RCC. When compared, tumour-specific CTLs were consistently superior to CTLs stimulated with telomerase RNA-transfected DCs in their ability to recognise and lyse tumour cells (Heiser A *et al.* 2001a). In addition to telomerase, PMBCs from patients vaccinated with RCC RNA-transfected DCs displayed reactivity to the oncofetal antigen and G250 (Su Z *et al.* 2003). The same group also worked with prostate cancer. Once again, DCs transfected with amplified tumour RNA stimulated T-cell responses directed against multiple TAAs. Only a fraction of these CTLs were activated against PSA and telomerase. Therefore, polyclonal tumour-specific CTLs were superior in recognising and killing tumour targets to CTLs specific for PSA only (Heiser A *et al.* 2001b). Similarly, epitopes derived from

MUC1 and Her-2/neu antigens were shown to contribute to the cytotoxic activity of CTLs primed with breast cancer RNA-pulsed DCs (Müller MR *et al.* 2003). MUC1-specific CTLs were also detected within the presumably polyclonal CTL pool primed with myeloma RNA-pulsed DCs (Milazzo C *et al.* 2003). All these studies prove that immunotherapeutically-induced tumour-specific CTLs indeed represent polyclonal responses and demonstrate the efficiency of strategies that prime CTLs against multiple antigens.

Another mechanism possibly contributing to immune escape is presentation of APLs. As explained above, the synthetic peptide ELAGIGILTV is an optimised analogue of the naturally presented Melan-A₂₆₋₃₅ peptide EAAGIGILTV. The altered amino acid sequence is a basis for quantitatively and qualitatively improved CTL responses (Valmori D *et al.* 1998, Rivoltini L *et al.* 1999). Therefore, when their impact on a CTL clone were compared, the natural peptide was described as an agonist and the synthetic peptide as a superagonist. At the other extreme, some APLs were observed to act on the same CTLs as partial agonists or antagonists rendering T-cells only partially activated or even anergised (Rivoltini L *et al.* 2002). Interestingly, EAAGIGILTV embodies a general sequence motif frequently occurring in a variety of endogenous peptides and proteins (Loftus DJ *et al.* 1996, Dutoit V *et al.* 2002). Since interaction with APLs with partial agonist or antagonist activities potentially plays a role in the functional impairment of self-reactive T-cells, presentation of APLs may be one of the mechanisms of maintaining peripheral tolerance to self-antigens, in this case Melan-A. Furthermore, given the genetic instability of tumour cells, it is conceivable that modifications of antigen structure, processing and/or presentation may lead to the expression of APLs by cancer cells and that the existence of partial agonist and antagonist peptides derived from TAAs may contribute to the development of peripheral tolerance to these antigens. Indeed, suboptimal activation of antigen-specific CTLs was detected in response to melanoma cells expressing endogenous Melan-A₂₆₋₃₅-like peptides. However, the phenomenon was overcome when CTLs were generated with the superagonist peptide (Carrabba MG *et al.* 2003). The RNA technology also benefited from these observations. DCs electroporated with Melan-A cRNA carrying an A27L amino acid substitution displayed higher stimulatory capacities than DCs pulsed with unmodified Melan-A cRNA (Abdel-Wahab Z *et al.* 2003).

When total cellular RNA is used as a source of TAAs for T-cell priming, identities of these antigens do not have to be known. If antigens associated with a certain tumour have been identified, single-species tumour-antigen cRNAs can be combined in DC-based immunotherapy to minimise effects of tumour escape. By concentrating on several well defined antigens, as opposed to the whole cellular repertoire, quantitatively better presentation of relevant antigenic epitopes and, thereby, more efficient T-cell activation can be achieved (Figures 4.26, 4.27 and 4.28). If necessary, components of the transfected cRNA pool can be manipulated so that peptides with optimised sequences are presented within both MHC class I and class II molecules.

5.7 Antigen competition and immunodominance

The use of multiple antigens in DC-based vaccination, either in the form of pooled single-species tumour-antigen cRNAs or in the form of amplified mRNA from tumour cells, automatically raises the question of immunodominance. If only one epitope will induce strong immune responses, there is no sense in developing a vaccine for several different antigens. However, advantages of simultaneous immunisation against multiple epitopes are becoming increasingly obvious with immunotherapeutic strategies applying more profound mechanisms to break tolerance against self-antigens and to fight tumour escape.

Grossman and colleagues (Grossmann ME *et al.* 2001) favour the use of strategies that utilise not only dominant, but also subdominant epitopes in the design of tumour vaccines. Whereas the immune system is likely to be tolerant to dominant epitopes from self-antigens, it may be easier to mount immune responses against subdominant epitopes. CTLs specific for subdominant epitopes more often bypass negative selection in the thymus and in the periphery. Pulsing with antigens in the form of RNA, allows DCs themselves to choose epitopes from antigens that are probably both dominant and subdominant. Unlike with antigenic peptides, the identity of epitopes and their ranking in the hierarchy of immunodominance do not have to be known if RNA coding for full antigens is used.

Which epitope will dominate an immune response is decided on two levels. The number of pMHC complexes expressed on the surface of a DC molecule may, to a certain extent,

be influenced by the competition of that peptide with other peptides present inside a DC at the same time. However, competition between CTLs specific for different epitopes seems to be the most important factor contributing to the phenomenon of immunodominance.

In my studies, combining tyrosinase, Melan-A and CDK4-R24C antigens was investigated to determine whether it is possible to activate epitope-specific CTLs with DCs that received large amounts of RNA coding for several different antigens (Figures 4.26, 4.27 and 4.28). Whereas the primary conclusion was that successful stimulation can be achieved, the experiments inspire a discussion about the quantities of peptides produced by DCs and their importance for vaccination strategies. In my experimental DC-RNA-CTL system, the variable of competition between CTLs with different specificities and different affinities for pMHC complexes was eliminated, since DCs transfected with either pooled tyrosinase, Melan-A and CDK4-R24C cRNAs or amplified melanoma mRNA were separately co-incubated with each of the five antigen-specific CTL clones. Therefore, arguments can be reduced to the competition of peptides inside the DC, even though CTLs were used to assess the immunogenicity of those peptides upon presentation.

The highest stimulation of CTLs was achieved within the system when DCs transfected with 48 μg of a single-species cRNA alone were utilised. As expected, 24 μg of a single-species cRNA alone led to lower but not proportional CTL stimulation. When 48 μg of each of the three single-species cRNAs were pooled, giving a total of 144 μg , and transfected into DCs, stimulations of individual CTL clones never reached their maximums, but were approximately in the range associated with 24 μg of each single-species cRNA applied alone. Responses to DCs transfected with 24 μg of each of the three single-species cRNAs, summing up to a total of 72 μg combined RNA, were similar or equal to the upper limit reached with 144 μg of pooled cRNAs. Since the CTLs had the capacity to secrete more IFN- γ , the argument can be made that the limiting factor in CTL activation was not the number of 2×10^4 CTLs, but rather the quantity of pMHC class I complexes expressed on the surface of 4×10^4 DCs. After transfection with either 144 μg or 72 μg of pooled cRNAs, so many antigenic peptides were produced that, in the context of a total cellular peptide pool, the antigen-presenting capacity of each DC was fully used. Tyrosinase, Melan-A and CDK4-R24C peptides possibly competed for free antigen-presenting molecules to some extent, but enough pMHC class I complexes were formed in all three cases for successful stimulation of epitope-specific CTL clones.

In comparison with single-species cRNA samples, amplified mRNA from a melanoma cell line contained much lower amounts of combined message for tyrosinase, Melan-A and CDK4-R24C. DCs transfected with 75 µg of this RNA seemed to produce significantly fewer peptides, as assessed by CTL recognition of pMHC class I complexes. It is possible that, the total cellular mRNA pool also contained factors that changed antigen processing and presentation in the DCs. However, since potential intracellular competition between peptides was not observed to strongly influence CTL stimulation when high doses of pooled single-species cRNAs were used, it is difficult to imagine that this kind of competition occurred upon transfection of total cellular mRNA.

If used as a vaccine, DCs pulsed with various RNA species will have the task of simultaneously activating CTLs of different specificities. For this reason, potential immunodominance, i.e. suppression of T-cell responses to subdominant epitopes by dominant epitopes, has to be taken into account. It has been hypothesised that competition between CTLs of different specificities occurs if peptides produced inside the same DC are not very abundant (Kedl RM *et al.* 2003). On the other hand, very high amounts of various peptides should result in expression of many pMHC class I complexes and eliminate the basis for CTL competition. As concluded above, DCs transfected with large quantities of pooled single-species tumour-antigen cRNAs produced large quantities of relevant peptides. These peptides possibly compete with irrelevant peptides and also among themselves, but nevertheless they do stimulate corresponding CTLs in the range where more RNA does not mean higher IFN- γ secretion by CTLs. This indirectly indicates that MHC class I molecules on the DCs are saturated with peptides, with possibly a high percentage of them presenting antigenic epitopes. Therefore, according to Kedl, these DCs should not cause immunodominance of an epitope from one antigen to epitopes from other antigens when used as a vaccine. Nevertheless, for DCs transfected with amplified mRNA from melanoma cells, a different set of rules may apply. Since antigenic peptides do not necessarily outnumber other peptides produced inside a transfected DC, fewer relevant complexes are expressed. According to Kedl, this may result in competition between CTLs of different specificities.

It was shown in numerous experiments that increasing the quantity of DCs used in vaccination, diminished or even abolished immunodominance. Furthermore, if separate DC populations were engineered to present single antigens and were pooled for

immunisation, immunodominance does not occur (Wolpert EZ 1998, Sandberg JK 1998, Grufman P 1999a, Grufman P 1999b). In other words, more DCs and more pMHC complexes expressed on their surfaces, meant less competition between responding CTLs, particularly if individual peptides were presented on separate DCs. Amplified mRNA from tumour cells is used when immunogenic antigens are unknown. In this case, message for different antigens can not be separated and the only way to avoid potential immunodominance seems to be administration of higher numbers of transfected DCs. If TAAs have been identified, as in the case of melanoma, two vaccination strategies can be considered. Each single-species tumour-antigen cRNA can be transfected into DCs separately and these DCs can be mixed before administration as a vaccine. According to experience of several groups, pooling pulsed DCs instead of antigens should eliminate immunodominance. Technically, it is easier to transfect pooled single-species tumour-antigen cRNAs into DCs. Whereas simultaneous presentation of different antigenic peptides may lead to immunodominance, the quantitation experiments performed with pooled tyrosinase, Melan-A and CDK4-R24C cRNAs demonstrated that peptides are abundant enough and should therefore minimise immunodominance.

5.8 Dangers of autoimmunity associated with immunotherapy

Some autoimmune phenomena seem to be associated with certain tumours. In some cases, antigen-specific immune responses have been described as the connection between malignancies and autoimmunity.

Paraneoplastic neurologic disorders are autoimmune neuronal degenerations that develop in some patients with systemic cancer. Such disorders are believed to be initiated when solid tumours (e.g. breast, ovarian, small-cell lung) present outside of the nervous system express neuronal proteins. Darnell proposed the following model (Darnell RB 1996). Antigens in question are normally expressed exclusively in neurons, both during development and adulthood. Because of the blood-brain barrier and/or the immunologically privileged state of neurons, the immune system most probably ignores T-cells specific for neuronal proteins. When these proteins are expressed elsewhere in the body, i.e. in tumour cells, they are recognised by the immune system and specific T-cells are activated. Anti-tumour responses based on these onconeural antigens may be followed

by the disruption of the blood-brain barrier or a change in the nature of the immune cells themselves. This establishes autoimmune neurologic degeneration and brings patients to clinical attention. There is a report regarding three patients with paraneoplastic neurological syndromes who experienced spontaneous regressions of small-cell lung carcinoma (Darnell RB and DeAngelis LM 1993).

Wegener's granulomatosis is a systemic disease of unknown origin. Autoimmune mechanisms and infection are suggested to play a role in its pathogenesis. It is characterised by a necrotising vasculitis involving lungs, upper airways and kidneys. Autoantibodies against proteinase 3, also known as Wegener's autoantigen, are closely associated with this disease (Kallenberg CG *et al.* 2002). The close temporal association between RCC and Wegener's granulomatosis suggests that the malignancy is, in some cases, a trigger for the development of the disease. However, proteinase 3 was not found in malignant tissues of patients suffering from both RCC and Wegener's granulomatosis (Tatsis E *et al.* 1999).

Vitiligo is an autoimmune condition characterised by the loss of epidermal melanocytes. Otherwise healthy patients suffering from this disorder were examined for the presence of immunity against antigens associated with melanocytes. Tyrosinase-specific autoantibodies were detected in 77% of individuals with vitiligo (Song YH *et al.* 1994). Another study showed that 77% had circulating CTLs specific for Melan-A (Ogg GS *et al.* 1998). This demonstrated that vitiligo is caused by autoimmune responses directed at the same antigens that are often used as targets in immunotherapy of melanoma. Indeed, vitiligo is more frequent in melanoma patients where its development may be associated with an ongoing spontaneous or therapeutically induced immune response against this type of cancer. Romero and colleagues found that Melan-A specific CTLs were expanded in tumour-infiltrated lymph nodes of melanoma patients with extremely high frequencies of 1 in every 30 to 400 CTLs (Romero P *et al.* 1998). Some of these patients had not received immunotherapy before the study was performed, indicating spontaneous T-cell priming. These Melan-A-specific CTLs displayed mostly an antigen-experienced phenotype and were capable of efficiently killing autologous tumour cells *in vitro*, providing direct evidence that an antigen-specific immune response had been triggered by the tumour. Similar results were obtained for the tyrosinase antigen. The same group also examined Melan-A-specific CTLs in the circulation (Pittet MJ *et al.* 1999). These cells were

detected in 77% of examined melanoma patients. Their frequency of approximately 1 in every 1500 CTLs was somewhat lower, compared to that measured in tumour-infiltrated lymph nodes, but still significantly high. Interestingly, just as many Melan-A specific CTLs were found in 60% of healthy controls. Circulating CTLs specific for Melan-A displayed a naïve phenotype in healthy individuals and 70% of melanoma patients, whereas an experienced CTL phenotype was observed in the remaining 30% of patients. Vitiligo developed in 23% of the patients, probably not as a spontaneous response, but occurring after antigen-unspecific immunotherapy with different combinations of the cytokines IL-2, IFN- α and TNF- α . The frequency of Melan-A-specific CTLs in patients with melanoma and vitiligo was 1 in every 430 CTLs. Another study found no vitiligo in melanoma patients who remained unresponsive to IL-2 immunotherapy (Rosenberg SA and White DE 1996). However, vitiligo was seen in 26% of melanoma patients who did react to the same therapy. These findings provided evidence that the presence of growing melanomas can sensitise patients to melanocyte differentiation antigens and that the immune response against these antigens is associated with cancer regression in patients undergoing immunotherapy.

Although paraneoplastic neurologic disorders, Wegener's granulomatosis and vitiligo are unwanted side-effects or even harmful diseases, their association with tumours shows that the immune system is indeed capable of mounting strong responses against TAAs. The responses can even be spontaneous or caused by antigen-unspecific immunotherapy. Unfortunately, these autoimmune conditions also indicate that efficient immune reactions to tumours can be dangerous because of autoimmune diseases that may accompany them. DC-based tumour immunotherapy is likely to generate immune responses more powerful than those induced spontaneously. Depending on the approach, either total cellular antigenic repertoires or well-defined individual self-antigens are used. This justifies the question, whether an improved efficiency of immunotherapy results in an even higher risk of autoimmunity.

Highly tumourigenic and poorly immunogenic mice were vaccinated with irradiated GM-CSF-transduced melanoma cells and antibodies blocking CTLA-4 (cytotoxic T-lymphocyte associated protein 4). The treatment was effective, but 56% of the animals developed vitiligo, starting at the site of vaccination and in most cases progressing to distant locations. Depigmentation occurred in T-helper cell-depleted mice, strongly

suggesting that the effect was mediated by CTLs (van Elsas A *et al.* 1999). Bondanza and colleagues also demonstrated potentially dangerous effects of vaccination against self-antigens (Bondanza A *et al.* 2003). DCs that phagocytosed autologous apoptotic cells were injected into healthy mice, genetically predisposed or not to the development of autoimmunity. In all vaccinated mice, high titres of anti-nuclear and anti-dsDNA autoantibodies were found. In normal mice, these antibodies progressively disappeared and did not cause autoimmune disease or tissue damage. In contrast, predisposed animals developed progressive and eventually lethal autoimmunity. In the study, DCs were pulsed with total cellular preparations that contained whole repertoires of expressed antigens, an approach similar to transfecting total cellular RNA into DCs. Whereas the existence of autoimmune reactions was confirmed, it was also observed that these reactions were transient in healthy mice. Therefore, the group concluded that autoantibody responses in treated patients may go undetected and that it should be relatively safe to use DCs pulsed with total cellular antigenic repertoires in vaccination. Potent anti-tumour immunity was observed in the absence of detectable autoimmunity in mice vaccinated with only irradiated GM-CSF transduced melanoma cells (Dranoff G *et al.* 1993), with DC-derived exosomes (Zitvogel L *et al.* 1998) and with DCs pulsed with total cellular RNA from ovalbumin-expressing tumour cells (Boczkowski D *et al.* 1996).

In humans, autoreactivity of CTLs primed with total cellular RNA-pulsed DCs was investigated thoroughly by Heiser and colleagues (Heiser A *et al.* 2001a). In their RCC model *in vitro*, DCs transfected with renal tumour RNA stimulated CTLs capable not only of killing autologous tumour cells, but also recognising antigens expressed by tumour cells from other RCC patients. The same CTLs did not react against autologous DC-targets that were transfected with either autologous or allogeneic RNA derived from normal tissue. This demonstrated that primed CTLs were indeed tumour-specific. Furthermore, foreign RNA, which included message for non-matched HLA molecules, did not induce alloreactive CTL responses after transfection into autologous DCs. In the context of vaccination strategies, antigens in the form of allogeneic tumour RNA may represent an attractive alternative because well-characterised and generic vaccines could substitute for expensive and time-consuming individual approaches. As a control, the group transfected DCs with RNA from normal tissues. CTLs primed by these DCs lysed neither tumour nor normal tissue targets. These data indicated that harmful autoimmunity with pathological consequences may not be a serious issue with this approach, even though self-antigens

might be presented in a highly stimulatory manner. After vaccination of RCC patients with total cellular tumour RNA-pulsed DCs, enhanced reactivity against RCC antigens was reported (Su Z *et al.* 2003). Even though there was minor reactivity of vaccine-induced T-cells against benign renal tissue, neither deterioration of renal function nor increases of autoimmune parameters were observed in the patients.

A similar study was performed with prostate cancer. DCs transfected with total cellular RNA from this tumour stimulated CTLs which not only recognised tumour-antigens, but also antigens expressed by normal prostatic tissue. Interestingly, these responses were exclusively directed against PSA shared between malignant and nonmalignant tissue. Other shared antigens were either insufficiently expressed by normal prostate cells or they contained only epitopes subdominant to PSA. In this particular case, the group evaluated the risk of autoimmunity as acceptable since prostates are nonessential for life (Heiser A *et al.* 2001b). When prostate cancer RNA-pulsed DCs were applied in a clinical trial, modest anti-tumour effects were suggested in the patients and no dose-limiting toxicity or adverse effects, including autoimmunity, were observed (Heiser A *et al.* 2002).

Even if DCs are pulsed with mixtures of self-antigens, the rules of immunodominance ensure that not all antigens will be efficiently presented and that their presentation will not necessarily generate strong T-cell responses, depending on the frequency and the avidity of antigen-specific T-cells and their competition for different factors associated with DCs pulsed with antigenic mixtures. However, quantitative differences in expression between usually over-expressed or re-expressed TAAs versus other self-antigens that are not over-expressed may permit more successful activation of TAA-specific T-cells. Mutated TAAs, that can no longer be classified as self-antigens, might have the advantage of winning the competition and becoming immunodominant, while still allowing the development of somewhat weaker responses against some subdominant TAAs. Based on these considerations, Gilboa concluded that most self-antigens should be underrepresented in a tumour-specific T-cell population. Furthermore, contrary to popular belief, vaccination with patient-specific tumour-derived antigenic mixtures may not only be more effective than vaccination with single shared tumour self-antigens, but may also entail a reduced risk of autoimmunity (Gilboa E 2001).

Immunotherapeutic approaches directed at multiple TAAs are likely to be more effective than strategies targeting individual TAAs. However, using a single antigen eliminates competition and potentially increases the strength of the immune response against this antigen, compared to simultaneous responses against different antigens. Depending on the antigen chosen, this may cause not only stronger tumour immunity, but also autoimmunity.

Immunisation of rats with a viral vector expressing human PAP (prostatic acid phosphatase), an antigen uniquely expressed in prostatic tissue and prostate cancer, generated a CTL response and destructive autoimmune prostatitis. A vector expressing rat PAP induced no immunity (Fong L *et al.* 1997). The study performed by Ludewig and colleagues (Ludewig *et al.* 2000) is also often cited in discussions about autoimmunity caused by immunotherapy against tumours. The mice they vaccinated developed life-threatening autoimmune diabetes and cardiovascular disease. It has to be noted that this immunotherapy targeted antigens that were selectively expressed in essential organs based on transgenes. Therefore, conclusions about the connection between immunotherapy and autoimmunity were drawn from a highly artificial model situation in which antigens with known distribution were chosen. Nevertheless, this study is a good example of a worst-case scenario, stressing the necessity of careful antigen selection in immunotherapy. In other transgenic mouse models, no autoimmune phenomena were detected. After vaccination, tumour cells expressing high levels of influenza virus hemagglutinin were rejected in mice, but pancreatic cells engineered to selectively express the same antigen were not destroyed (Morgan DJ *et al.* 1998). Even though skin epithelial cells in transgenic mice expressed the viral E7 antigen, the skin remained unaffected after immunisation with the E7 peptide. These mice were protected against subsequent challenge with tumour cells expressing a transfected E7 gene (Melero I *et al.* 1997). When CTLs specific for a viral envelope protein were adoptively transferred into mice with lymphoid cells selectively expressing this protein, tumour cells positive for the same antigen were eradicated, but no detectable autoimmune damage to the lymphoid tissue was induced (Hu J *et al.* 1993). The tumour suppressor protein p53 is over-expressed in close to 50% of all human malignancies. Mice immunised with murine p53-overexpressing tumour cells completely rejected this tumour upon challenge. No demonstrable damage to normal tissue was observed (Vierboom MP *et al.* 1997).

Based on some data, the development of vitiligo was associated with vaccination against individual MAAs. However, there are other studies that found no such correlation. Immunisation of mice with purified murine TRP-1, a melanocyte differentiation antigen, failed to induce antibody or CTL responses, but when human TRP-1 was used, mice rejected metastatic melanomas and developed vitiligo (Naftzger C *et al.* 1996). Skin depigmentation and melanocyte destruction were also observed in mice inoculated with a viral vector encoding murine TRP-1 (Overwijk WW *et al.* 1999). However, mice vaccinated with either a plasmid or a viral vector encoding murine TRP-2 rejected the melanoma tumour and did not develop generalised vitiligo (Bronte V *et al.* 2000). Vaccination of mice with TRP-2 peptide-loaded DCs also resulted in protective antitumour immunity, but only minor depigmentation restricted to the vaccination site was seen, despite the observed CTL-mediated melanocyte destruction *in vitro* (Schreurs MW *et al.* 2000).

In vitro, CTLs usually kill isolated normal cells with the same efficiency that they kill tumour cells. Nevertheless, experimental data presented above strongly indicate that structured normal tissues and tumour masses *in vivo* display different susceptibilities to effector cells of the immune system. Therefore, Gilboa concluded that vaccination against individual self-antigens expressed in tumour cells should be capable of inducing therapeutic immunity in the absence of devastating autoimmune consequences. However, increasing the effectiveness and/or intensity of vaccination with a self-antigen could result in mild to serious autoimmune pathology. Careful selection of TAAs is the safest solution to this problem. Good candidates can be found in the group of antigens that are expressed in immunoprivileged sites and are reactivated in cancer cells (e.g. MAGE) and in the group of fetal and embryonic antigens that are re-expressed in cancer cells (e.g. CEA and oncofetal antigen). Most importantly, since tumour cells themselves are not able to shuttle their own antigens to the secondary lymphoid organs, professional APCs are necessary to activate the naïve and the memory T-cells. For that reason, it should be possible to control unwanted autoimmune reactions by simply stopping vaccination (Gilboa E 2001).

5.9 Conclusions and prospects

Even though RNA is rapidly degraded and, therefore, difficult to work with, electroporation of RNA encoding TAAs was confirmed to be a highly efficient method of introducing antigens into DCs in order to improve their presentation to the immune system. It is unclear whether RNA should be electroporated into DCs of an immature or mature stage. Whereas these studies indicated that *in vitro* mature DCs express more antigen than immature DCs, allowing transfected DCs to mature *in situ* may prove to be a good compromise between initial manipulation *ex vivo* and subsequent adaptation *in vivo*. Kinetic studies demonstrated that after electroporation there is an initial surge in antigen expression which subsequently decreases, depending on transfected RNA degradation and protein half-life. Therefore, considering the right time-frame for T-cell activation by engineered DCs might be advantageous in designing immunotherapeutic strategies. Quantitation experiments explained the significantly different stimulatory capacities of DCs pulsed with total cellular tumour RNA and single-species tumour-antigen cRNAs. Transferring more antigen message into DCs indeed resulted in higher antigen expression, better epitope presentation and stronger T-cell stimulation. Amplification of total cellular RNA samples increased the proportions of TAAs that have higher expression levels in the tumour and, thereby, enhanced their presentation, but a normally-expressed mutated TAA was hardly amplified in RT-PCR and, consequently, only weakly presented. If immunogenic TAAs are not known in a tumour model, total cellular RNA is the only source of antigenic material than can be utilised. Single-species RNAs encoding identified TAAs not only guarantee stronger T-cell stimulation, but also allow fine-tuning of immune responses by adjusting antigenic sequences and combining antigens. RNA coding for a protein fused with a signal sequence was described to induce tumour epitope presentation not only to CTLs but also to T-helper cells. Priming of T-cells against more than one antigen is necessary to minimise the effects of potential tumour escape from immune surveillance. Electroporation with a combination of RNAs encoding different TAAs was shown to stimulate CTLs on levels only slightly lower than those achieved with individual RNAs alone, indicating that possible competition of antigens inside the DCs did not inhibit T-cell responses. It remains to be seen whether pooling RNAs before transfection or mixing individually-transfected DCs before vaccination helps avoid immunodominance due to competition between T-cells. Having established and discussed approaches to enhance TAA presentation and T-cell activation, the risk of autoimmunity associated with

immunotherapy requires attention. Examples from the literature indicate that vaccination against TAAs, most of which are self-antigens, may not be as dangerous as previously postulated.

The described methodology was optimised and thoroughly explained in the context of immunology and cellular biology. This was only possible in a well-defined system with highly sensitive antigen-specific CTL clones. Further research should show if the observed quantitative differences in antigen presentation have an impact on priming of immune responses *in vitro* and subsequently *in vivo*, as another small step is made in mobilising the immune system to fight cancer.

6. Summary

In situations where well-established approaches such as surgery, radiation therapy and chemotherapy fail to help cancer patients, immunotherapy has the potential to be an effective alternative. Tumour cells can sometimes be distinguished from corresponding normal cells due to their expression of tumour-associated antigens (TAAs), most of which are unaltered self-molecules. These molecules must be presented to the immune system in the context of danger in order to achieve their specific recognition. If dendritic cells (DCs), the most potent professional antigen-presenting cells, are loaded with RNA, they will translate the RNA into protein, process the protein into peptides and present the peptides within MHC molecules (pMHC) on their surface to cytotoxic T-lymphocytes (CTLs) and T-helper cells in a stimulatory manner. These effector cells can, in turn, recognise tumour cells. The goal of these studies was to find optimal conditions for producing a DC-based vaccine for cancer patients using TAAs in the form of RNA. The studies were designed to quantitate RNA transfer into DCs, to determine the intracellular stability of transfected RNA in DCs and to analyse the kinetics of protein expression and the generation of functional pMHC ligands that could activate effector memory CTLs. Simultaneous activation of CTLs with specificities for different antigens minimises the potential for tumour escape through immune selection of tumour variants showing loss of individual antigens. Thus, generation of multiplex pMHC ligands for CTLs may improve clinical efficiency. On the other hand, peptide competition for MHC molecules within the DC may limit pMHC ligand generation. This central immunological question was addressed by comparing DCs loaded with total cellular tumour RNA, amplified total cellular tumour mRNA and pools of defined single-species tumour-antigen cRNAs versus individual single-species tumour-antigen cRNAs for their capacity to display various pMHC ligands and activate CTLs of corresponding specificities.

Experiments performed with RNA encoding the enhanced green fluorescence protein (EGFP), a reporter protein, showed that the highest efficiency of RNA transfection into DCs was achieved with electroporation, reaching levels of 90% positive cells. The fact that mature DCs expressed more EGFP than immature DCs suggests that this stage of DC maturation will be optimal for vaccine development. Importantly, electroporation and RNA transfer did not alter the expression of antigen-presenting and co-stimulatory molecules on the surface of DCs.

The melanoma model was chosen for extensive analyses because its characterisation at the cellular and molecular levels has made it a very informative model for understanding cancer immunity. In addition to total cellular melanoma RNA, single-species cRNAs were used encoding the melanoma-associated antigens, tyrosinase, Melan-A and CDK4-R24C. Antigen presentation was detected with the help of effector memory CTL clones specific for each of these antigens. The CTL stimulatory capacity of RNA-transfected DCs was higher if they were allowed one day to recuperate from electroporation and to produce pMHC complexes. Tyrosinase cRNA dose-finding showed that more RNA would indeed result in higher stimulatory capacities of transfected DCs. Kinetics of tyrosinase cRNA degradation, similar to kinetics of EGFP cRNA degradation, revealed that the amount of transfected RNA rapidly decreased inside the DCs within 1.5 hr after electroporation. The smallest decrease was observed with the highest amount of RNA applied in electroporation. The kinetics of RNA degradation and protein half-life will be important parameters to consider in defining the right time-frame for T-cell activation by engineered DCs. When reverse transcription PCR (RT-PCR) was performed with total cellular melanoma RNA samples to generate amplified mRNA, the Melan-A, tyrosinase and CDK4/CDK4-R24C message was amplified 62-fold, 24-fold and 2-fold, respectively. These differences likely reflect variations in the expression levels of the corresponding antigen message in melanoma cells from which the RNA was isolated. Approximately 17240-fold more CDK4-R24C message, at least 500-fold more tyrosinase message and at least 480-fold more Melan-A message was found in single-species cRNAs when the same masses of single-species cRNA and amplified melanoma mRNA samples were compared. This explained why electroporation of single-species cRNAs into DCs yielded the highest DC stimulatory capacities. Combinations of tyrosinase, Melan-A and CDK4-R24C cRNAs were studied for their capacity to induce satisfactory levels of T-cell stimulation when presented by DCs. Here it was demonstrated that antigen competition was not a critical factor, since CTL responses to pooled RNAs were not inhibited even though competition for MHC class I molecules may have occurred within the DCs. DCs also developed CTL stimulatory capacities, but at much lower levels, using amplified melanoma mRNA. Two antigen-specific CTL clones displayed higher reactivities upon exposure to pMHC produced naturally by RNA-transfected DCs than to synthetic peptides pulsed onto DCs. In one case, this could be explained by a post-translational modification of the peptide, which normally occurs within cells. Since this particular modification was

not represented in the synthetic peptide, which was chosen from the protein sequence, the synthetic peptide was not well recognised. This demonstrated that the use of RNA technology eliminates the need to know the correct sequences of immunogenic peptides. Thereby, DCs are better than scientists at choosing antigens and their epitopes for presentation to T-cells.

These data provided a better understanding of antigen presentation by DCs based on the use of RNA, giving insight into antigen competition and paving the way for the use of pooled RNAs of defined species for the development of a multiplex vaccine. They also allowed a precise protocol for efficient T-cell activation to be defined. Further experiments will demonstrate whether quantitative differences detected in antigen presentation between DCs loaded with total cellular tumour RNA and amplified total cellular tumour mRNA versus single-species tumour-antigen cRNAs have an impact on *de novo* T-cell priming *in vitro* and *in vivo*.

7. References

Abdel-Wahab Z, Kalady MF, Emani S, Onaitis MW, Abdel-Wahab OI, Cisco R, Wheless L, Cheng TY, Tyler DS, Pruitt SK

Induction of anti-melanoma CTL response using DC transfected with mutated mRNA encoding full-length Melan-A/MART-1 antigen with an A27L amino acid substitution.

Cell Immunol 2003, 224(2):86-97.

Banchereau J, Briere F, Caux C, Davoust J, Lebecque S, Liu YJ, Pulendran B, Palucka K
Immunobiology of dendritic cells.

Annu Rev Immunol 2000, 18:767-811.

Barker CF, Billingham RE

Immunologically privileged sites.

Adv Immunol 1977, 25:1-54.

Bevan MJ

Cross-priming for a secondary cytotoxic response to minor H antigens with H-2 congenic cells which do not cross-react in the cytotoxic assay.

J Exp Med 1976, 143(5):1283-8.

Bhardwaj N, Young JW, Nisanian AJ, Baggers J, Steinman RM

Small amounts of superantigen, when presented on dendritic cells, are sufficient to initiate T cell responses.

J Exp Med 1993, 178(2):633-42.

Bhardwaj N

Processing and presentation of antigens by dendritic cells: implications for vaccines.

Trends Mol Med 2001, 7(9):388-94.

Birkeland SA, Storm HH, Lamm LU, Barlow L, Blohme I, Forsberg B, Eklund B, Fjeldborg O, Friedberg M, Frodin L

Cancer risk after renal transplantation in the Nordic countries, 1964-1986.

Int J Cancer 1995, 60(2):183-9.

Boczkowski D, Nair SK, Snyder D, Gilboa E

Dendritic cells pulsed with RNA are potent antigen-presenting cells in vitro and in vivo.

J Exp Med 1996, 184(2):465-72.

Boczkowski D, Nair SK, Nam JH, Lyerly HK, Gilboa E

Induction of tumor immunity and cytotoxic T lymphocyte responses using dendritic cells transfected with messenger RNA amplified from tumor cells.

Cancer Res 2000, 60(4):1028-34.

Bondanza A, Zimmermann VS, Dell'Antonio G, Dal Cin E, Capobianco A, Sabbadini MG, Manfredi AA, Rovere-Querini P

Cutting edge: dissociation between autoimmune response and clinical disease after vaccination with dendritic cells.

J Immunol 2003, 170(1):24-7.

Boon T, van der Bruggen P

Human tumor antigens recognized by T lymphocytes.

J Exp Med 1996, 183(3):725-9.

Brady CS, Bartholomew JS, Burt DJ, Duggan-Keen MF, Glenville S, Telford N, Little AM, Davidson JA, Jimenez P, Ruiz-Cabello F, Garrido F, Stern PL

Multiple mechanisms underlie HLA dysregulation in cervical cancer.
Tissue Antigens 2000, 55(5):401-11.

Bronte V, Apolloni E, Ronca R, Zamboni P, Overwijk WW, Surman DR, Restifo NP, Zanovello P

Genetic vaccination with "self" tyrosinase-related protein 2 causes melanoma eradication but not vitiligo.
Cancer Res 2000, 60(2):253-8.

Burnet FM

The concept of immunological surveillance.
Prog Exp Tumor Res 1970, 13:1-27.

Butz EA, Bevan MJ

Differential presentation of the same MHC class I epitopes by fibroblasts and dendritic cells.
J Immunol 1998, 160(5):2139-44.

Cappello P, Novelli F, Forni G, Giovarelli M

Death receptor ligands in tumors.
J Immunother 2002, 25(1):1-15.

Carbone E, Terrazzano G, Ruggiero G, Zanzi D, Ottaiano A, Manzo C, Karre K, Zappacosta S

Recognition of autologous dendritic cells by human NK cells.
Eur J Immunol 1999, 29(12):4022-9.

Carrabba MG, Castelli C, Maeurer MJ, Squarcina P, Cova A, Pilla L, Renkvist N, Parmiani G, Rivoltini L

Suboptimal activation of CD8(+) T cells by melanoma-derived altered peptide ligands: role of Melan-A/MART-1 optimized analogues.
Cancer Res 2003, 63(7):1560-7.

Castelli C, Rivoltini L, Andreola G, Carrabba M, Renkvist N, Parmiani G

T-cell recognition of melanoma-associated antigens.
J Cell Physiol 2000, 182(3):323-31.

Cella M, Scheidegger D, Palmer-Lehmann K, Lane P, Lanzavecchia A, Alber G

Ligation of CD40 on dendritic cells triggers production of high levels of interleukin-12 and enhances T cell stimulatory capacity: T-T help via APC activation.
J Exp Med 1996, 184(2):747-52.

Cella M, Engering A, Pinet V, Pieters J, Lanzavecchia A

Inflammatory stimuli induce accumulation of MHC class II complexes on dendritic cells.
Nature 1997, 388(6644):782-7.

Cella M, Salio M, Sakakibara Y, Langen H, Julkunen I, Lanzavecchia A

Maturation, activation, and protection of dendritic cells induced by double-stranded RNA.
J Exp Med 1999, 189(5):821-9.

Chen L, McGowan P, Ashe S, Johnston J, Li Y, Hellstrom I, Hellstrom KE

Tumor immunogenicity determines the effect of B7 costimulation on T cell-mediated tumor immunity.
J Exp Med 1994, 179(2):523-32.

Clemente CG, Mihm MC Jr, Bufalino R, Zurrida S, Collini P, Cascinelli N

Prognostic value of tumor infiltrating lymphocytes in the vertical growth phase of primary cutaneous melanoma.

Cancer 1996, 77(7):1303-10.

Conry RM, LoBuglio AF, Wright M, Sumerel L, Pike MJ, Johanning F, Benjamin R, Lu D, Curiel DT

Characterization of a messenger RNA polynucleotide vaccine vector.

Cancer Res 1995, 55(7):1397-400.

Darnell RB, DeAngelis LM

Regression of small-cell lung carcinoma in patients with paraneoplastic neuronal antibodies.

Lancet 1993, 341(8836):21-2.

Darnell RB

Onconeural antigens and the paraneoplastic neurologic disorders: at the intersection of cancer, immunity, and the brain.

Proc Natl Acad Sci USA 1996, 93(10):4529-36.

de Mazière AM, Muehlethaler K, van Donselaar E, Salvi S, Davoust J, Cerottini JC, Levy F, Slot JW, Rimoldi D

The melanocytic protein Melan-A/MART-1 has a subcellular localization distinct from typical melanosomal proteins.

Traffic 2002, 3(9):678-93.

Dermime S, Armstrong A, Hawkins RE, Stern PL

Cancer vaccines and immunotherapy.

Br Med Bull 2002, 62:149-62.

de Vries TJ, Fourkour A, Wobbes T, Verkroost G, Ruiter DJ, van Muijen GN

Heterogeneous expression of immunotherapy candidate proteins gp100, MART-1, and tyrosinase in human melanoma cell lines and in human melanocytic lesions.

Cancer Res 1997, 57(15):3223-9.

de Vries E, Bray FI, Coebergh JW, Parkin DM

Changing epidemiology of malignant cutaneous melanoma in Europe 1953-1997: rising trends in incidence and mortality but recent stabilizations in western Europe and decreases in Scandinavia.

Int J Cancer 2003, 107(1):119-26.

Dighe AS, Richards E, Old LJ, Schreiber RD

Enhanced in vivo growth and resistance to rejection of tumor cells expressing dominant negative IFN gamma receptors.

Immunity 1994, 1(6):447-56.

Dranoff G, Jaffee E, Lazenby A, Golumbek P, Levitsky H, Brose K, Jackson V, Hamada H, Pardoll D, Mulligan RC

Vaccination with irradiated tumor cells engineered to secrete murine granulocyte-macrophage colony-stimulating factor stimulates potent, specific, and long-lasting anti-tumor immunity.

Proc Natl Acad Sci USA 1993, 90(8):3539-43.

Dunn GP, Bruce AT, Ikeda H, Old LJ, Schreiber RD

Cancer immunoediting: from immunosurveillance to tumor escape.

Nat Immunol 2002, 3(11):991-8.

Dutoit V, Rubio-Godoy V, Pittet MJ, Zippelius A, Dietrich PY, Legal FA, Guillaume P, Romero P, Cerottini JC, Houghten RA, Pinilla C, Valmori D

Degeneracy of antigen recognition as the molecular basis for the high frequency of naive A2/Melan-a peptide multimer(+) CD8(+) T cells in humans.

J Exp Med 2002, 196(2):207-16.

Dyall R, Bowne WB, Weber LW, LeMaoult J, Szabo P, Moroi Y, Piskun G, Lewis JJ, Houghton AN, Nikolic-Zugic J

Heteroclitic immunization induces tumor immunity.

J Exp Med 1998, 188(9):1553-61.

Engelhard VH, Brickner AG, Zarling AL

Insights into antigen processing gained by direct analysis of the naturally processed class I MHC associated peptide repertoire.

Mol Immunol 2002, 39(3-4):127-37.

Eppler E, Horig H, Kaufman HL, Groscurth P, Filgueira L

Carcinoembryonic antigen (CEA) presentation and specific T cell-priming by human dendritic cells transfected with CEA-mRNA.

Eur J Cancer 2002, 38(1):184-93.

Fong L, Ruegg CL, Brockstedt D, Engleman EG, Laus R

Induction of tissue-specific autoimmune prostatitis with prostatic acid phosphatase immunization: implications for immunotherapy of prostate cancer.

J Immunol 1997, 159(7):3113-7.

Fontana A, Frei K, Bodmer S, Hofer E, Schreier MH, Palladino MA Jr, Zinkernagel RM

Transforming growth factor-beta inhibits the generation of cytotoxic T cells in virus-infected mice.

J Immunol 1989, 143(10):3230-4.

Garbe C, Blum A

Epidemiology of cutaneous melanoma in Germany and worldwide.

Skin Pharmacol Appl Skin Physiol 2001, 14(5):280-90.

Garcia-Lora A, Algarra I, Garrido F

MHC class I antigens, immune surveillance, and tumor immune escape.

J Cell Physiol 2003, 195(3):346-55.

Garrido F, Ruiz-Cabello F, Cabrera T, Perez-Villar JJ, Lopez-Botet M, Duggan-Keen M, Stern PL

Implications for immunosurveillance of altered HLA class I phenotypes in human tumours.

Immunol Today 1997, 18(2):89-95.

Garrido F, Algarra I

MHC antigens and tumor escape from immune surveillance.

Adv Cancer Res 2001, 83:117-58.

Gerosa F, Baldani-Guerra B, Nisii C, Marchesini V, Carra G, Trinchieri G

Reciprocal activating interaction between natural killer cells and dendritic cells.

J Exp Med 2002, 195(3):327-33.

Gilboa E

The risk of autoimmunity associated with tumor immunotherapy.

Nat Immunol 2001, 2(9):789-92.

Gileadi U, Moins-Teisserenc HT, Correa I, Booth BL Jr, Dunbar PR, Sewell AK, Trowsdale J, Phillips RE, Cerundolo V

Generation of an immunodominant CTL epitope is affected by proteasome subunit composition and stability of the antigenic protein.

J Immunol 1999, 163(11):6045-52.

Girolomoni G, Ricciardi-Castagnoli P

Dendritic cells hold promise for immunotherapy.

Immunol Today 1997, 18(3):102-4.

Glennie MJ, Johnson PW

Clinical trials of antibody therapy.

Immunol Today 2000, 21(8):403-10.

Greenberg PD

Adoptive T cell therapy of tumors: mechanisms operative in the recognition and elimination of tumor cells.

Adv Immunol 1991, 49:281-355.

Grossmann ME, Davila E, Celis E

Avoiding Tolerance Against Prostatic Antigens With Subdominant Peptide Epitopes.

J Immunother 2001, 24(3):237-241.

Grufman P, Sandberg JK, Wolpert EZ, Karre K

Immunization with dendritic cells breaks immunodominance in CTL responses against minor histocompatibility and synthetic peptide antigens.

J Leukoc Biol 1999a, 66(2):268-71.

Grufman P, Wolpert EZ, Sandberg JK, Karre K

T cell competition for the antigen-presenting cell as a model for immunodominance in the cytotoxic T lymphocyte response against minor histocompatibility antigens.

Eur J Immunol 1999b, 29(7):2197-204.

Grünebach F, Muller MR, Nencioni A, Brossart P

Delivery of tumor-derived RNA for the induction of cytotoxic T-lymphocytes.

Gene Ther 2003, 10(5):367-74.

Halaban R, Cheng E, Zhang Y, Moellmann G, Hanlon D, Michalak M, Setaluri V, Hebert DN

Aberrant retention of tyrosinase in the endoplasmic reticulum mediates accelerated degradation of the enzyme and contributes to the dedifferentiated phenotype of amelanotic melanoma cells.

Proc Natl Acad Sci USA 1997, 94(12):6210-5.

Heiser A, Dahm P, Yancey DR, Maurice MA, Boczkowski D, Nair SK, Gilboa E, Vieweg J

Human dendritic cells transfected with RNA encoding prostate-specific antigen stimulate prostate-specific CTL responses in vitro.

J Immunol 2000, 164(10):5508-14.

Heiser A, Maurice MA, Yancey DR, Coleman DM, Dahm P, Vieweg J

Human dendritic cells transfected with renal tumor RNA stimulate polyclonal T-cell responses against antigens expressed by primary and metastatic tumors.

Cancer Res 2001a, 61(8):3388-93.

Heiser A, Maurice MA, Yancey DR, Wu NZ, Dahm P, Pruitt SK, Boczkowski D, Nair SK, Ballo MS, Gilboa E, Vieweg J

Induction of polyclonal prostate cancer-specific CTL using dendritic cells transfected with amplified tumor RNA.

J Immunol 2001b, 166(5):2953-60.

Heiser A, Coleman D, Dannull J, Yancey D, Maurice MA, Lallas CD, Dahm P, Niedzwiecki D, Gilboa E, Vieweg J

Autologous dendritic cells transfected with prostate-specific antigen RNA stimulate CTL responses against metastatic prostate tumors.

J Clin Invest 2002, 109(3):409-17.

Helmbach H, Rossmann E, Kern MA, Schadendorf D

Drug-resistance in human melanoma.

Int J Cancer 2001, 93(5):617-22.

Herr W, Ranieri E, Olson W, Zarour H, Gesualdo L, Storkus WJ

Mature dendritic cells pulsed with freeze-thaw cell lysates define an effective in vitro vaccine designed to elicit EBV-specific CD4(+) and CD8(+) T lymphocyte responses.

Blood 2000, 96(5):1857-64.

Hersey P, Zhang XD

How melanoma cells evade trail-induced apoptosis.

Nat Rev Cancer 2001, 1(2):142-50.

Hicklin DJ, Wang Z, Arienti F, Rivoltini L, Parmiani G, Ferrone S

Beta2-Microglobulin mutations, HLA class I antigen loss, and tumor progression in melanoma.

J Clin Invest 1998, 101(12):2720-9.

Hofbauer GF, Kamarashev J, Geertsens R, Boni R, Dummer R

Melan A/MART-1 immunoreactivity in formalin-fixed paraffin-embedded primary and metastatic melanoma: frequency and distribution.

Melanoma Res 1998, 8(4):337-43.

Hu J, Kindsvogel W, Busby S, Bailey MC, Shi YY, Greenberg PD

An evaluation of the potential to use tumor-associated antigens as targets for antitumor T cell therapy using transgenic mice expressing a retroviral tumor antigen in normal lymphoid tissues.

J Exp Med 1993, 177(6):1681-90.

Huang M, Stolina M, Sharma S, Mao JT, Zhu L, Miller PW, Wollman J,

Herschman H, Dubinett SM

Non-small cell lung cancer cyclooxygenase-2-dependent regulation of cytokine balance in lymphocytes and macrophages: up-regulation of interleukin 10 and down-regulation of interleukin 12 production.

Cancer Res 1998, 58(6):1208-16.

Hung K, Hayashi R, Lafond-Walker A, Lowenstein C, Pardoll D, Levitsky H

The central role of CD4(+) T cells in the antitumor immune response.

J Exp Med 1998, 188(12):2357-68.

Irmeler M, Thome M, Hahne M, Schneider P, Hofmann K, Steiner V, Bodmer JL, Schroter M, Burns K, Mattmann C, Rimoldi D, French LE, Tschopp J

Inhibition of death receptor signals by cellular FLIP.

Nature 1997, 388(6638):190-5.

Jenne L, Schuler G, Steinkasserer A

Viral vectors for dendritic cell-based immunotherapy.

Trends Immunol 2001, 22(2):102-7.

Kalady MF, Onaitis MW, Padilla KM, Emani S, Tyler DS, Pruitt SK

Enhanced dendritic cell antigen presentation in RNA-based immunotherapy.

J Surg Res 2002, 105(1):17-24.

Kallenberg CG, Rarok A, Stegeman CA, Limburg PC

New insights into the pathogenesis of antineutrophil cytoplasmic autoantibody-associated vasculitis.

Autoimmun Rev 2002, 1(1-2):61-6.

Kawakami Y, Eliyahu S, Sakaguchi K, Robbins PF, Rivoltini L, Yannelli JR, Appella E, Rosenberg SA

Identification of the immunodominant peptides of the MART-1 human melanoma antigen recognized by the majority of HLA-A2-restricted tumor infiltrating lymphocytes.

J Exp Med 1994, 180(1):347-52.

Kedl RM, Kappler JW, Marrack P

Epitope dominance, competition and T cell affinity maturation.

Curr Opin Immunol 2003, 15(1):120-7.

Kersh GJ, Allen PM

Essential flexibility in the T-cell recognition of antigen.

Nature 1996, 380(6574):495-8.

Kesmir C, van Noort V, de Boer RJ, Hogeweg P

Bioinformatic analysis of functional differences between the immunoproteasome and the constitutive proteasome.

Immunogenetics 2003, 55(7):437-49.

Khong HT, Restifo NP

Natural selection of tumor variants in the generation of "tumor escape" phenotypes.

Nat Immunol 2002, 3(11):999-1005.

Kim CJ, Reintgen DS, Balch CM, AJCC Melanoma Staging Committee

The new melanoma staging system.

Cancer Control 2002, 9(1):9-15.

Kirk CJ, Mulé JJ

Gene-modified dendritic cells for use in tumor vaccines.

Hum Gene Ther 2000, 11(6):797-806.

Kirkin AF, Dzhandzhugazyan K, Zeuthen J

The immunogenic properties of melanoma-associated antigens recognized by cytotoxic T lymphocytes.

Exp Clin Immunogenet 1998, 15(1):19-32.

Kowalczyk DW

Tumors and the danger model.

Acta Biochim Pol 2002, 49(2):295-302.

Kugler A, Stuhler G, Walden P, Zoller G, Zobywalski A, Brossart P, Trefzer U, Ullrich S, Muller CA, Becker V, Gross AJ, Hemmerlein B, Kanz L, Muller GA, Ringert RH

Regression of human metastatic renal cell carcinoma after vaccination with tumor cell-dendritic cell hybrids.

Nat Med 2000, 6(3):332-6.

Kurnick JT, Ramirez-Montagut T, Boyle LA, Andrews DM, Pandolfi F, Durda PJ, Butera D, Dunn IS, Benson EM, Gobin SJ, van den Elsen PJ

A novel autocrine pathway of tumor escape from immune recognition: melanoma cell lines produce a soluble protein that diminishes expression of the gene encoding the melanocyte lineage melan-A/MART-1 antigen through down-modulation of its promoter.

J Immunol 2001, 167(3):1204-11.

Kurts C, Heath WR, Kosaka H, Miller JF, Carbone FR

The peripheral deletion of autoreactive CD8+ T cells induced by cross-presentation of self-antigens involves signaling through CD95 (Fas, Apo-1).

J Exp Med 1998, 188(2):415-20.

Lanzavecchia A

Immunology: Licence to kill.

Nature 1998, 393(6684):413-4.

Lee KH, Panelli MC, Kim CJ, Riker AI, Bettinotti MP, Roden MM, Fetsch P, Abati A, Rosenberg SA, Marincola FM

Functional dissociation between local and systemic immune response during anti-melanoma peptide vaccination.

J Immunol 1998, 161(8):4183-94.

Lee SP, Thomas WA, Blake NW, Rickinson AB

Transporter (TAP)-independent processing of a multiple membrane-spanning protein, the Epstein-Barr virus latent membrane protein 2.

Eur J Immunol 1996, 26(8):1875-83.

Lengauer C, Kinzler KW, Vogelstein B

Genetic instabilities in human cancers.

Nature 1998, 396(6712):643-9.

Li J, Schuler-Thurner B, Schuler G, Huber C, Seliger B

Bipartite regulation of different components of the MHC class I antigen-processing machinery during dendritic cell maturation.

Int Immunol 2001, 13(12):1515-23.

Li X, Zhao X, Fang Y, Jiang X, Duong T, Fan C, Huang CC, Kain SR

Generation of destabilized green fluorescent protein as a transcription reporter.

J Biol Chem 1998, 273(52):34970-5.

Loftus DJ, Castelli C, Clay TM, Squarcina P, Marincola FM, Nishimura MI, Parmiani G, Appella E, Rivoltini L

Identification of epitope mimics recognized by CTL reactive to the melanoma/melanocyte-derived peptide MART-1(27-35).

J Exp Med 1996, 184(2):647-57.

Ludewig B, Graf D, Gelderblom HR, Becker Y, Kroczeck RA, Pauli G

Spontaneous apoptosis of dendritic cells is efficiently inhibited by TRAP (CD40-ligand) and TNF-alpha, but strongly enhanced by interleukin-10.

Eur J Immunol 1995, 25(7):1943-50.

- Ludewig B, Ochsenbein AF, Odermatt B, Paulin D, Hengartner H, Zinkernagel RM**
Immunotherapy with dendritic cells directed against tumor antigens shared with normal host cells results in severe autoimmune disease.
J Exp Med 2000, 191(5):795-804.
- Lundqvist A, Noffz G, Pavlenko M, Saeboe-Larssen S, Fong T, Maitland N, Pisa P**
Nonviral and viral gene transfer into different subsets of human dendritic cells yield comparable efficiency of transfection.
J Immunother 2002, 25(6):445-54.
- Lutz MB, Schuler G**
Immature, semi-mature and fully mature dendritic cells: which signals induce tolerance or immunity?
Trends Immunol 2002, 23(9):445-9.
- Macagno A, Kuehn L, de Giuli R, Groettrup M**
Pronounced up-regulation of the PA28alpha/beta proteasome regulator but little increase in the steady-state content of immunoproteasome during dendritic cell maturation.
Eur J Immunol 2001, 31(11):3271-80.
- Mackay CR**
Homing of naive, memory and effector lymphocytes.
Curr Opin Immunol 1993, 5(3):423-7.
- Marin R, Ruiz-Cabello F, Pedrinaci S, Mendez R, Jimenez P, Geraghty DE, Garrido F**
Analysis of HLA-E expression in human tumors.
Immunogenetics 2003, 54(11):767-75.
- Matzinger P**
Tolerance, danger, and the extended family.
Annu Rev Immunol 1994, 12:991-1045.
- Melero I, Singhal MC, McGowan P, Haugen HS, Blake J, Hellstrom KE, Yang G, Clegg CH, Chen L**
Immunological ignorance of an E7-encoded cytolytic T-lymphocyte epitope in transgenic mice expressing the E7 and E6 oncogenes of human papillomavirus type 16.
J Virol 1997, 71(5):3998-4004.
- Milazzo C, Reichardt VL, Muller MR, Grunebach F, Brossart P**
Induction of myeloma-specific cytotoxic T cells using dendritic cells transfected with tumor-derived RNA.
Blood 2003, 101(3):977-82.
- Mitchell DA, Nair SK**
RNA-transfected dendritic cells in cancer immunotherapy.
J Clin Invest 2000, 106(9):1065-9.
- Morgan DJ, Kreuwel HT, Fleck S, Levitsky HI, Pardoll DM, Sherman LA**
Activation of low avidity CTL specific for a self epitope results in tumor rejection but not autoimmunity.
J Immunol 1998, 160(2):643-51.

Mosse CA, Meadows L, Luckey CJ, Kittlesen DJ, Huczko EL, Slingluff CL, Shabanowitz J, Hunt DF, Engelhard VH

The class I antigen-processing pathway for the membrane protein tyrosinase involves translation in the endoplasmic reticulum and processing in the cytosol.

J Exp Med 1998, 187(1):37-48.

Mumberg D, Monach PA, Wanderling S, Philip M, Toledano AY, Schreiber RD, Schreiber H
CD4(+) T cells eliminate MHC class II-negative cancer cells in vivo by indirect effects of IFN-gamma.

Proc Natl Acad Sci USA 1999, 96(15):8633-8.

Müller MR, Grunebach F, Nencioni A, Brossart P

Transfection of dendritic cells with RNA induces CD4- and CD8-mediated T cell immunity against breast carcinomas and reveals the immunodominance of presented T cell epitopes.

J Immunol 2003, 170(12):5892-6.

Naftzger C, Takechi Y, Kohda H, Hara I, Vijayasaradhi S, Houghton AN

Immune response to a differentiation antigen induced by altered antigen: a study of tumor rejection and autoimmunity.

Proc Natl Acad Sci USA 1996, 93(25):14809-14.

Nair SK, Boczkowski D, Morse M, Cumming RI, Lyerly HK, Gilboa E

Induction of primary carcinoembryonic antigen (CEA)-specific cytotoxic T lymphocytes in vitro using human dendritic cells transfected with RNA.

Nat Biotechnol 1998, 16(4):364-9.

Nair SK, McLaughlin C, Weizer A, Su Z, Boczkowski D, Dannull J, Vieweg J, Gilboa E

Injection of immature dendritic cells into adjuvant-treated skin obviates the need for ex vivo maturation.

J Immunol 2003, 171(11):6275-82.

Niehans GA, Brunner T, Frizelle SP, Liston JC, Salerno CT, Knapp DJ, Green DR, Kratzke RA

Human lung carcinomas express Fas ligand.

Cancer Res 1997, 57(6):1007-12.

Ogg GS, Rod Dunbar P, Romero P, Chen JL, Cerundolo V

High frequency of skin-homing melanocyte-specific cytotoxic T lymphocytes in autoimmune vitiligo.

J Exp Med 1998, 188(6):1203-8.

Oldstone MB, Nerenberg M, Southern P, Price J, Lewicki H

Virus infection triggers insulin-dependent diabetes mellitus in a transgenic model: role of anti-self (virus) immune response.

Cell 1991, 65(2):319-31.

Ossendorp F, Mengede E, Camps M, Filius R, Melief CJ

Specific T helper cell requirement for optimal induction of cytotoxic T lymphocytes against major histocompatibility complex class II negative tumors.

J Exp Med 1998, 187(5):693-702.

Overwijk WW, Lee DS, Surman DR, Irvine KR, Touloukian CE, Chan CC, Carroll MW, Moss B, Rosenberg SA, Restifo NP

Vaccination with a recombinant vaccinia virus encoding a "self" antigen induces autoimmune vitiligo and tumor cell destruction in mice: requirement for CD4(+) T lymphocytes.

Proc Natl Acad Sci USA 1999, 96(6):2982-7.

Oyama T, Ran S, Ishida T, Nadaf S, Kerr L, Carbone DP, Gabrilovich DI

Vascular endothelial growth factor affects dendritic cell maturation through the inhibition of nuclear factor-kappa B activation in hemopoietic progenitor cells.

J Immunol 1998, 160(3):1224-32.

Peltenburg LT, Schrier PI

Transcriptional suppression of HLA-B expression by c-Myc is mediated through the core promoter elements.

Immunogenetics 1994, 40(1):54-61.

Penn I

Posttransplant malignancies.

Transplant Proc 1999, 31(1-2):1260-2.

Pittet MJ, Valmori D, Dunbar PR, Speiser DE, Lienard D, Lejeune F, Fleischhauer K, Cerundolo V, Cerottini JC, Romero P

High frequencies of naive Melan-A/MART-1-specific CD8(+) T cells in a large proportion of human histocompatibility leukocyte antigen (HLA)-A2 individuals.

J Exp Med 1999, 190(5):705-15.

Ponsaerts P, Van Tendeloo VF, Cools N, Van Driessche A, Lardon F, Nijs G,

Lenjou M, Mertens G, Van Broeckhoven C, Van Bockstaele DR, Berneman ZN

mRNA-electroporated mature dendritic cells retain transgene expression, phenotypical properties and stimulatory capacity after cryopreservation.

Leukemia 2002, 16(7):1324-30.

Ponsaerts P, Van Tendeloo VF, Berneman ZN

Cancer immunotherapy using RNA-loaded dendritic cells.

Clin Exp Immunol 2003, 134(3):378-84.

Prota G

Melanins, melanogenesis and melanocytes: looking at their functional significance from the chemist's viewpoint.

Pigment Cell Res 2000, 13(4):283-93.

Qin Z, Blankenstein T

CD4+ T cell--mediated tumor rejection involves inhibition of angiogenesis that is dependent on IFN gamma receptor expression by nonhematopoietic cells.

Immunity 2000, 12(6):677-86.

Ramal LM, Maleno I, Cabrera T, Collado A, Ferron A, Lopez-Nevot MA, Garrido F

Molecular strategies to define HLA haplotype loss in microdissected tumor cells.

Hum Immunol. 2000, 61(10):1001-12.

Ramirez-Montagut T, Turk MJ, Wolchok JD, Guevara-Patino JA, Houghton AN

Immunity to melanoma: unraveling the relation of tumor immunity and autoimmunity.

Oncogene 2003, 22(20):3180-7.

- Restifo NP, Antony PA, Finkelstein SE, Leitner WW, Surman DP, Theoret MR, Touloukian CE**
Assumptions of the tumor 'escape' hypothesis.
Semin Cancer Biol 2002, 12(1):81-6.
- Ribas A, Butterfield LH, Glaspy JA, Economou JS**
Current developments in cancer vaccines and cellular immunotherapy.
J Clin Oncol 2003, 21(12):2415-32.
- Rivoltini L, Barracchini KC, Viggiano V, Kawakami Y, Smith A, Mixon A, Restifo NP, Topalian SL, Simonis TB, Rosenberg SA**
Quantitative correlation between HLA class I allele expression and recognition of melanoma cells by antigen-specific cytotoxic T lymphocytes.
Cancer Res 1995, 55(14):3149-57.
- Rivoltini L, Squarcina P, Loftus DJ, Castelli C, Tarsini P, Mazzocchi A, Rini F, Viggiano V, Belli F, Parmiani G**
A superagonist variant of peptide MART1/Melan A27-35 elicits anti-melanoma CD8+ T cells with enhanced functional characteristics: implication for more effective immunotherapy.
Cancer Res 1999, 59(2):301-6.
- Rivoltini L, Carrabba M, Huber V, Castelli C, Novellino L, Dalerba P, Mortarini R, Arancia G, Anichini A, Fais S, Parmiani G**
Immunity to cancer: attack and escape in T lymphocyte-tumor cell interaction.
Immunol Rev 2002, 188:97-113.
- Rodriguez A, Regnault A, Kleijmeer M, Ricciardi-Castagnoli P, Amigorena S**
Selective transport of internalized antigens to the cytosol for MHC class I presentation in dendritic cells.
Nat Cell Biol 1999, 1(6):362-8.
- Rojas M, Donahue JP, Tan Z, Lin YZ**
Genetic engineering of proteins with cell membrane permeability.
Nat Biotechnol 1998, 16(4):370-5.
- Romero P, Dunbar PR, Valmori D, Pittet M, Ogg GS, Rimoldi D, Chen JL, Lienard D, Cerottini JC, Cerundolo V**
Ex vivo staining of metastatic lymph nodes by class I major histocompatibility complex tetramers reveals high numbers of antigen-experienced tumor-specific cytolytic T lymphocytes.
J Exp Med 1998, 188(9):1641-50.
- Rosenberg SA**
Karnofsky Memorial Lecture. The immunotherapy and gene therapy of cancer.
J Clin Oncol 1992, 10(2):180-99.
- Rosenberg SA, White DE**
Vitiligo in patients with melanoma: normal tissue antigens can be targets for cancer immunotherapy.
J Immunother Emphasis Tumor Immunol 1996, 19(1):81-4.
- Sallusto F, Lanzavecchia A**
Efficient presentation of soluble antigen by cultured human dendritic cells is maintained by granulocyte/macrophage colony-stimulating factor plus interleukin 4 and downregulated by tumor necrosis factor alpha.
J Exp Med 1994, 179(4):1109-18.

Sallusto F, Lanzavecchia A

Mobilizing dendritic cells for tolerance, priming, and chronic inflammation.
J Exp Med 1999, 189(4):611-4.

Salter RD, Howell DN, Cresswell P

Genes regulating HLA class I antigen expression in T-B lymphoblast hybrids.
Immunogenetics 1985, 21(3):235-46.

Sandberg JK, Grufman P, Wolpert EZ, Franksson L, Chambers BJ, Karre K

Superdominance among immunodominant H-2Kb-restricted epitopes and reversal by dendritic cell-mediated antigen delivery.
J Immunol 1998, 160(7):3163-9.

Santin AD, Hermonat PL, Ravaggi A, Chiriva-Internati M, Zhan D, Pecorelli S, Parham GP, Cannon MJ

Induction of human papillomavirus-specific CD4(+) and CD8(+) lymphocytes by E7-pulsed autologous dendritic cells in patients with human papillomavirus type 16- and 18-positive cervical cancer.
J Virol 1999, 73(7):5402-10.

Schendel DJ, Gansbacher B, Oberneder R, Kriegmair M, Hofstetter A, Riethmuller G, Segurado OG

Tumor-specific lysis of human renal cell carcinomas by tumor-infiltrating lymphocytes. I. HLA-A2-restricted recognition of autologous and allogeneic tumor lines.
J Immunol 1993, 151(8):4209-20.

Schild H, Rotzschke O, Kalbacher H, Rammensee HG

Limit of T cell tolerance to self proteins by peptide presentation.
Science 1990, 247(4950):1587-9.

Schott M, Feldkamp J, Schattenberg D, Krueger T, Dotzenrath C, Seissler J, Scherbaum WA

Induction of cellular immunity in a parathyroid carcinoma treated with tumor lysate-pulsed dendritic cells.
Eur J Endocrinol 2000, 142(3):300-6.

Schreiber H, Wu TH, Nachman J, Kast WM

Immunodominance and tumor escape.
Semin Cancer Biol 2002, 12(1):25-31.

Schreurs MW, Eggert AA, de Boer AJ, Vissers JL, van Hall T, Offringa R, Figdor CG, Adema GJ

Dendritic cells break tolerance and induce protective immunity against a melanocyte differentiation antigen in an autologous melanoma model.
Cancer Res 2000, 60(24):6995-7001.

Sharma S, Stolina M, Lin Y, Gardner B, Miller PW, Kronenberg M, Dubinett SM

T cell-derived IL-10 promotes lung cancer growth by suppressing both T cell and APC function.
J Immunol 1999, 163(9):5020-8.

Shevach EM

Certified professionals: CD4(+)CD25(+) suppressor T cells.
J Exp Med 2001, 193(11):F41-6.

Shin MS, Park WS, Kim SY, Kim HS, Kang SJ, Song KY, Park JY, Dong SM, Pi JH, Oh RR, Lee JY, Yoo NJ, Lee SH

Alterations of Fas (Apo-1/CD95) gene in cutaneous malignant melanoma.
Am J Pathol 1999, 154(6):1785-91.

Sigal LJ, Rock KL

Bone marrow-derived antigen-presenting cells are required for the generation of cytotoxic T lymphocyte responses to viruses and use transporter associated with antigen presentation (TAP)-dependent and -independent pathways of antigen presentation.
J Exp Med 2000, 192(8):1143-50.

Skipper JC, Hendrickson RC, Gulden PH, Brichard V, Van Pel A, Chen Y, Shabanowitz J, Wolfel T, Slingluff CL Jr, Boon T, Hunt DF, Engelhard VH

An HLA-A2-restricted tyrosinase antigen on melanoma cells results from posttranslational modification and suggests a novel pathway for processing of membrane proteins.
J Exp Med 1996, 183(2):527-34.

Song YH, Connor E, Li Y, Zorovich B, Balducci P, Maclaren N

The role of tyrosinase in autoimmune vitiligo.
Lancet 1994, 344(8929):1049-52.

Soong TW, Hui KM

Locus-specific transcriptional control of HLA genes.
J Immunol 1992, 149(6):2008-20.

Steinman RM, Turley S, Mellman I, Inaba K

The induction of tolerance by dendritic cells that have captured apoptotic cells.
J Exp Med 2000, 191(3):411-6.

Stoler DL, Chen N, Basik M, Kahlenberg MS, Rodriguez-Bigas MA, Petrelli NJ, Anderson GR

The onset and extent of genomic instability in sporadic colorectal tumor progression.
Proc Natl Acad Sci USA 1999, 96(26):15121-6.

Strobel I, Berchtold S, Gotze A, Schulze U, Schuler G, Steinkasserer A

Human dendritic cells transfected with either RNA or DNA encoding influenza matrix protein M1 differ in their ability to stimulate cytotoxic T lymphocytes.
Gene Ther 2000, 7(23):2028-35.

Su Z, Peluso MV, Raffegerst SH, Schendel DJ, Roskrow MA

The generation of LMP2a-specific cytotoxic T lymphocytes for the treatment of patients with Epstein-Barr virus-positive Hodgkin disease.
Eur J Immunol 2001, 31(3):947-58.

Su Z, Vieweg J, Weizer AZ, Dahm P, Yancey D, Turaga V, Higgins J, Boczkowski D, Gilboa E, Dannull J

Enhanced induction of telomerase-specific CD4(+) T cells using dendritic cells transfected with RNA encoding a chimeric gene product.
Cancer Res 2002, 62(17):5041-8.

Su Z, Dannull J, Heiser A, Yancey D, Pruitt S, Madden J, Coleman D, Niedzwiecki D, Gilboa E, Vieweg J

Immunological and clinical responses in metastatic renal cancer patients vaccinated with tumor RNA-transfected dendritic cells.
Cancer Res 2003, 63(9):2127-33.

Takeda K, Oshima H, Hayakawa Y, Akiba H, Atsuta M, Kobata T, Kobayashi K, Ito M, Yagita H, Okumura K

CD27-mediated activation of murine NK cells.
J Immunol 2000, 164(4):1741-5.

Tatsis E, Reinhold-Keller E, Steindorf K, Feller AC, Gross WL

Wegener's granulomatosis associated with renal cell carcinoma.
Arthritis Rheum. 1999, 42(4):751-6.

Thurner B, Haendle I, Roder C, Dieckmann D, Keikavoussi P, Jonuleit H, Bender A, Maczek C, Schreiner D, von den Driesch P, Brocker EB, Steinman RM, Enk A, Kampgen E, Schuler G

Vaccination with mage-3A1 peptide-pulsed mature, monocyte-derived dendritic cells expands specific cytotoxic T cells and induces regression of some metastases in advanced stage IV melanoma.
J Exp Med 1999, 190(11):1669-78.

Toi M, Taniguchi T, Yamamoto Y, Kurisaki T, Suzuki H, Tominaga T

Clinical significance of the determination of angiogenic factors.
Eur J Cancer 1996, 32A(14):2513-9.

Tsien RY

The green fluorescent protein.
Annu Rev Biochem 1998, 67:509-44.

Turk MJ, Wolchok JD, Guevara-Patino JA, Goldberg SM, Houghton AN

Multiple pathways to tumor immunity and concomitant autoimmunity.
Immunol Rev 2002, 188:122-35.

Urban JL, Holland JM, Kripke ML, Schreiber H

Immunoselection of tumor cell variants by mice suppressed with ultraviolet radiation.
J Exp Med 1982, 156(4):1025-41.

Uyttenhove C, Van Snick J, Boon T

Immunogenic variants obtained by mutagenesis of mouse mastocytoma P815. I. Rejection by syngeneic mice.
J Exp Med 1980, 152(5):1175-83.

Valmori D, Fonteneau JF, Lizana CM, Gervois N, Lienard D, Rimoldi D, Jongeneel V, Jotereau F, Cerottini JC, Romero P

Enhanced generation of specific tumor-reactive CTL in vitro by selected Melan-A/MART-1 immunodominant peptide analogues.
J Immunol 1998, 160(4):1750-8.

van der Bruggen P, Traversari C, Chomez P, Lurquin C, De Plaen E, Van den Eynde B, Knuth A, Boon T

A gene encoding an antigen recognized by cytolytic T lymphocytes on a human melanoma.
Science 1991, 254(5038):1643-7.

van Elsas A, Hurwitz AA, Allison JP

Combination immunotherapy of B16 melanoma using anti-cytotoxic T lymphocyte-associated antigen 4 (CTLA-4) and granulocyte/macrophage colony-stimulating factor (GM-CSF)-producing vaccines induces rejection of subcutaneous and metastatic tumors accompanied by autoimmune depigmentation.
J Exp Med 1999, 190(3):355-66.

van Tendeloo VF, Snoeck HW, Lardon F, Vanham GL, Nijs G, Lenjou M, Hendriks L, Van Broeckhoven C, Moulijn A, Rodrigus I, Verdonk P, Van Bockstaele DR, Berneman ZN

Nonviral transfection of distinct types of human dendritic cells: high-efficiency gene transfer by electroporation into hematopoietic progenitor- but not monocyte-derived dendritic cells.
Gene Ther 1998, 5(5):700-7.

van Tendeloo VF, Ponsaerts P, Lardon F, Nijs G, Lenjou M, Van Broeckhoven C, Van Bockstaele DR, Berneman ZN

Highly efficient gene delivery by mRNA electroporation in human hematopoietic cells: superiority to lipofection and passive pulsing of mRNA and to electroporation of plasmid cDNA for tumor antigen loading of dendritic cells.
Blood 2001, 98(1):49-56.

Vax VV, Bibi R, Diaz-Cano S, Gueorguiev M, Kola B, Borboli N, Bressac-de Paillerets B, Walker GJ, Dedov II, Grossman AB, Korbonits M

Activating point mutations in cyclin-dependent kinase 4 are not seen in sporadic pituitary adenomas, insulinomas or Leydig cell tumours.
J Endocrinol 2003, 178(2):301-10.

Vierboom MP, Nijman HW, Offringa R, van der Voort EI, van Hall T, van den Broek L, Fleuren GJ, Kenemans P, Kast WM, Melief CJ

Tumor eradication by wild-type p53-specific cytotoxic T lymphocytes.
J Exp Med 1997, 186(5):695-704.

Wang RF, Parkhurst MR, Kawakami Y, Robbins PF, Rosenberg SA

Utilization of an alternative open reading frame of a normal gene in generating a novel human cancer antigen.
J Exp Med 1996, 183(3):1131-40.

Wang RF

The role of MHC class II-restricted tumor antigens and CD4+ T cells in antitumor immunity.
Trends Immunol 2001, 22(5):269-76.

Wang RF, Wang HY

Enhancement of antitumor immunity by prolonging antigen presentation on dendritic cells.
Nat Biotechnol 2002, 20(2):149-54.

Weissman D, Ni H, Scales D, Dude A, Capodici J, McGibney K, Abdool A, Isaacs SN, Cannon G, Kariko K

HIV gag mRNA transfection of dendritic cells (DC) delivers encoded antigen to MHC class I and II molecules, causes DC maturation, and induces a potent human in vitro primary immune response.
J Immunol 2000, 165(8):4710-7.

Wolpert EZ, Grufman P, Sandberg JK, Tegnesjo A, Karre K

Immunodominance in the CTL response against minor histocompatibility antigens: interference between responding T cells, rather than with presentation of epitopes.
J Immunol 1998, 161(9):4499-505.

Wölfel T, Hauer M, Klehmann E, Brichard V, Ackermann B, Knuth A, Boon T, Meyer Zum Buschenfelde KH

Analysis of antigens recognized on human melanoma cells by A2-restricted cytolytic T lymphocytes (CTL).
Int J Cancer 1993, 55(2):237-44.

- Wölfel T, Schneider J, Meyer Zum Buschenfelde KH, Rammensee HG, Rotzschke O, Falk K**
Isolation of naturally processed peptides recognized by cytolytic T lymphocytes (CTL) on human melanoma cells in association with HLA-A2.1.
Int J Cancer 1994a, 57(3):413-8.
- Wölfel T, Van Pel A, Brichard V, Schneider J, Seliger B, Meyer zum Buschenfelde KH, Boon T**
Two tyrosinase nonapeptides recognized on HLA-A2 melanomas by autologous cytolytic T lymphocytes.
Eur J Immunol 1994b, 24(3):759-64.
- Wölfel T, Hauer M, Schneider J, Serrano M, Wolfel C, Klehmann-Hieb E, De Plaen E, Hankeln T, Meyer zum Buschenfelde KH, Beach D**
A p16INK4a-insensitive CDK4 mutant targeted by cytolytic T lymphocytes in a human melanoma.
Science 1995, 269(5228):1281-4.
- Wu TC, Guarnieri FG, Staveley-O'Carroll KF, Viscidi RP, Levitsky HI, Hedrick L, Cho KR, August JT, Pardoll DM**
Engineering an intracellular pathway for major histocompatibility complex class II presentation of antigens.
Proc Natl Acad Sci USA 1995, 92(25):11671-5.
- Yang TT, Cheng L, Kain SR**
Optimized codon usage and chromophore mutations provide enhanced sensitivity with the green fluorescent protein.
Nucleic Acids Res 1996, 24(22):4592-3.
- Yee C, Savage PA, Lee PP, Davis MM, Greenberg PD**
Isolation of high avidity melanoma-reactive CTL from heterogeneous populations using peptide-MHC tetramers.
J Immunol 1999, 162(4):2227-34.
- Yewdell JW, Norbury CC, Bennink JR**
Mechanisms of exogenous antigen presentation by MHC class I molecules in vitro and in vivo: implications for generating CD8+ T cell responses to infectious agents, tumors, transplants, and vaccines.
Adv Immunol 1999, 73:1-77.
- Zhao Y, Boczkowski D, Nair SK, Gilboa E**
Inhibition of invariant chain expression in dendritic cells presenting endogenous antigens stimulates CD4+ T-cell responses and tumor immunity.
Blood 2003, 102(12):4137-42.
- Zinkernagel RM**
Immunology taught by viruses.
Science 1996, 271(5246):173-8.

8. Abbreviations

Ag	antigen
APC	antigen-presenting cell
APL	altered peptide ligand
bp	base pair
CAMEL	CTL-recognised antigen on melanoma
CCR	chemokine (CC motif) receptor
CD	cluster of differentiation
CD40L	CD40 ligand
CDC27	cell division control 27
CDK4	cyclin-dependent kinase 4
cDNA	complementary DNA
CEA	carcinoembryogenic antigen
cFLIP	cellular FLICE-inhibitory protein
cRNA	complementary RNA
CTL	cytotoxic T-lymphocyte
CTLA-4	cytotoxic T-lymphocyte associated protein 4
DC	dendritic cell
DC-SIGN	DC-specific ICAM-grabbing nonintegrin
DEPC	diethyl pyrocarbonate
DNA	deoxyribonucleic acid
DNase	deoxyribonuclease
DMSO	dimethyl sulfoxide
dsDNA	double-stranded DNA
dsRNA	double-stranded RNA
EDTA	ethylenediamine-tetra-acetate
elp.	electroporation or electroporated
ER	endoplasmic reticulum
EGFP	enhanced green fluorescence protein
ELISA	enzyme-linked immunosorbent assay
Fab	fragment antigen binding
FACS™	fluorescence-activated cell sorter
Fc	fragment crystallisable

FcR	Fc receptor
FITC	fluorescein isothiocyanate
GFP	green fluorescence protein
GM-CSF	granulocyte macrophage colony stimulating factor
gp	glycoprotein
GnT-V	beta 1,6-N-acetylglucosaminyltransferase V
HIV	human immunodeficiency virus
HLA	human leukocyte antigen
HSP	heat-shock protein
iDC	immature DC
IFN	interferon
Ig	immunoglobulin
IL	interleukin
LAMP-1	lysosome-associated membrane protein 1
LDLR	low density lipoprotein receptor
LMP	low molecular protein
LPS	lipopolysaccharide
MIIC	MHC class II compartment
MAA	melanoma-associated antigen
MAGE	melanoma antigen gene
MART-1	melanoma antigen recognised by T-cells 1
mDC	mature DC
Melan-A	melanoma antigen A
MFI	mean fluorescence intensity
MIC	MHC class I chain-related gene
MIF	macrophage migration inhibitory factor
MMR	macrophage mannose receptor
mRNA	messenger RNA
NK	natural killer
NKT	natural killer T
OX-40L	OX40 ligand
PAP	prostatic acid phosphatase
PBMC	peripheral blood mononuclear cells
PBS	phosphate buffered saline

PCR	polymerase chain reaction
pDNA	plasmid DNA
PE	phycoerythrin
PGE ₂	prostaglandin E2
pMHC	peptide-MHC
PRAME	preferentially expressed antigen of melanoma
PSA	prostate-specific antigen
RCC	renal cell carcinoma
RNA	ribonucleic acid
RNase	ribonuclease
rpm	rotations per minute
rRNA	ribosomal RNA
RT	reverse transcriptase
RT-PCR	reverse transcription PCR
ru	relative unit
TAA	tumour-associated antigen
TAE	tris acetate EDTA
TAP	transporter associated with antigen processing
TBE	tris borate EDTA
TCR	T-cell receptor
TGF	transforming growth factor
TIL	tumour-infiltrating lymphocyte
TLR	Toll-like receptor
TNF	tumour necrosis factor
TRAIL	TNF-related apoptosis-inducing ligand
tRNA	transfer RNA
TRP	tyrosinase related protein
UV	ultraviolet
VEGF	vascular endothelial growth factor

9. Acknowledgments

Two days ago, having typed in the last corrections of the summary, I felt relieved for the first time in three months because the most important chapters of this thesis were written and the grand finale was in sight! And I really wanted to share my happiness with someone... In other words, what has become increasingly obvious over the past three and a half years is that it is not as much about seeing blue in the ELISA plate (after a whole year of seeing nothing) as it is about telling someone that the experiment has finally worked. Or that it has not. The following are the people who happily smiled to my positive reports or, when the news was not so good, replied with "It's going to be fine". They also constantly supported me and helped me, thereby becoming or continuing to be an important part of my life.

When I was not sure in which direction to go with my research, my tutor, Prof. Dolores Schendel, was. When I did not know which experiments to do, she did. When I could not find the right word or phrase for my thesis, she had one ready. And when I gave her the first draft of the results chapter, she already asked about the discussion because she was correcting faster than I had imagined it to be possible. I was lucky to have not only one but two tutors. Dr. Heike Pohla never said no to my ideas (... and some of them were not inexpensive) and always said yes when I asked if she had a minute for my questions (... and I did so on many many occasions, the one minute turning into at least ten). She also took the time to read and correct this thesis. On a more personal note, Dolores kindly motivated me with positive comments about my work and Heike's gentle personality defined the relaxed and friendly atmosphere I felt privileged to work in. Dolores and Heike, thank you!

From the beginning on, Dr. Dirk Eick, my university "Doktorvater", showed interest in the project, suggested additional experiments and, in the end, made an effort to read the thesis. Thank you!

Roswitha Fischer and Birgit Konkoll helped me in the lab, laughed with me a lot and were very often forced to listen to my singing (they did so without complaining). Rosi, thank you for letting me be part of the "Wunderbare Welt der Roswitha Fischer"! Birgit, thank you for all your nice smiles and kind words! Bernhard Frankenberger taught me

everything I know about real-time PCR. Sybille Regn was my DC expert. They both answered my numerous questions and helped me with experiments. Bernhard and Sybille, thank you! Elfriede Nößner also always found the time to help me with my theoretical and practical problems. Elfriede, thank you! Many other colleagues not only offered their help immediately when I asked but they also, every so often, wanted to know how things were going. Therefore, Rainer Riesenberg, Alex Buchner, Birgit Stadlbauer, Anna Brandl, Konrad Kronenberger, Wolfgang Zimmermann, Sandra Neckermann, Mirna Castro, Sylvia Donhauser, Chris Falk, Valeria Milani, Josef Mysliwietz,, Falk Nimmerjahn, Joseph Mautner, Nicole Baur, Sibylle Ruhland, Julia Schleypen, Christine Hennard, Barbara Mosetter, Christoph von Hesler, Sonja Hirschmüller, Oksana Heinz and Doreen Hammer, thank you! I hope I haven't forgotten anyone.

At first, my friends themselves made an effort to enquire about the mice and viruses in my experiments (... one short look at the methods chapter reveals that I worked with human and bacterial cells only). With time, they had no choice but to listen about how my dendritic cells were annihilated in electroporation and how difficult it was to get all diagrams in the thesis to have the same format. And about other problems... They did so very patiently and with a lot of support. Therefore, Mose, Dusan, Andi, Massimo, Roland, Jochen, Susan, Carmen, Robert, Torsten, Ana, Maja, Nina, Marijana, Tomo and Bojan, thank you!

Going back to my emotional state that, two days ago, came a bit too early (the abbreviations section of the thesis cost me a whole afternoon and a lot of nerves yesterday)... I sent a message to my mom saying how relieved I was. And, like in so many situations before, she was happy for me. Simply knowing that I can count on my mom no matter what, when or how far away (OK, it is just 8 hours by bus between Munich and Zagreb but still...) made everything so much easier. Mom, thank you!

Munich, 11th January 2004

10. Curriculum vitae

Personal data

Name: Miran Javorović
Date and place of birth: 9th July, 1976 in Zagreb, Croatia
Nationality: Croatian
Marital status: single

Address (Croatia): Hatzova 28, 10000 Zagreb, Croatia
Address (Germany): Rolf-Pinegger-Str. 10, 80689 München, Germany
Address (e-mail): mjavorovic@hotmail.com

School education

Primary school (1983-1991): Izidor Kršnjavi, Zagreb, Croatia
Secondary school (1991-1995): Klasična gimnazija (ancient Latin and Greek programme school), Zagreb, Croatia
Scholarships (1993-1995): "Scholarship of the City of Zagreb" for the academic year 93/94
"Scholarship of the City of Zagreb" for the academic year 94/95

Academic education

Undergraduate (1995-2000): Molekularna biologija, Biološki odsjek, Prirodoslovno-matematički fakultet, Zagrebačko sveučilište (Molecular biology programme, Department of Biology, Faculty of Natural Sciences and Mathematics, University of Zagreb), Zagreb, Croatia
Honours (1998): "Certificate of Merit" as the best student of biology at the Faculty of Natural Sciences and Mathematics for the academic year 97/98
Scholarship (1998-1999): "Scholarship of the City of Zagreb" for the academic year 98/99
Undergraduate thesis (2000): "Influence of dexamethazone on peripheral blood mononuclear cells" at the Institute of Immunology, Zagreb, Croatia
Undergraduate degree (2000): engineer in molecular biology
Graduate thesis (2000-2004): "T-cell stimulation by melanoma RNA-pulsed dendritic cells" at the Institute of Molecular Immunology, GSF Research Centre for Environment and Health, Munich, Germany and at Biologische Fakultät, Ludwig-Maximilians-Universität (Faculty of Biology, Ludwig-Maximilian University), Munich, Germany

Languages

Languages spoken and written: Croatian (fluent), English (fluent), German (fluent),
French (basic knowledge)

Certificates: Cambridge First Certificate in English
Cambridge Certificate in Advanced English
TOEFL in English